Antimicrobial activity of polyethyleneimine/polyurethane (PEI/PU) colloidal films

by

Minghui Liu

A thesis

presented to the University of Waterloo

in fulfillment of the

thesis requirement for the degree of

Master of Applied Science

in

Chemical Engineering

Waterloo, Ontario, Canada, 2021

Author's declaration

I hereby declare that I am the sole author of this thesis. This is a true copy of the thesis, including any required final revisions, as accepted by my examiners.

I understand that my thesis may be made electronically available to the public.

Abstract

With the occurrence of healthcare associated infections (HAIs), the development of novel antimicrobial materials has drawn significant research attention. However, developing an antimicrobial material that can be long-term effective and environmentally friendly without cytotoxicity is still a technical challenge and normally results in large production costs. In this thesis research, we fabricated, characterized and evaluated a polyethyleneimine/polyurethane (PEI/PU) colloidal film for antimicrobial coating applications. Following the previous work in our group, the colloidal film was obtained by introducing polyethyleneimine into a waterborne polyurethane. This colloidal film was found having excellent mechanical properties. From tensile tests it was found that the PU/PEI composites displayed superior mechanical properties compared to pure PU with an ultimate tensile strength of 23 MPa compared to 18 MPa for pure PU. In addition to tensile tests, scratch tests were performed on the coatings. It was found that at 5 wt% PEI the coatings displayed the best abrasion resistance at 2000 g of applied force on the tip compared to 1200 g for pure PU. The antimicrobial activities were investigated in this work with the hypothesis of PU/PEI colloidal films being a dual-functional antibacterial material. The ion-releasing activity and contact-killing efficiency of PU/PEI colloidal films were tested separately. Though there have not been conclusive results showing the existence of ion-releasing antibacterial working principle, a high killing rate of contact-active antibacterial activity was observed. Furthermore, explorative evaluations were performed to check possible virucidal effect against baculovirus.

Acknowledgements

I would like to formally thank my supervisor Dr. Boxin Zhao, and co-supervisor Dr. William A. Anderson for their professional support and expertise throughout this work. Completing this thesis would not be possible without their guidance.

Besides, I would like to acknowledge Dr. Pengxiang Si for his mentorship in the study of polyethyleneimine/polyurethane system. I would also like to express my appreciation to Scott Joseph Boegel (PhD candidate in Dr. Marc Aucoin's research group) with the antiviral experiments he performed for my polyethyleneimine/polyurethane samples. The patience and knowledge they provided helped me better understand my material.

Last but not the least, I would like to thank my beloved fiancé, Lukas Bauman for his support and company within these 2 years. It would be more difficult for me to get used to the life in a foreign country and quickly concentrated on academic study without him. Significantly, the emotional support he provided encouraged me to overcome the challenges, accomplishing my goals during this pandemic.

Table of Contents

Table of Figures

List of Tables

List of Abbreviations

QACs	Quaternary Ammonium Compounds
PEI	Polyethyleneimine
QA-PEI	Quaternized Polyethyleneimine
PU	Polyurethane
WPU	Waterborne Polyurethane
IPDI	Isophorone Diisocyanate
DMPA	Dimethylol Propionic Acid
PPG-2000	Polypropylene Glycol 2000 mw
FTIR	Fourier Transform Infrared Spectroscopy
UMT	Universal Mechanical Tester
DLS	Dynamic Light Scattering
SEM	Scanning Electron Microscopy
CFUs	Colony Forming Units
HAIs	Healthcare Associated Infections

Chapter 1. Introduction

Healthcare associated infections (HAI) have seen a significant increase along with the development of modern clinical treatments, including central line-associated bloodstream infections, catheter-associated urinary tract infections, and ventilator-associated pneumonia. Data from the HAI Hospital Prevalence Survey shows on any given day, about one in 31 hospital patients has at least one healthcare-associated infection. 687,000 HAIs in U.S. acute care hospitals in 2015, and about 72,000 hospital patients with HAIs died during their hospitalizations[1]. To prevent HAIs, the development of novel antimicrobial materials has drawn significant research attention. Antimicrobial materials contain antimicrobial agents, which have the ability to inhibit the growth or directly kill microorganisms so as to reduce the occurrence of HAIs. However, developing an antimicrobial material which can be long-term effective and environmentally friendly without cytotoxicity to human cells is still a technical challenge and normally results in large production costs.

With the purpose of reducing the health threat from microbial contaminants, antimicrobial polymers have been substantially developed and used in varies application. Current antimicrobial polymers were roughly sorted into passive and active types based on their action against microbes. Furthermore, a category of their antimicrobial principles was proposed as repelling, ion-release and contact-active antimicrobial polymers. However, each of these antimicrobial principles has its inherent shortage respectively. Due to this, multifunctional antimicrobial surfaces have been developed and focused on in recent research since with only one antimicrobial principle, the effectiveness of antimicrobial materials is insufficient in practice because of the inherent

limitations of each principle[2]. A literature review was performed in Chapter 2 to provide context for the antimicrobial agent applied in this project and the study of its antimicrobial mechanisms.

The objective of this project is to evaluate the antimicrobial properties including both ion-releasing and contact-active antibacterial activity as well as antiviral property of a recently-developed PU/PEI colloidal film. Previous research with this system by Si et al. found that PEI could be incorporated into polyurethane to form a colloidal film and it enhanced the material strength at low concentrations[3]. The PEI was bonded to the polyurethane in this system by both ionic interactions and hydrogen bonds[4], and it was expected to maintain the surface charge density under leaching conditions. PEI contains primary, secondary and tertiary amine groups, which shall provide a certain antimicrobial activity. In addition to the antibacterial contact-killing activity of the bonded PEI in the system, there also existed some mobile PEI. These mobile molecules could migrate or leach out of the film and provide biocide releasing activity. In this study, multiple antimicrobial tests were performed on the surface to characterize the PU/PEI colloidal film's antimicrobial activity without any surface modifications and gain insights into the antimicrobial mechanism. The details and results of antimicrobial and antiviral tests with this material are subsequently described in Chapter 3 and Chapter 4. Chapter 5 presents the conclusion and a discussion of future work.

Chapter 2. Literature Review

2.1 Antimicrobial material

Antimicrobial polymeric materials were first characterized in 1965 by Cornell and Donaruma claiming antibacterial activity of polymers and copolymers prepared from 2-methacryloxytroponones[5,6]. In the 1970s researchers synthesized various antimicrobial polymeric molecules such as polymerized salicylic acid [7], polymers with quaternary ammonium groups[8]. Since then, a large number of polymeric structures with such actions have been discovered or synthesized and widely applied in both industrial and academic areas. Furthermore, with the development of FDA-approved disinfecting polymers, antimicrobial materials have attracted substantial attention in pharmaceutical, and household applications, where microbial contaminants could directly cause a serious threat to human health or indirectly by spreading contagion. Julieta et al. performed a comprehensive analysis of Google Patent Search database and found more than 27,845 patents filed since 2013 relating to antimicrobial polymers[9].

Figure 1. Typical formations of biofilm:(a) biofilm of mold; (b) algae biofilm and (c) bacterial biofilm[6]. Reproduced from ref 6. Copyright held by original authors.

The way microbes contaminate a substance has been found to be through the adhesion of biofilms (Fig. 1) that microbe excrete to anchor themselves to the surface of the substance[10,11]. Under satisfactory growth conditions, microbial cells grow and aggregate while producing a biofilm (Fig. 2) consisting of extracellular polymeric substance surrounding them[10,11]. Such extracellular polymeric substance is a polymeric conglomeration composed of polysaccharides, proteins, lipids and DNA[10–12]. Defective biofilms are not able to provide satisfactory growth conditions[9]. Therefore, some conventional antimicrobial materials were developed to prevent microbial adhesion or viability. Antibiotics, cytotoxic chemical composites, or metal particles were often contained in the material and gradually released into the microbial environment to disrupt the completion of the biofilm, leading to the inhibition of growth or death of microbes. For example, sulphonated poly (ether ether ketone) (SPEEK) significantly reduced the pH level of the surface environment, creating an acidic environment which reacted with the anionic membrane of the cells, remarkably inhibiting the growth of microbes[13].

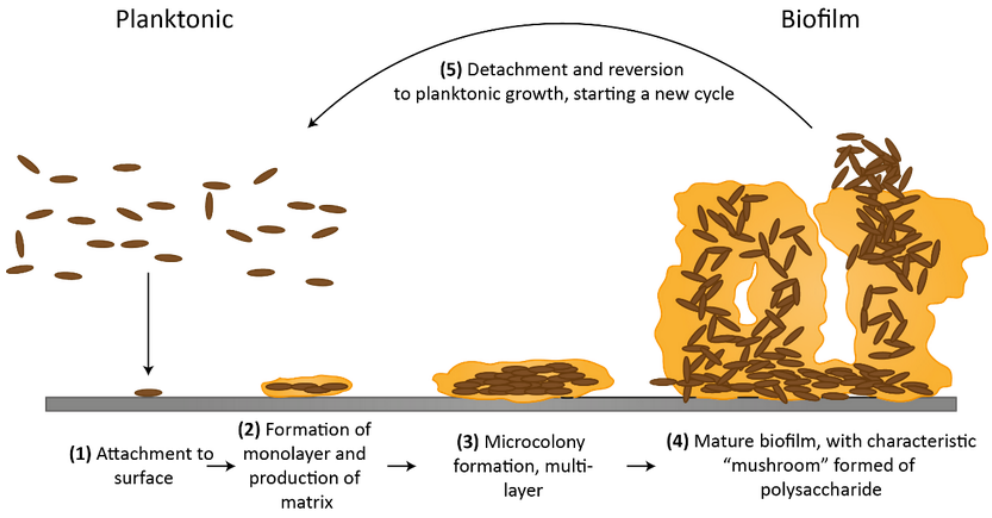

Figure 2. Forming process and structure of biofilms[14]. Reproduced from ref 14. Copyright held by original author.

Biofilms functionally provide resistance and protection to microbes. However, the rise of biocide resistance in microbes, specifically infectious pathogens, presents a challenge for the selection of antimicrobial agents and mechanisms, which requires alternatives to antimicrobial agents. Therefore, while preventing the spread of infections, exhibiting superior efficiency, minimizing toxicity, environmental problems and production costs are also current criteria for antimicrobial material development.

2.2 Mechanisms of antimicrobial activity

With the dramatic development of disinfecting polymers, the mechanisms of their antimicrobial activity have drawn great attention in the research field. Though some of the discovered polymeric structures' disinfecting mechanisms have not been fully understood, current work has divided them into two types: passive action-repelling and active action-killing (as shown in Fig. 3).

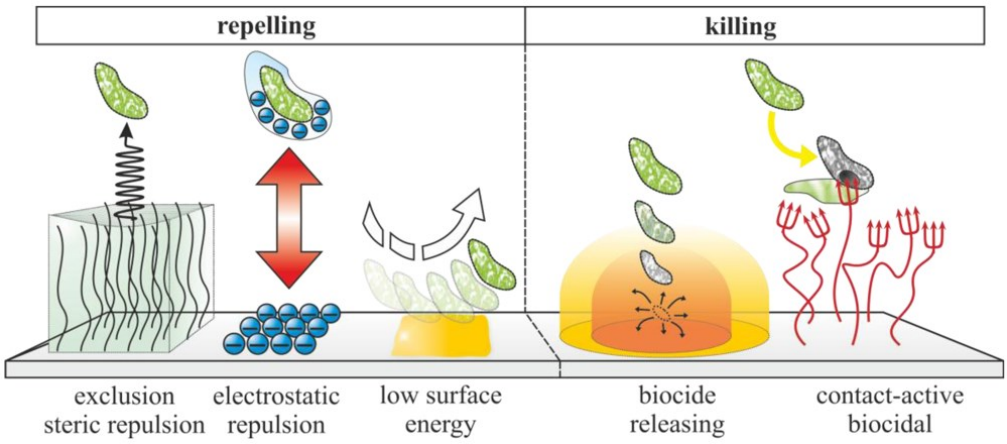

Figure 3. General categories on mechanisms of antimicrobial polymers[6]. Reproduced from ref 6. Copyright held by original authors.

2.2.1 Passive antimicrobial action

Due to the typical properties of microbial membrane of being hydrophobic and negatively charged, the surface of a polymer with passive antimicrobial action has a property, such as being hydrophilic, containing negative charges, or having a low surface free energy to prevent the adhesion from surroundings of planktonic microbes by reducing protein adsorption on it. Nevertheless, passive antimicrobial surfaces do not actively react with the microbial membrane or kill microbes, though repelling them[15,16]. Passive polymers are typically designed with one of 3 approaches, the first is a self-healing, slippery liquid-infused porous surface (SLIPS), most commonly this is made of microtextured poly(dimethyl siloxane). The second approach uses uncharged polymers, such as poly(2-methyl-2-oxazoline), polypeptoid, polypoly(n-vinyl-pyrrolidone), poly(ethylene glycol) (PEG), and poly(dimethyl acrylamide). Finally the third approach consists of zwitterionic polymers and charged polyampholytes, examples of these polymers include phosphobetaine, sulfobetaine, and phospholipid polymers[17,18]. PEG (Fig. 4), as the most generally used passive antimicrobial polymer, has been well studied and has shown relatively wide-range targets of pathogens, including *Staphylococcus aureus*, *Escherichia coli* and *Pseudomonas aeruginosa*. Also it has demonstrated remarkable antimicrobial effects and antifouling ability with the polymer brush system[19](Fig. 5). This behaviour is attributed to PEG's high chain mobility, large exclusion volume (Fig. 5), and steric hindrance effect of the highly hydrated layer[15] (as shown in Fig. 5) to prevent protein adsorption and bacterial adhesion[19].

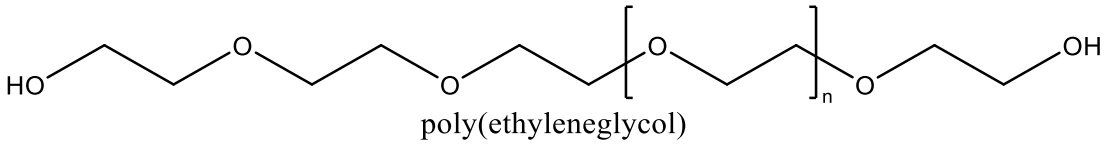

Figure 4. Chemical structure of poly(ethylene glycol) (PEG).

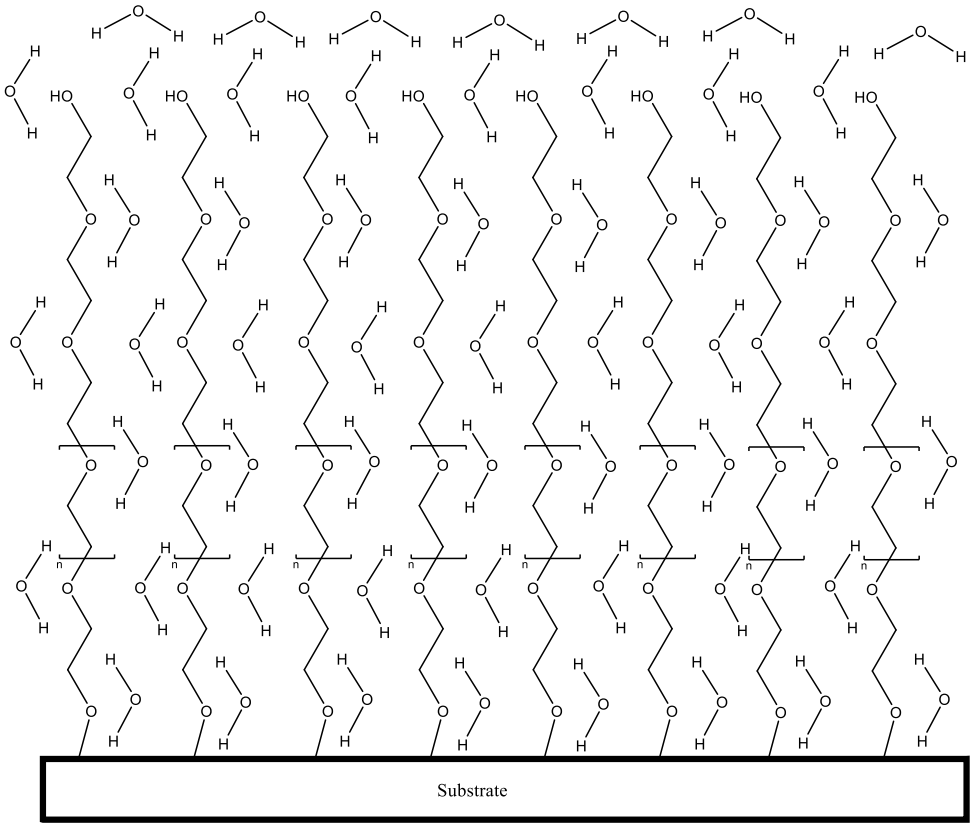

Figure 5. Polymer brush system of poly(ethylene glycol) (PEG).

2.2.2 Active antimicrobial action

Broadly speaking, active antimicrobial actions can be classified as either biostatic or biocidal as seen in Fig 6. Biostatic action refers to a surface that keeps the organisms in the stationary non-

reproducing phase. This contrasts with biocidal action, which actively kills microbes in addition to preventing growth. Of the two, biocidal activity is more desirable as it completely prevents the microbes from growing after leaving the surface by killing microbes on the surface. Depending on the situation, biostatic surfaces can be suitable for some applications such as coatings on certain medical instruments. An example of these coatings are plasma polymerized organic nitrites which can be produced from a variety of organic monomers containing at least 1 nitrite group, these coatings prevent colonization of bacteria on the coated surface[20].

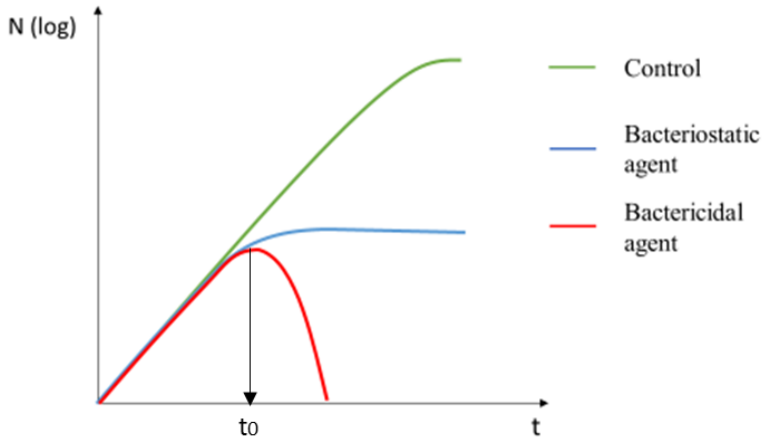

Figure 6. Effects of incorporation of bacteriostatic agent versus bactericidal agent at t_0 on the number of bacterial colony forming units.

Antimicrobial polymers act differently from the passive ones, as they actively interact with microbes and kill any which adhere from surroundings onto the polymer surface. Such polymers normally are functionalized with biocidal agents, which are basically summarized into three types:

antibiotics, positively-charged biocides, or antimicrobial peptides that are able to damage the integrity of the microbial cell leading to the death of microbes[21].

Differentiating from biocides directly destroying and killing the living organisms, another active antimicrobial approach is limiting the growth of organisms by a biostatic agent. For example, bacteriostatic agents are known being able to interfere with intracellular metabolism, such as protein production or DNA replication of bacteria in order to keep the growth of bacteria in a stationary phase (as shown in Fig. 6). However, bacteria can regain the ability of proliferation once the bacteriostatic agents are removed. Hence, with the applications of bacteriostatic antibiotics in clinical practice, the duration of treatment must be sufficient to allow the host defense mechanisms of the immune system to eradicate the bacteria[22]. Nevertheless, there is not an absolute distinction between bacteriostatic agents and bactericidal agents. Some bacteriostatic agents show bactericidal activity against susceptible bacteria at high concentration. Macrolides are categorized as one of the most general bacteriostatic antibiotics, whereas clarithromycin, erythromycin, and azithromycin have been observed exhibiting bactericidal property to *Streptococcus pneumoniae* and *Streptococcus pyogenes*[23–26]. Similarly, some bactericidal agents can merely be bacteriostatic at low concentration. Furthermore, one type of antibiotic exhibits differently to different bacteria. Chloramphenicol is generally considered to be bactericidal against *S. pneumoniae* but is bacteriostatic to *S. aureus* and group B Streptococci[27–30]; Linezolid is known as a bacteriostatic antibiotic to treat staphylococci and enterococci infections but it shows bactericidal property when treating infections by streptococci, including *S. pneumoniae*[31,32]. Quinupristin-dalfopristin typically has bactericidal activity to most strains of staphylococci and streptococci but bacteriostatic action against *Enterococcus faecium*[33,34].

The antimicrobial activities of polymers are based on their active biocidal agents. Antimicrobial polymers functionalized with positively-charged quaternary ammonium have been extensively studied and have been the most widely used. The positively-charged quaternary ammonium is a biocidal agent, which interacts with the microbial cell by the electrostatic interaction between the polymer and the cell membrane and damages the cytoplasmic membrane, the rupture of the membranes causes the leakage of intracellular components leading to the subsequent cell death[21]. In addition to positively-charged quaternary ammonium, other active antimicrobial polymers have been actively studied. Two examples of these compounds are polyguanidine, and N-halamine. Polyguanidine. As seen in Fig. 7 b), N-halamine inhibits or inactivates cells through the oxidative halogen present in the structure that attacks the amino or thio groups of cell receptors[35].

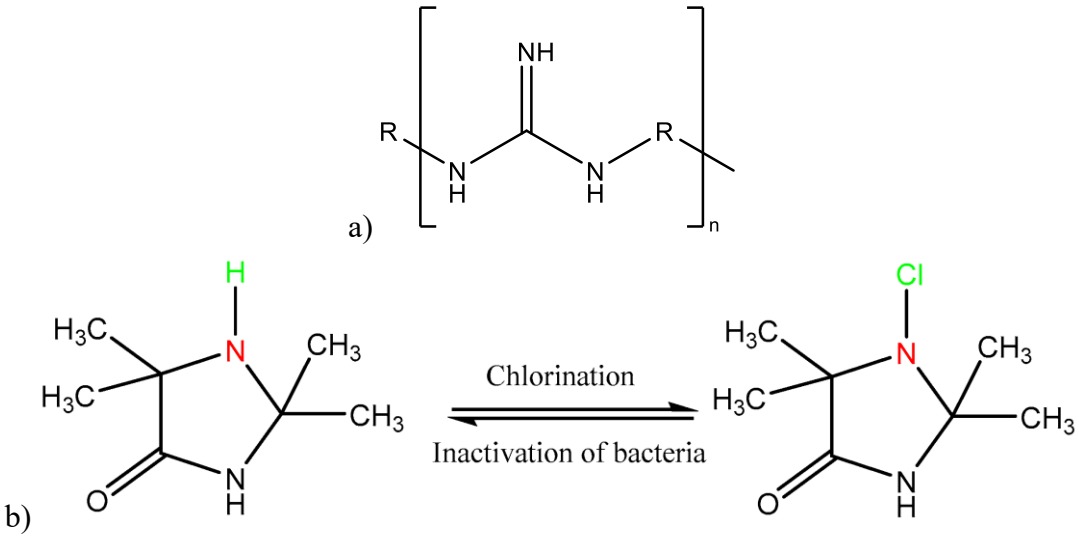

Figure 7. a) Chemicail structure of polyguanidine; b) Bacterial inactivation loop of N-halamine[36]. Reproduced from ref 36. Copyright held by original authors.

2.3 Antimicrobial polymers

Comprehensive studies have classified current antimicrobial polymers into three main types: polymeric biocides, biocidal polymers, and biocide-releasing polymers[6]. As they are shown in Fig. 8 a) polymeric biocides are formed by the interconnection of repeating active biocidal units[16,37,38], which is not necessarily required in Fig. 8 b) biocidal polymers. Due to this, the antimicrobial activity of biocidal polymers includes the whole macromolecule with the biocidal group embedded. Alternatively, Fig. 8 c) biocide releasing polymers normally are loaded with biocides and hence their biocidal activity is not performed due to the polymeric matrix. Instead, the matrix acts as a carrier of the biocidal agents and releases them to contact and attack the targeted organisms[39–42]. Additionally, these antimicrobial polymers can also be categorized into surface-bound polymers or solution-based polymers based on their working principles. Generally, biocidal polymers are surface-bound with antimicrobial action occurring by surface contact, whereas biocide-releasing polymers are solution-based, performing antimicrobial activity in solutions. Besides, polymeric biocides can be either surface-bond or solution-based. It is determined by the antimicrobial repeating groups they contain.

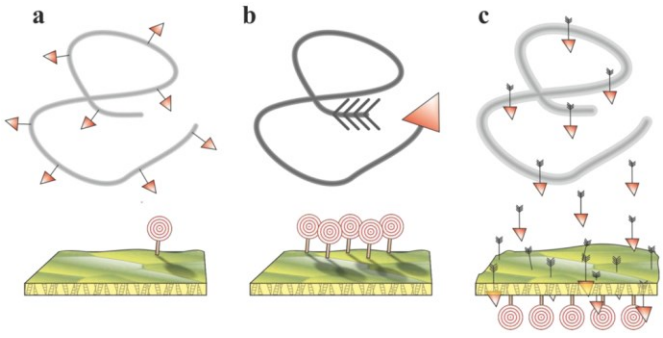

Figure 8. General classification of antimicrobial polymers: a) Polymeric biocides; b) biocidal polymers; c) Biocide releasing polymers[6]. Reproduced from ref 6. Copyright held by original authors.

2.3.1 Polymeric biocides

Polymeric biocides are polymers are composed of active repeating antimicrobial units such as amino, carboxyl, or hydroxyl groups, covalently link to each other[16,37,38] and the whole macromolecules act analogously to the monomers. Also included in this classification are polymers with side groups consisting of hydrophobic quaternary ammonium functional groups[43]. Compared to the active monomers, the antimicrobial effectiveness of the polymers should be lower due to the steric hindrance maintained by the polymer matrix. The polymerization of the 4-vinyl-N-benzylpyridinium chloride-antimicrobial molecules is a respective example. The crosslinking process leads to a water-insoluble polymer which has no active biocidal property but has biostatic activity[44]. Another example of the effect of different linkages on the efficacy can be seen with the antibiotics Penicillin V and Cephradine. The resulting polymer of Cephradine does not display antimicrobial activity when stably bonded to PEG-Lysine [Fig. 9 a)]. However when the Penicillin V is bonded by an ester linkage to PEG-Lysine, it still exhibits antimicrobial behavior because the linkage can be hydrolyzed to release free Penicillin V [45] [as shown in Fig. 9 b)]. This demonstrates that the bonding method for polymeric biocides plays a major role in their activity. This behavior must be considered when designing polymeric biocides as it seriously impacts the activity of the final material.

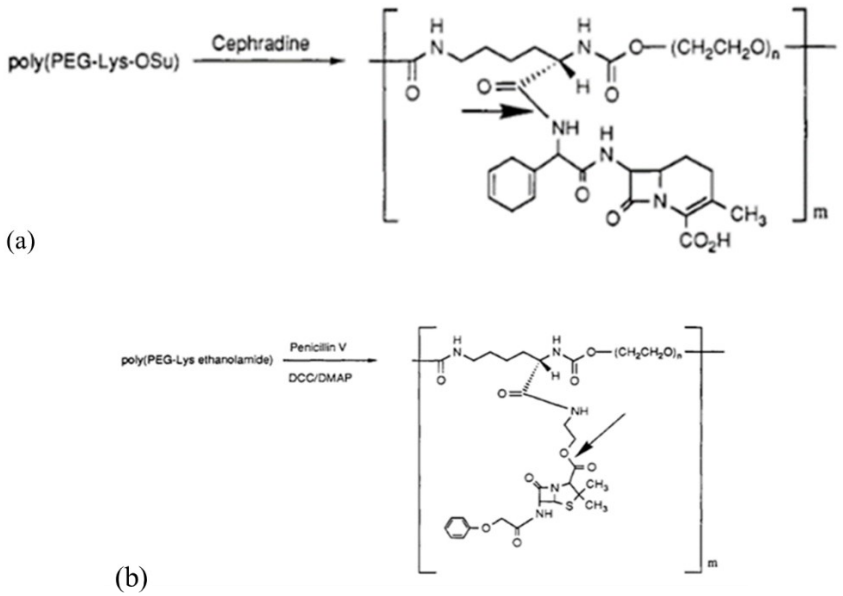

Figure 9. a) Cephradine is stably bonded to PEG-Lysine; b) Penicillin V is bonded by an ester linkage to PEG-Lysine[45]. Reprinted (adapted) with permission from ref 45. Copyright 1993 American Chemical Society.

Other examples of polymeric biocides synthesised recently includes the copolymerization of methacrylate modified Norfloxacin and PEG-methacrylates[46] and the copolymerization of modified Vancomycin and PEG-methacrylates[47]. Both these systems showed significant reduction in the efficacy of the biocidal units with activities up to 6-fold lower than unmodified antibiotics. This trend, while common, does not always hold true and penicillin functionalized polyacrylate nanoparticles showed increased efficacy when compared to unmodified biocides[48]. This indicates that the activity of these polymers is not determined by the monomer alone and another mechanism may be present.

2.3.2 Biocidal polymers

In contrast with polymeric biocides, biocidal polymers do not necessarily require repeat active antimicrobial units. Instead, the antimicrobial activity of such polymers is generally exhibited by the whole macromolecule. Studies on microbial cell membranes have shown that the surfaces of cell membranes of both Gram-positive bacteria and Gram-negative bacteria (see Fig. 10) are normally negatively charged, as the cytoplasmic membrane of Gram-positive bacteria consists of membrane proteins and teichoic acids as well as phospholipids providing negative charges to the surface of Gram-negative bacteria[49]. Hence, biocidal polymers containing antimicrobial polycations have drawn great attention with their ability to electrostatically interact and disrupt the microbial cell membrane, completing an antimicrobial action and leading to the ultimate death of microbes[50]. Such functional groups include tertiary sulfonium[51], phosphonium[52,53], quaternary ammonium[44], and guanidinium cation. While significant research has studied incorporating antimicrobial side groups on linear polymers, dendritic and hyperbranched polymers have also been studied for their antimicrobial properties. One commonly used example of these structures is quaternized hyperbranched PEI which displays strong antimicrobial properties[54]. Both commonly available as a water solution and a low cost n-alkylated material, quaternized polyethyleneimine nanoparticles have remarkable antimicrobial activity against both Gram-positive bacteria and Gram-negative bacteria based on the immobilized quaternary ammonium compound (QAC) embedded on the long polymeric chain and its hydrophobicity[55].

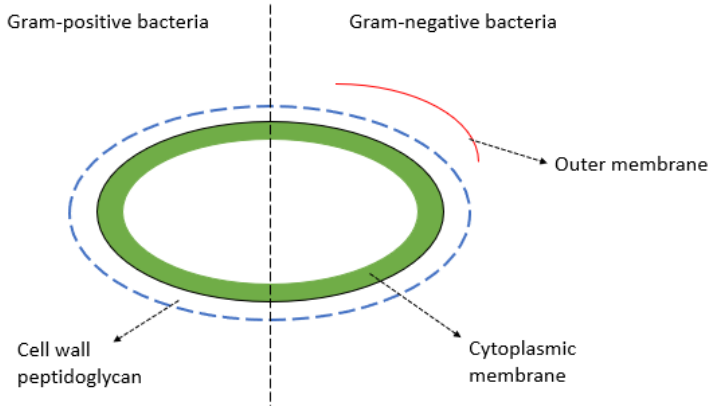

Figure 10. Cell wall and membrane structure of Gram-positive versus Gram-negative bacteria.

It is observed that if the polymer backbone is hydrophobic, bioactive repeating units are not required in this biocidal polymer. Furthermore, if the polymer backbone is hydrophilic, then this polymer needs hydrophobic side groups parallel to the backbone to form a hydrophobic surrounding area. The mechanism of antimicrobial peptides (AMP) has been discovered that follows the statement above. Examples include magainin and defensin[56–60]. These two peptides both contain highly stiff backbones, and there are side groups distributed in the way that one side of the backbones is hydrophobic and the other is positively charged (as shown in Fig. 11). Such a structure has a high effectiveness in antimicrobial activity by invading the microbial both outer and cytoplasmic membrane with the whole molecule and destroys the structural and functional integrity of the cell membrane, leading to the final death of the microbial cell[61,62].

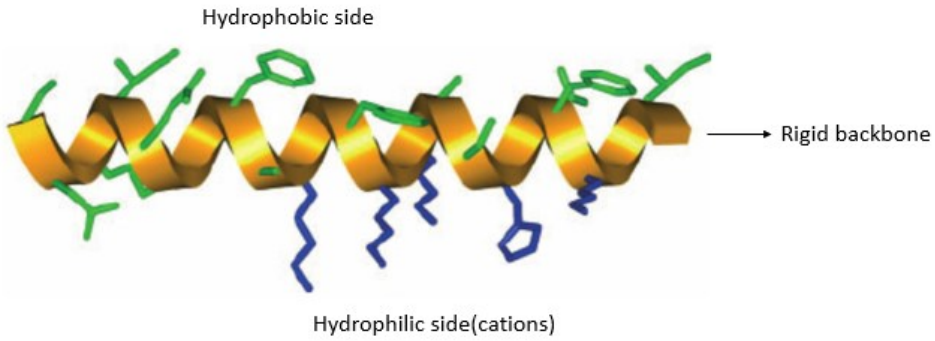

Figure 11. Structure of a rigid backbone, hydrophobic side and hydrophilic side with cations in magainin and defensin[63]. Reproduced with permission from ref 63. Copyright 2006 Microbiology Society.

Besides biocidal polymers with cationic groups being organized along the polymer backbone, polymers with only one antimicrobial end cap have also been found showing high antimicrobial efficiency. This type of biocidal polymer has mainly focused on the addition of a terminal endcap during ring-opening polymerization. Commonly a cationic surfactant is used for this purpose, and one example is the cation of 2-alkyl-1,3-oxazolines. By utilizing this technique, the polymer is only functionalized on one end with another group on the distal end. Within such a polymerization process, the introduction of specific different endcaps on either end of the polymers can be controlled and varied by utilizing the suitable initiator and terminator. From Waschinski et al. it can be seen that when the molecular weight of poly(2-methyl-1,3-oxazolines) (PMOx) and its ethyl-derivative (PEtOx) varied between 2k-10k g/mol there was no change in the efficacy of the antimicrobial endcap dimethyldodecylammonium bromide (DDA)[64]. Moreover, by changing the polymer backbone to polyethylene glycol (PEG), a 5 to 10 times reduction in antimicrobial activity was shown compared to the polyoxazolines. Furthermore, the antimicrobial efficiency could be tuned by the group distal to the biocide. This satellite group determines the molecule's

antimicrobial activity within 3 orders of magnitude[65]. It is hypothesized the behavior is caused by the amphipathic nature of the macromolecules. When in solution they can form unimolecular micelles, that on contact with microbial cells, unfold and deliver the antimicrobial group as shown in Fig. 12[65,66]. The satellite group plays an important role in this process as it determines the micelle formation and aids in the penetration of the biocide through the membrane.

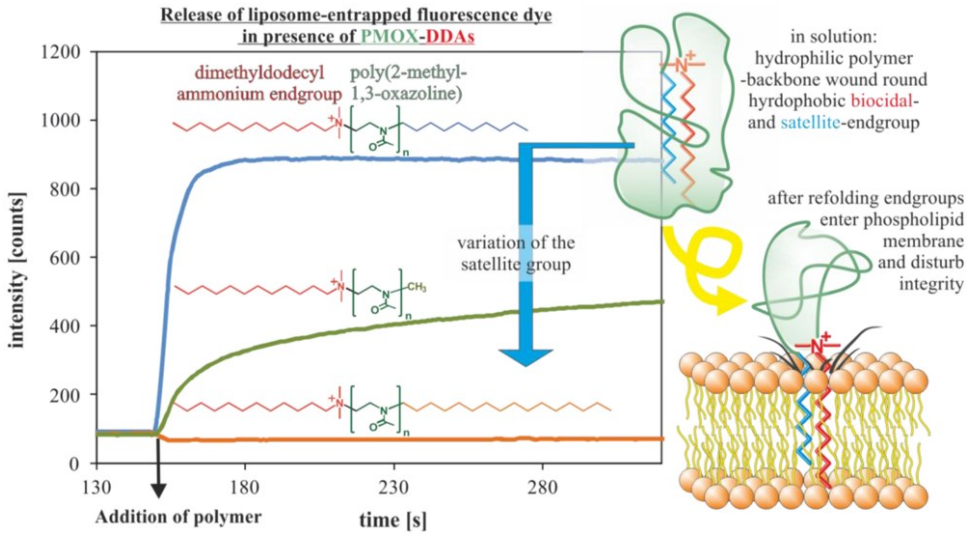

Figure 12. Release of liposome-entrapped fluorescence dye in presence of PMOx-DDAs[6]. Reproduced from ref 6. Copyright held by original authors.

2.3.3 Biocide-releasing polymers

Biocide-releasing polymers are generally composed of biocides and a polymer matrix as the carrier for the biocidal agents. The antimicrobial activity of such polymers is embodied by releasing the antimicrobial compounds. Extensive studies have achieved the development of biocide-releasing polymers through either bonding the antimicrobial molecules to polymer matrix by polymerization or compounding antimicrobial molecules with the polymer. These polymers have been frequently

utilized as carriers for antibiotics in clinical trials with their ability to maintain a high local concentration of biocides and deliver their biocides quickly and comparably close to the targets[39–42].

Rodriguez et al. designed a type of disinfecting cement with both sufficient antimicrobial efficiency and cement strength retention by incorporating chlorhexidine into acrylic bone cements. The system contains brushite as a calcium phosphate filler and chlorhexidine as the antimicrobial agent, which can release chlorhexidine cation to disrupt the microbial cell membrane[67]. Incorporation of brushite increased the porosity, enhancing the kinetics of chlorhexidine release from cements, leading to a higher antimicrobial effectiveness[68]. Alternatively, in other applications a similar delayed release can be achieved by modifying polymers with N-halamine groups attached to the backbone [69,70]. This class of functionalized polymers can release chlorine or hypochlorite into the solution. The active chlorine can then oxidize the phospholipids of the microbial cytoplasmic membrane, resulting in the death of microbes[71].

While significant research has focused on the release of organic antimicrobial agents from a polymer matrix, another active area of research utilizes the release of metal ions for antimicrobial purposes. The antimicrobial properties varied with the type of metal. Silver has been well studied as the most commonly used metallic antibacterial agent with its significant antibacterial effectiveness against both Gram-positive and Gram-negative bacteria. The studies of the antibacterial mechanism of silver ions have shown that the ions interact with multiple membrane proteins, resulting in the disruption of the membrane and eventually cell death[72]. Additionally, it was also found that silver ions are capable of disrupting the DNA replication cycle[73] and

interrupting the respiratory chain of bacteria[74,75] (as shown in Fig. 13). Lyutakov et al. has developed light-activated antimicrobial materials against both *Staphylococcus* and *Pseudomonas aeruginosa* by doping porphyrin and silver nanoparticles in polymethylmethacrylate. Under illumination, porphyrin absorbs light and produces reactive oxygen, affecting the release of silver ions[76].

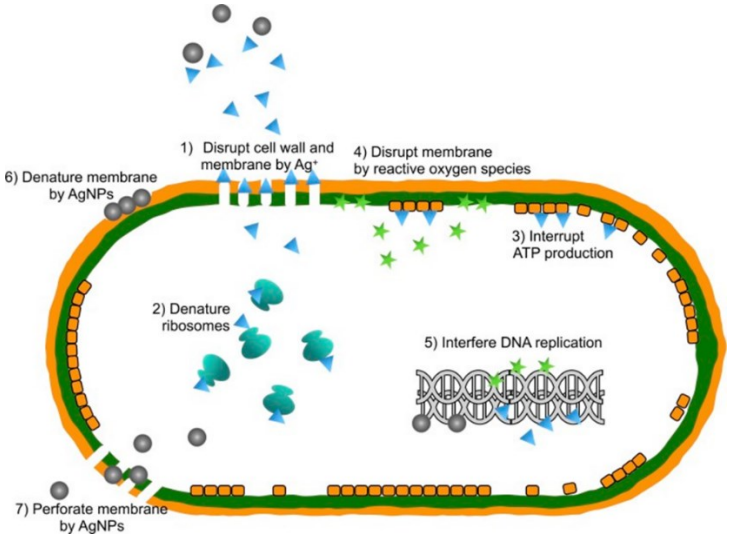

Figure 13. The antibacterial principles of silver ions (Ag+) and silver nanoparticles (AgNPs) [77]. Reproduced from ref 77. Copyright held by Dove Medical Press Limited

2.3.4 Contact-active antimicrobial polymers

Within the discussion of surface-bonded and solution-based antimicrobial polymers, the non-leaching polymeric biocides or biocidal polymers can obtain antimicrobial activity on the surface, disintegrating microbial cells' structure and killing them by contact. Despite claims of contact-killing surfaces, it is difficult to distinguish the mechanism from the biocide-releasing system just by general antimicrobial tests with indeterminacy of the bond between biocidal groups and

polymer matrix. In addition, if the concentration of the antimicrobial components is over the minimal inhibitory concentration (MIC) within 1 micrometer of the surface, the results indicate the possibility of contact-killing action. The most frequent and well-regarded method to prove this activity so far is by long-term leaching tests, constantly monitoring and comparing the antimicrobial performance of the concentrated washing solution with the polymer surface.

As one of the earliest hypotheses, the polymeric spacer effect was proposed in 2001 (see Fig. 14) which assumes that when bacterial cells adhere on the polymer surface, the grafted antimicrobial polymer could penetrate the cell wall and break up the phospholipid bilayer of cytoplasmic membrane killing the microbial cells. This mechanism was further proved in their study by the observation that N-hexylated poly(4-vinylpyridine) in solution showed no antibacterial effect on *Pseudomonas aeruginosa* which was one of the targets of the surface modified with N-hexylated poly(4-vinylpyridine)[78]. Another strong evidence of the polymeric spacer effect was shown by grafted quarternized polyethyleneimine with a dependency of antimicrobial efficiency on its molecular weight[79].

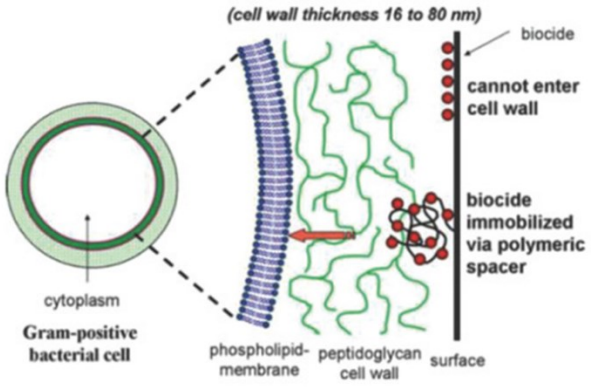

Figure 14. The hypothesis of polymeric spacer effect on contact-active antibacterial activity[80]. Reproduced from ref 80. Copyright 2018 John Wiley and Sons.

The second possible mechanism of contact-killing, a phospholipid sponge effect, was proposed in 2011, claiming that surfaces that are not biocidal groups grafted on polymeric spacers performed their antimicrobial activity through removal of negatively charged phospholipids from cell membranes (see Fig. 15). Bieser and Tiller have studied a variety of cellulose-derivative surfaces modified with different quaternary ammonium compounds and additional hydrophobic groups. The conclusion was made that the antibacterial action of such surfaces against *S. aureus* was mostly determined by the cationic/hydrophobic balance rather than by their charge density[81]. Also, by treating with negatively charged phospholipids, the antibacterial performance of all investigated surfaces was inhibited[82]. Both results supported the phospholipid sponge effect. While validity of this hypothesis has been approved by some studies, the way water-insoluble phospholipids approach the antimicrobial surface through the cell wall has not been clear.

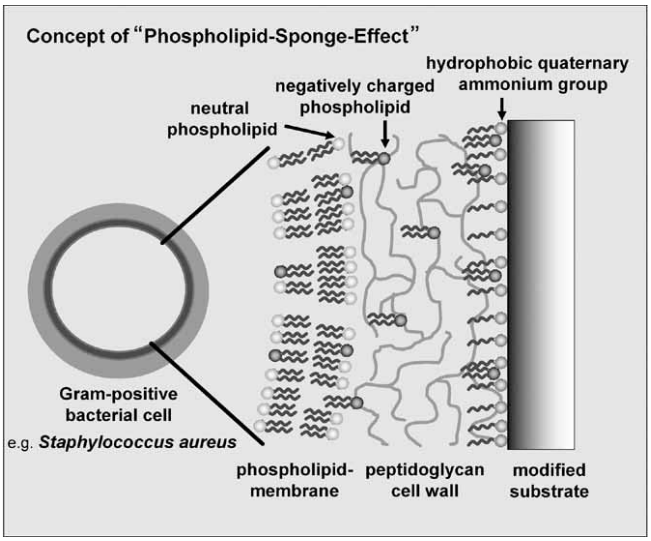

Figure 15. The hypothesis of phospholipid sponge effect for bacterial contact-killing mechanism[81]. Reproduced from ref 81. Copyright 2011 John Wiley and Sons.

2.3.5 Multifunctional antimicrobial surfaces

With only one of the three mechanisms being discussed above – repelling, biocide-releasing and contact-active activities, antimicrobial polymers can not always work sufficiently for practical applications as each of them has its respective inherent defects[2]. Therefore, multifunctional antimicrobial surfaces have been developed to be more effective and practical in application.

Surface modification on both biocide-releasing and contact-active polymers can repel the adhering microbe corpses killed by antimicrobial functional groups, providing a self-cleaning property to the resulting polymers. This technique specifically increases the effectiveness and longevity of water-soluble or hydrophilic antimicrobial polymers. For example, the antifouling paint frequently used on ship's hulls is a hydrophobic coating of copper-based acrylate copolymers[83]. While releasing biocidal copper ions, the movement of the ship can shear the swollen layer with contamination off the hydrophobic coating, revealing self polishing[84]. Examples of combination repelling and contact-killing properties include the surface developed by Laloyaux et al., comprising surface attached magainin grafted with oligo(ethylene glycol) methacrylate. The contact-killing action of this surface is activated at room temperature with the polymer brushes stretched. It switches to repel microbes when the PEG brush structures collapse by increasing the temperature to over 35°C (Tcoll)[85] (Fig. 16).

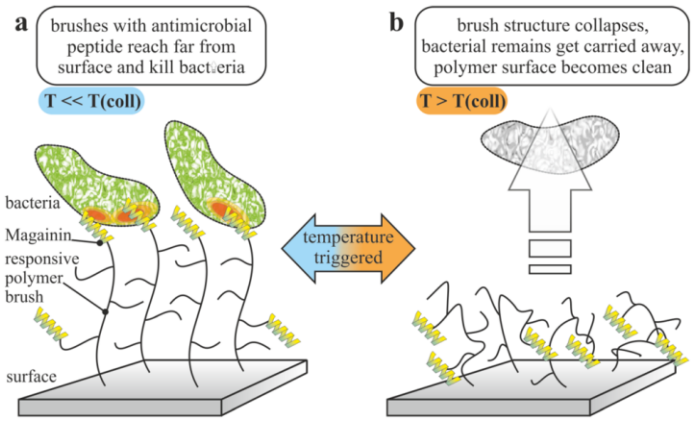

Figure 16. Antibacterial surface combines thermo-responsive repelling [T above the collapse temperature (Tcoll)] and contact-killing properties (T below Tcoll) [6]. Reproduced from ref 6. Copyright held by original authors.

The combination of biocide-releasing and contact-active approaches has been demonstrated to increase the antimicrobial efficiency and lifetime of antimicrobial activity of the entire system. Liang et al. combined *N*-halamine siloxane with quaternary ammonium salt siloxane to form a composite polyurethane coating. It was found that the coating displayed lasting antimicrobial activity due to the addition of the quaternary ammonium compounds. These contact killing QACs continued to provide antimicrobial action after the hypochlorite release system ceased to function, giving the coating long term functionality[86]. A similar behaviour could be achieved by the coating approach Li et al. developed based on a layer-by-layer assembled antibacterial coating with immobilized quaternary ammonium salts and releasable silver ions on a polystyrene surface (as seen in Fig. 17). The antimicrobial efficiency of silver ion-releasing was accompanied by the contact-killing activity from the layer of quaternary ammonium compounds[87].

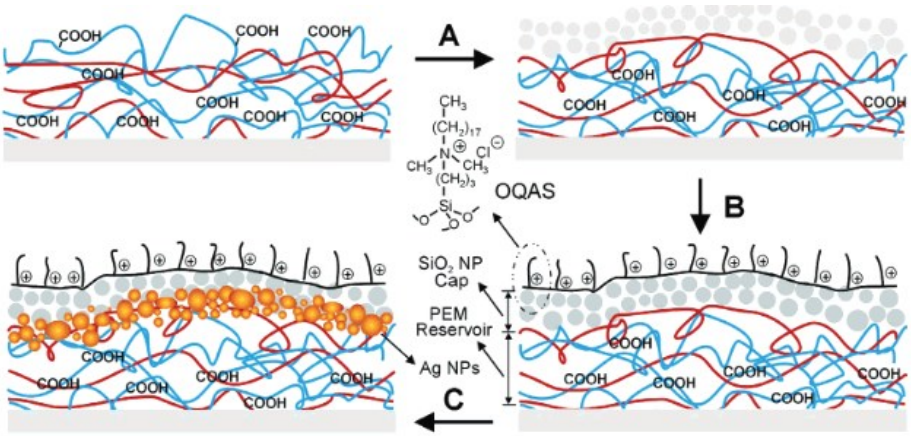

Figure 17. Layer-by-layer assembled antibacterial surface comprising both contact-killing and release-killing antibacterial properties[87]. Reproduced (adapted) with permission from ref 87. Copyright 2006 American Chemical Society.

2.4 Polyethyleneimine (PEI)

Polyethyleneimine (PEI), also called polyaziridine is known as a polymeric molecule comprising repeating amine units and ethylene spacers. Generally, linear-formed and branch-formed PEI have been classified by their structural architectures. All amine units in linear PEI (LPEI) are secondary amino groups (the primary amino groups at the ends are neglected since there are only 2 of them), but branched PEI (BPEI) is composed of primary, secondary, and tertiary amino groups [as shown in Fig. 18 a)] with a ratio of 1:2:1[88]. As shown in Fig. 19 a), the general synthesis of LPEI is achieved through hydrolysis of poly(2-ethyl-2-oxazoline)[89], while BPEI is available via the open-ring polymerization of aziridine[90][see Fig. 19 b)]. LPEI and BPEI (see Fig. 20) have fundamental differences in properties as independent of molecular weight. For example, BPEI is a liquid at room temperature while LPEI is a solid with a melting point around 73–75 °C[91]. In addition, the solid LPEI is insoluble in cold water, acetone, benzene and ethyl ether but soluble in hot water at low pH and ethanol, chloroform, methanol[92].

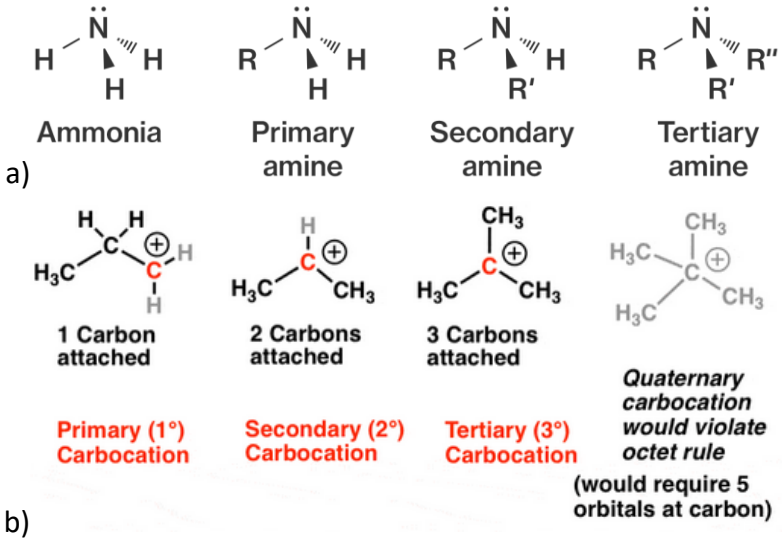

Figure 18. a) Scheme of ammonia, primary amine, secondary amine and tertiary amine[93] Reproduced with permission from ref 93. Copyright 2021 Course Hero Inc.; b) Schemes of primary, secondary, tertiary and quaternary ammonium cations[94]. Reproduced with permission from ref 94. Copyright 2021 Master Organic Chemistry.

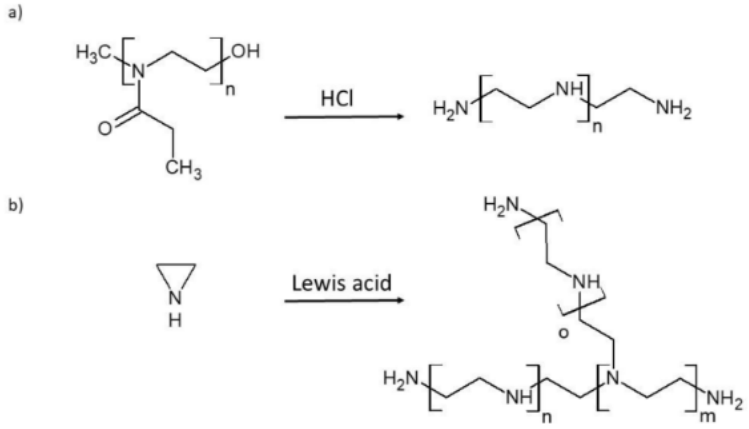

Figure 19. General synthesis approaches of (a) linear polyethyleneimine (LPEI), (b) branched polyethyleneimine (BPEI) [79]. Reproduced from ref 79. Copyright held by original authors.

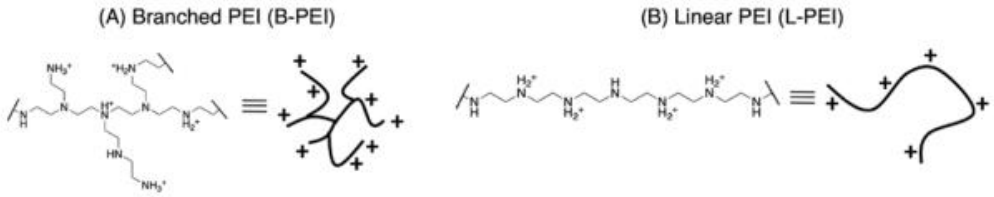

Figure 20. Cationic amphiphilic structures of (A) Branched PEI (BPEI) and (B) Linear PEI (LPEI) [95]. Reproduced from ref 94. Copyright 2012 John Wiley and Sons.

2.4.1 Polyethyleneimine (PEI) and quaternized PEI (QA-PEI)

With the amino groups, PEI can be quaternized to obtain quaternized PEI (QA-PEI) consisting of quaternary nitrogen cations[88]. As a polycation with quaternary ammonium compounds (QACs), QA-PEI is known to have remarkable antimicrobial activity against a broad spectrum of organisms[95–99] with selective cytotoxicity only towards pathogens but not mammalian cells[100–103]. QACs are salts of quaternary ammonium cations (quats). As seen in Fig. 18 b), the structure of quats is NR_4^+ with four alkyl groups or aryl groups[104]. Additionally, QACs permanently contain their positive charges, whereas the charges in primary, secondary, and tertiary ammonium cations are dependent on their solution pH. The antibacterial mechanism of mobilized QA-PEI molecules includes disrupting the lipid bilayers of the cytoplasmic membrane and additionally the outer-membrane of Gram-negative bacteria through the electrolyte attraction between positively charged ammonium groups with the negatively charged bacterial surface and the replacement of divalent cations, calcium ions (Ca^{2+}) and magnesium ions (Mg^{2+}) from the cytoplasmic membrane[105]. Further damage of the cytoplasmic membrane occurs when the hydrophobic alkyl chain interdigitates into the hydrophobic bacterial membrane leading to the loss of the proton motive force, leakage of intracellular fluid and ultimate death of the bacterial cell[106–108]. In addition,

compared to the QA-LPEI, the primary amino groups in QA-BPEI provide stronger tensile strength and the formed three-dimensional network of QA-BPEI while tethering onto polymeric matrix has been reported to exhibit contact-active antimicrobial activity through the polymeric spacer effect[6] in addition to the biocide-release antimicrobial action. Thus, to approach the same killing efficiency, lower concentration of QA-PEI is required in the entire polymeric macromolecule, resulting in less release of the QACs in environment, minimizing the potential impacts of QACs to aquatic systems and microbial drug-resistant mutation[98].

2.4.2 Factors impact the antimicrobial activity of PEI

Polyethyleneimine (PEI) as an antimicrobial polycation has been stated with advantages of being non-volatile and being long-term antimicrobial comparing to small-molecule antimicrobial agents. The higher chemical stability reduces the possibility of antimicrobial agents permeating through human skin, risking human health consequently[109–111]. Owing to these advantages of polycations, the factors that impact their antimicrobial effect have also been specifically focused on in relevant studies. Antimicrobial polycations are antimicrobial cationic polymers. Cationic groups and hydrophobic groups are the two essential functional components in these polymers. Generally, the antimicrobial activity of polycations starts with electrostatic adsorption between the cationic groups and microbial membrane. Then it follows with an insertion of the microbial membrane by the hydrophobic groups, leading to the disruption of the membrane and death of the microbial cells.

PEI derives its antimicrobial activity from the primary, secondary and tertiary amine groups within its chain. With protonation of the respective amines, the primary, secondary and tertiary

ammonium groups can become cationic. These cationic ammonium groups are commonly used to make antimicrobial polycations. Note that studies have shown that when compared to antimicrobial cationic polymer with quaternary ammonium compounds (QACs), antimicrobial polycations containing primary, secondary, or tertiary ammino groups display significant antimicrobial potency while still showing lower hemolytic activity than QACs. Additionally, when incorporated into a copolymer, polycations with primary and tertiary amine groups (see Fig. 21) can be used to tune the bactericidal activity while minimizing the risk of hemolysis. Of the different amine groups present in the copolymers, it was found that primary amino groups displayed the best biocidal performance compared to other amino groups while also being highly selective with negligeable damage to red blood cells at physiologically relevant concentrations[112].

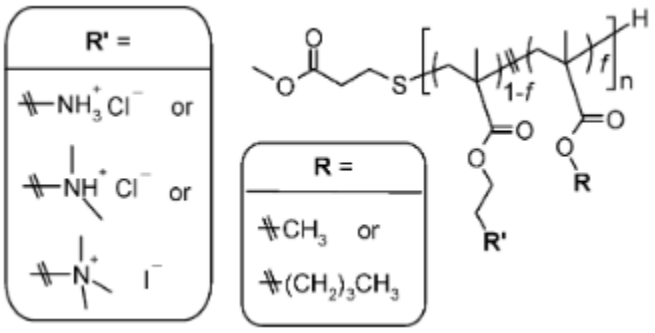

Figure 21. Design scheme of polymethacrylate with different cationic ammonium groups[112]. Reprinted (adapted) with permission from ref 112. Copyright 2009 American Chemical Society.

Other than the cationic groups, the length of the hydrophobic alkyl chains also impacts the antimicrobial effectiveness of antimicrobial polycations. For instance, n-Alkyltrimethylammonium bromides (CnTAB) have been synthesized with a series of n-alkyl chain lengths (C_5 - C_{22}) by Gilbert et al. to study the effect of the n-alkyl chain lengths on antibacterial

performance. The results have shown a disproportional increase in inhibitory performance up to 2-3 orders of magnitude of CnTAB when the n-alkyl chain lengths increased from C_{10} to C_{12}. A hypothesis was proposed that the antimicrobial mechanism might differ with a long alkyl chain from with a short alkyl chain due to the presence of 2 distinct binding sites with each having an affinity for either the long or short alkyl chains[113]. The other possibility is the formation of dimers or aggregates of the longer alkyl chains below the critical micelle concentration that then interact with the microbial cell membrane, while this phenomenon does not occur in short alkyl chains due to their proximity to the quaternized nitrogen[114]. The correlation of the substituted alkyl chain length and antibacterial activity has also been reported by the investigation of dental resin comprising a group of quaternary ammonium methacrylate monomers (QAM) with lengths from C10 to C18 of the substituted alkyl chain. It was found that the copolymer with longer alkyl chain of QAM displayed a higher antibacterial effectiveness. QAM with a longer alkyl chain (n=16 and n=18) showed optimal inhibition on both newly-formed biofilm and mature biofilm, while QAM with alkyl chain of 11 carbons and 12 carbons could only inhibit newly-formed biofilm, and neither of these biofilms were sensitive to the QAM containing 10 carbons[115].

2.4.3 Antivirus activities of QA-PEI and PEI

As discussed above, quaternized PEI has many potential antimicrobial applications as a hydrophobic QACs polycation, and it is also additionally applied as an antiviral agent inhibiting enveloped viruses, such as hepatitis B virus (HBV), hepatitis C virus (HCV), human immunodeficiency virus (HIV), and influenza viruses. Also disinfectants containing QACs have been recommended to be employed to inactivate SARS-CoV-2 (COVID-19) virus by U.S. Environmental Protection Agency (EPA)[116]. Haldar et al. have tested glass slides coated with linear

or branched N, N-dodecyl methyl-polyethyleneimines (PEIs) and the results showed a 100% inactivation efficiency of those hydrophobic PEI derivatives against influenza virus (minimal reduction was up to 4 orders of magnitude in the viral titer within minutes)[117]. Notably the reason that QACs are effective against these viruses is that enveloped viruses have a similar membrane structure to that of bacterial cells, constituting bilayers of phospholipid due to their infection and replication approaches[118] (as shown in Fig. 22).

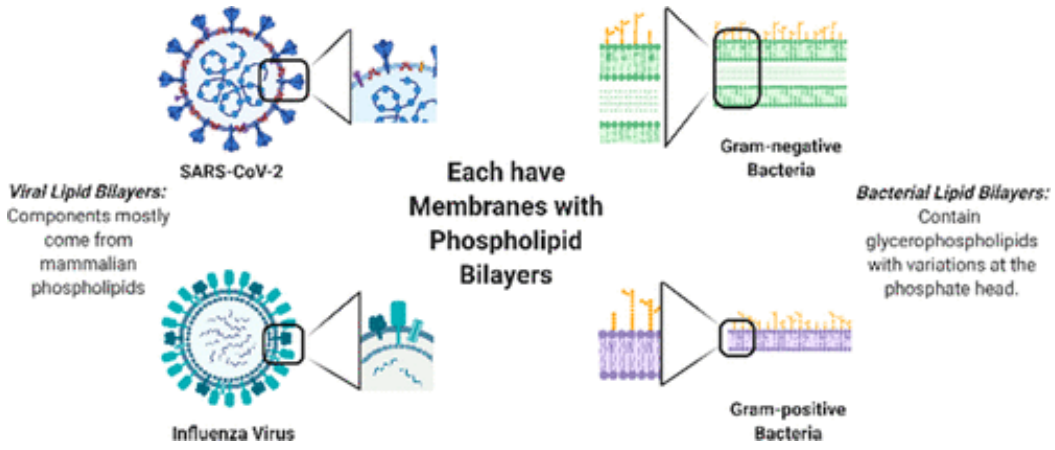

Figure 22. Comparing the membrane structure of viral envelopes of SARA-CoV-2 and influenza virus to bacterial membranes[118]. Reprinted (adapted) with permission from ref 118. Copyright 2020 American Chemical Society.

Schrank et al. have reviewed and summarized a series of QACs against different coronaviruses (enveloped) as seen in Table 1[118]. It was found that the QACs had significant differences in their efficacy against different coronaviruses with no QAC providing comprehensive sterilization against all members of the Coronaviridae family. While the QACs did provide some killing efficacy, many were unable to significantly damage the cell monolayer alone. For example while BAC at 1% w/v reduced the replication of SARS-CoV after 5 min exposure, it was unable to

eradicate traces of the SARS-CoV RNA on the surface after 3 min of exposure[119]. In addition to the antiviral activity of QACs against enveloped viruses, Tuladhar et al. have also tested and reported no virucidal effect of QACs on poliovirus[120].

Table 1. Summary of QACs inactivate different coronaviruses (enveloped) [118]. Reprinted (adapted) with permission from ref 118. Copyright 2020 American Chemical Society.

QAC	conc. (% w/v)	type of assay	virus tested	exposure time	quantified viral load reduction (log_{10})	effective viral load reduction (>99.9%)? (Y/N)
BAC	0.04	QCT	HCoV	1 min	3.0	N
BAC, HCl	0.04 (pH 1.0)	QCT	HCoV	1 min	>3.0	Y
BAC, EtOH	0.04, 70	QCT	HCoV	1 min	>3.0	Y
BAC	0.2	suspension	HCoV	10 min	0.0	N
BAC	1	suspension	SARS-CoV	5−30 min	reduced growth; RNA still detectable by RT-PCR	Y
Mikrobac Forte (BAC)	0.5	suspension	SARS-CoV	30, 60 min	≥6.13	Y
Kohrsolin FF (BAC)	0.5	suspension	SARS-CoV	30, 60 min	≥3.75	Y
BAC	0.01	suspension	TGEV	5 min	≥3.0	Y
CG	0.008	QCT	HCoV 229E	5 min	<3.0	N
CG, EtOH	0.008, 70	QCT	HCoV229E	5 min	≥3.0	Y
mix of BAC/CG	0.066	QCT	HCoV 229E	10 min	4.0	Y
DDAC	0.0025	suspension	CCoV	3 d	>4.0	Y
BAC	0.00175	suspension	CCoV	3 d	3.0	N
BAC, EtOH	0.1, 79	suspension	MHV	30 s	≥3.0	Y

However, branched PEI without quaternization does not contain QACs. Studies have been performed on overall protonation level of high MW PEI (1616k D) and it was found that the PEI acts as a proton sponge with protonation highly dependant on the solution pH. When the pH of the solution was 7 the overall protonation of the PEI was found to be 20% compared to 45% at a pH of 5. Due to this, in a neutral solution PEI with positive charges is more likely to act as a vector of gene delivery rather than antiviral agent. It can potentially prevent DNA degradation with its lysosomal buffering capacity[121–123].

Chapter 3. Antibacterial activity of PU/PEI based on release-killing and contact-killing mechanisms

3.1 Synthesis of polyethylenimine/polyurethane (PU/PEI) colloidal film

Polyurethane systems are polymers containing multiple urethane units in the molecular backbone. These urethane groups are generally obtained from bonding of alcohol group (–OH) and isocyanate (NCO) (see Fig. 23) with additional activation from either catalysts or ultraviolet light. Waterborne PUs (WPUs) are known as environmentally friendly materials, differing from other general types of polyurethane that normally consist of a large portion of volatile organic compounds (VOCs)[124,125].

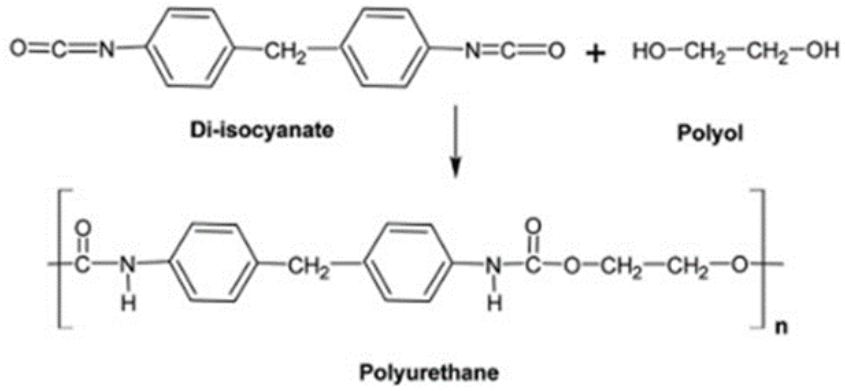

Figure 23. General synthesis approach of polyurethane[126]. Reproduced from ref 126. Copyright 2016 Royal Society of Chemistry

Polyurethanes have been widely used in a variety of applications due to its excellent mechanical properties, such as high tensile strength, resistance of abrasion and tear propagation. Such excellent

mechanical properties are offered by the alternate linkages of hard segments and soft segments in the polymer. The immobile hard segments constitute isocyanate and chain extenders, whereas the mobile soft segments are composed of polyols[126].

In this project, the resulting PU/PEI elastomeric networks containing three types of dynamic non-covalent interactions. As shown in Figure. 24, hydrogen bonds, ionic bonds and polymer entanglement interactions are all included. Note the PEI is a branched polyethyleneimine containing primary, secondary and ternary amino group but there is no quaternary amino group as incorrectly indicated by the schematic. During the coating procedure the water in the emulsion slowly evaporates at room temperature causing the PU micelles to slowly approach each other and entangle together. These actions are main factors for the resulting PU film to reach a high mechanical strength. Furthermore, both hydrogen bonds and ionic bonds improve the mechanical properties of the whole PU/PEI system because both hydrogen and ionic bonds can be simply broken then rebuilt, when the elastomeric PU/PEI film is stretched, the breaking and rebuilding process of these bonds can dissipate energy at high stress areas. This allows for relaxation of the polymer chains and maintains the mechanical integrity of the network. Hydrogen bonds exist between urethane groups and urea groups, and PEI groups are incorporated into PU colloidal system through additional ionic bonds. However, when the amount of PEI incorporated into the PU colloidal system is too high, an over-crosslinked PU/PEI network can be formed from the high ion concentration. This over-crosslinked network tends to inhibit the polymer entanglement of PU matrix and results in a reduction of mechanical properties. Hence the number of ionic bonds referring to the concentration of PEI is critical to the overall PU/PEI network[3,4].

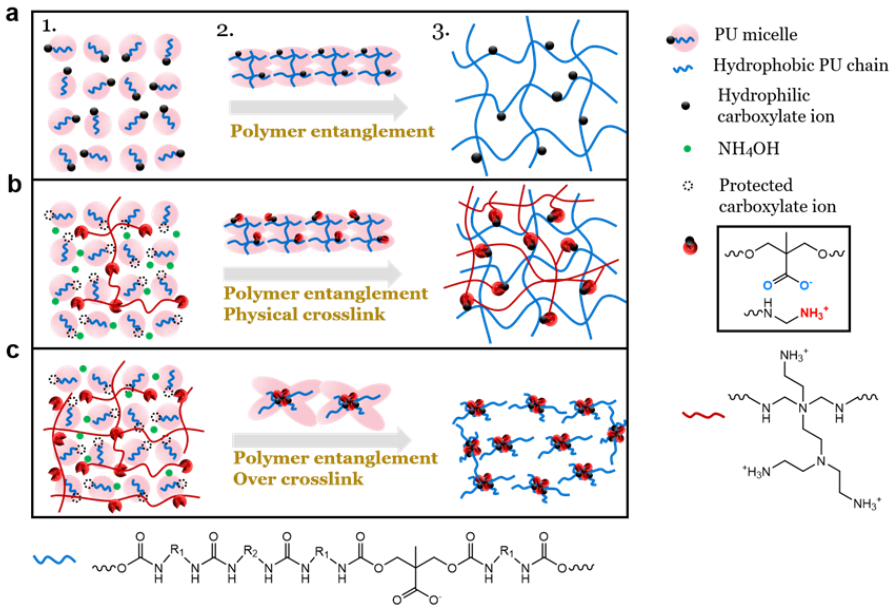

Figure 24. Crosslinked network in PU and PU/PEI colloidal film[4]. Reproduced from ref 4. Copyright 2020 Royal Society of Chemistry.

3.1.1 Materials and instruments

3.1.1.1 Materials

All chemicals used were of analytical reagent grade unless otherwise stated. The following chemicals were purchased from Sigma Aldrich. Isophorone diisocyanate (IPDI); polypropylene glycol-2000 (PPG-2000); dimethylolpropanic acid (DMPA); Ethylenediamine (EDA); Triethylamine (TEA); branched polyethyleneimine (PEI) (average Mw ~25000); Acetone(Plc); Ammonium hydroxide, ACS reagent (28-30% solution) was purchased from ACROS Organics.

3.1.1.2 Instruments

A mechanical stirrer and vacuum oven were used in the synthesis of the waterborne polyurethane dispersions. A Thinky Planetary mixer and environment chamber were applied in the process of coating PU and PU/PEI colloidal films. The compounds of the polymer films were tested by Fourier-transform infrared spectroscopy (FTIR) to confirm that the PU/PEI composites were successfully synthesized. Universal Macro-Tribometer (UMT) (T1377, Centre for Tribology Inc.) was used for testing the tensile strength of different ratios of PU/PEI polymer films. The cation concentration of the water solution used to soak the polymer films was measured by a conductivity meter . The morphology changes of PU/PEI film after treatment with DI water, PBS buffer and UV Ozone PSDP-UVT (benchtop UV cleaner from Novascan) for 1 h were observed by Scanning Electron microscopy (SEM).

3.1.2 Synthesis of PU emulsions

To synthesize the PU emulsion (see Fig. 25), PPG-2000 (50 g) and DMPA (3.4 g) were dried at 110^{o}C under nitrogen before they were mixed with IPDI (16 mL) in a 250 mL three-necked flask. The flask was set up on a hot plate with a mechanical stirrer, thermometer and nitrogen inlet. The reaction mixture was kept at 110^{o}C for about 5 h, the mixture was cooled down to 40^{o}C after. Then 38 mL reagent acetone was added into the reaction while stirring. Meanwhile, a 110 mL acetone solution mixed with 5.35 mL EDA and 13.95 mL TEA was prepared then this mixed solution was dropped into the reaction to adjust the viscosity of the prepolymers with high shear rate agitation throughout the dispersion process. The viscosity is dependent on the rate of the above-mentioned acetone solution being added to the PU prepolymer. When the rate of addition is too high, the PU

prepolymer could significantly increase in viscosity and climb up the mechanical stirrer. If this occurred, the addition rate of the acetone solution was reduced, along with the addition of 1 mL of DI water if needed. During the process of adding the mixture of EDA and TEA, the formation of the PU emulsion can be observed by the change of solution from translucent to opaque, resulting in a creamy white emulsion. Acetone was removed in a vacuum oven with no heat under low vacuum for 20 minutes from these PU dispersions and consequently the final PU dispersions had 30% solids content[3].

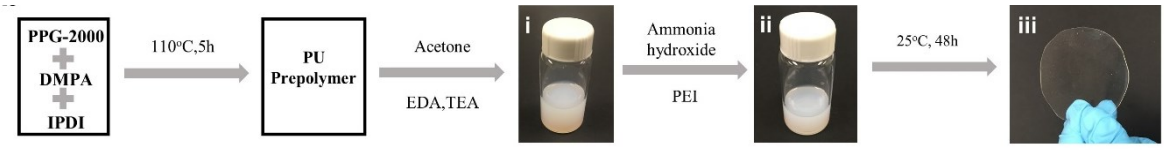

Figure 25. Synthesis process of waterborne polyurethane[3]. Reproduced from ref 3. Copyright 2020 University of Waterloo.

3.1.3 Coating PU/PEI films

PEI (10 g) was dissolved in 90 mL deionized water to get a solution of 10wt% concentration. Before mixing this PEI solution with PU dispersions, 1 mL 30wt% ammonium hydroxide solution (28-30%) was added to prevent the PU/PEI colloidal solution from aggregating. Six different concentrations of PU/PEI colloidal solution were prepared as such PU, PU/2wt% PEI, PU/5wt% PEI, PU/10wt% PEI, PU/15wt% PEI, PU/20wt% PEI. The measurement of the water content of PU emulsion was determined to be 70wt%. For each sample in petri dish (60 mm diameters), 2.5 grams of PU emulsion was added, the weight of polyurethane in this emulsion was 30wt% of the

PU emulsion, which means there is 0.75 grams of polyurethane in each sample. The weight of PEI introduced for each concentration is following the equation below:

$$x\ wt\%\ PEI = \frac{Weight\ of\ PEI}{Weight\ of\ PEI + 0.75\ grams}$$

For example, to prepare the PU/2wt% PEI, 0.155 mL of 10wt% PEI water solution was added to 2.5 mL of 30wt% PU emulsion that was previously mixed with 1mL 30wt% ammonium hydroxide.

$$2\ wt\%\ PEI = \frac{0.155\ mL(volume\ of\ PEI\ solution) * \frac{0.1g}{mL}(concentration\ of\ PEI\ solution)}{\left(0.155\ mL * \frac{0.1g}{mL}\right) + 0.75g(weight\ of\ PU\ in\ 2.5\ mL\ PU\ emulsion)}$$

$$2\ wt\%\ PEI = \frac{0.0155g}{0.7655g}$$

Each solution was intensely mixed at 2000 rpm with 5 min mixing and 2 min defoaming at 2200 rpm in the Thinky Planetary mixer to avoid the appearance of bubbles during coating. The PU and PU/PEI film samples were made by evaporating the well-mixed solution at room temperature (20°C) with 50% humidity in petri dishes in the environment chamber.

3.1.4 Results and discussion

With concentrations lower than 15wt% of PEI, the PU/PEI films formed completely in the petri dish during the coating process. PU film with 15wt% PEI started to partially show cracks on the surface due to the internal stresses that form during unidirectional drying. As the top layer fully

dried the shrinking of the material underneath pulled it apart. This can be mitigated through controlled drying. Due to this phenomenon the samples were dried in a humidity chamber at 20°C and 50% humidity. By increasing the humidity, the drying rate was reduced, and the top layer remained more ductile. This technique reduced the likelihood of lower wt% PEI films cracking during drying and minimized the cracking seen in the 15wt% PEI samples [see Fig. 26 e)] with cracks only occurring on the exterior edge where the thickness increased due to the meniscus. It was hypothesized that the increased content of PEI increases the crosslinking seen in the PU network, and this in turn makes the composite stiffer. While this property is desirable in some cases, the increased stiffness reduces the compliance of the top layer during coating leading to cracks forming. As shown in Fig. 26 f), in films with 20wt% PEI, the cracks were exhibited all over the surface. Pure PU does not have this issue as the linear chains interact through entanglement and can unravel to relieve these stresses.

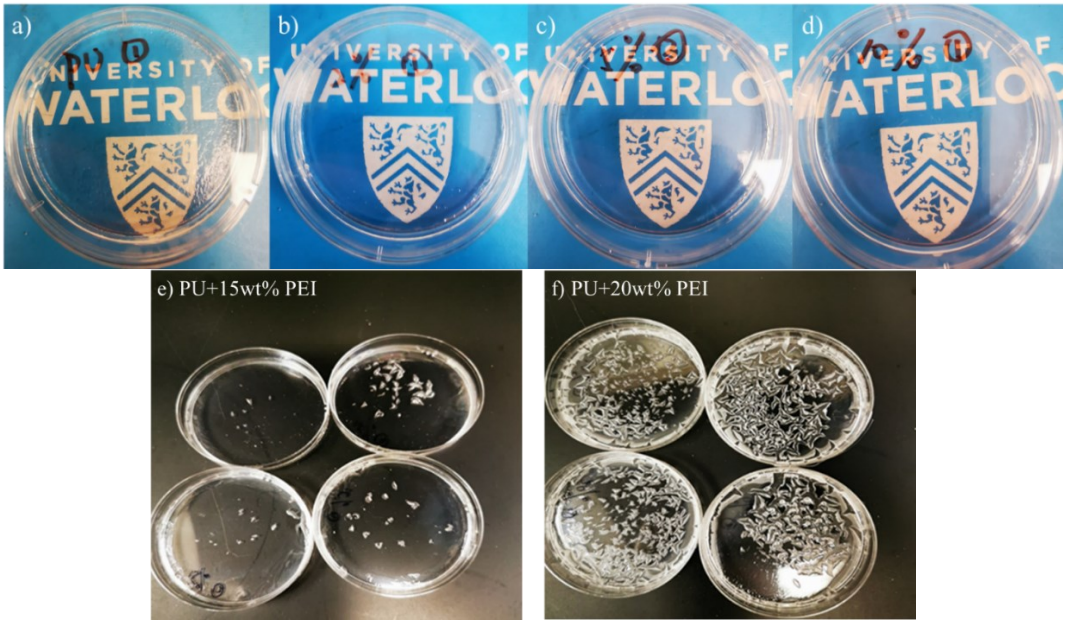

Figure 26. Coatings of a) PU and PU with b) 2wt%; c) 5wt%; d) 10wt%; e) 15wt% and f) 20wt% PEI.

3.1.4.1 Fourier-transform infrared spectroscopy (FTIR)

In this study, the carbamate group in polyurethane was prepared by the reaction of the hydroxyl group from dimethylolpropanic acid (DMPA) and cyanate group from isophorone diisocyanate (IPDI). As shown in Fig. 27, the peak at around 3340 cm^{-1} of DMPA shows O-H stretching and the significant absorption peak in the range of 2275-2250 cm^{-1} indicates N=C=O stretching in IPDI. The peak at 1100 cm^{-1} of PPG-2000, which is the polymer chain extender in the reaction, shows C-O stretching, while the smaller peak at 1370 cm^{-1} indicates C-H. Comparing the FTIR spectra of these three with the spectrum of PU, the disappearance of the hydroxyl bonds at 3350 cm^{-1} and cyanate bonds in 2275-2250 cm^{-1}, the appearance of new bands at around 1200,1700 cm^{-1}, which were assigned to the C-N and C=O of the carbamate groups respectively, confirmed that the carbonate groups were completely converted into carbamate groups. The introduction of PEI into the polyurethanes backbone mainly occurred through the direct reaction of isocyanate with amine groups of PEI forming urea bonds. As seen in Fig. 27, the broad absorption peaks at about 2800-3500 cm^{-1} show the overlapped absorptions of primary and secondary amine groups, and amine salt. Absorbance bands due to the ester and carbamate groups of PU/PEI (10wt%) were overlapped in the spectra. Therefore, FTIR results confirmed the formation of a polyurethane network and successful introduction of PEI.

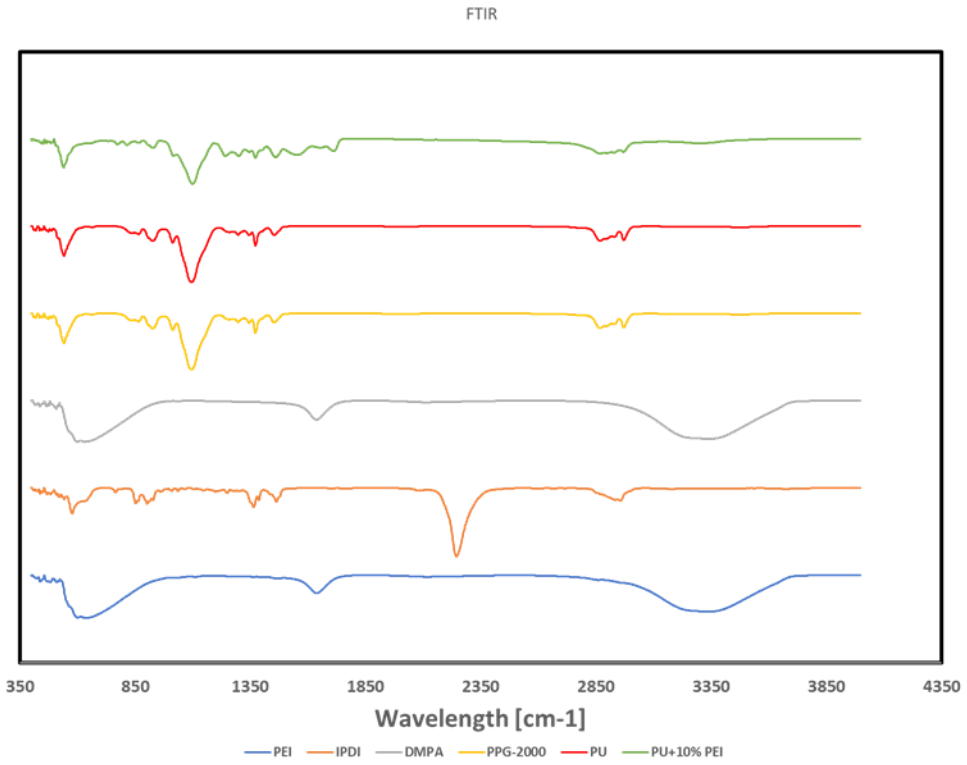

Figure 27. FTIR measurements of PEI, IPDI, DMPA, PPG-2000, PU and PU/10wt% PEI.

3.1.4.2 Conductivity

In this project, branched polyethyleneimine was introduced into the PU/PEI system as the polycation to provide antibacterial properties, which has a cation nitrogen in each repeating group. From the mechanism of antibacterial activity of antimicrobial polycation, the concentration of PEI was expected having direct impact on the antimicrobial effectiveness of the PU/PEI system[127]. Therefore, knowing either the amount of PEI leached out of the PU/PEI film or the amount left within the polymer matrix significantly helps to prove the existence of both ion-releasing and contact-killing antimicrobial actions in this system. However, it is difficult to directly detect either of these amounts of PEI. Conductivity measurements have been significantly studied and used as

a reliable indirect method to determine the ion concentration in a solution. Therefore, a conductivity test was applied in this project to confirm the rate of mobile and immobile cationic PEI molecules in the PU/PEI colloidal system.

The conductivity of the PU/PEI solution in this project was measured by a conductivity meter. As seen in Fig. 28 a), the increase in conductivity of DI water with PU/PEI samples soaked in indicated that there were PEI cations leached out from sample films. This indicates that the PU/PEI collodial films likely have ion-releasing antibacterial activity. Sample solutions with PU/2wt% PEI and PU/5wt% PEI soaked in showed very minor conductivity due to the low concertration of PEI. Since conductivity meters become unreliable at low conductivities, these results could either be due to errors within the meter or the PEI preventing conductive small molecules from leaving the PU. At concentrations below 7wt% the PEI appears to be fully bound to the PU with little free PEI able to leave the sample. This can be seen in the 2wt% having the lowest conductivity of all the samples, while 5wt% is slightly higher with some PEI releasing into solution and both having lower conductivities than pure PU. Conversely, with higer wt% PEI, the solutions showed significant increase in conductivity. As seen in Figure. 28 b), the conductivity results showed highest rate of release compaired to other leaching periods in the first 20min of leaching for PU/2wt%-20wt% PEI samples. As the soaking time was increased above 1 hour, the conductivity curves of all PU/PEI samples in the test tend to reach equilibrium.

a)

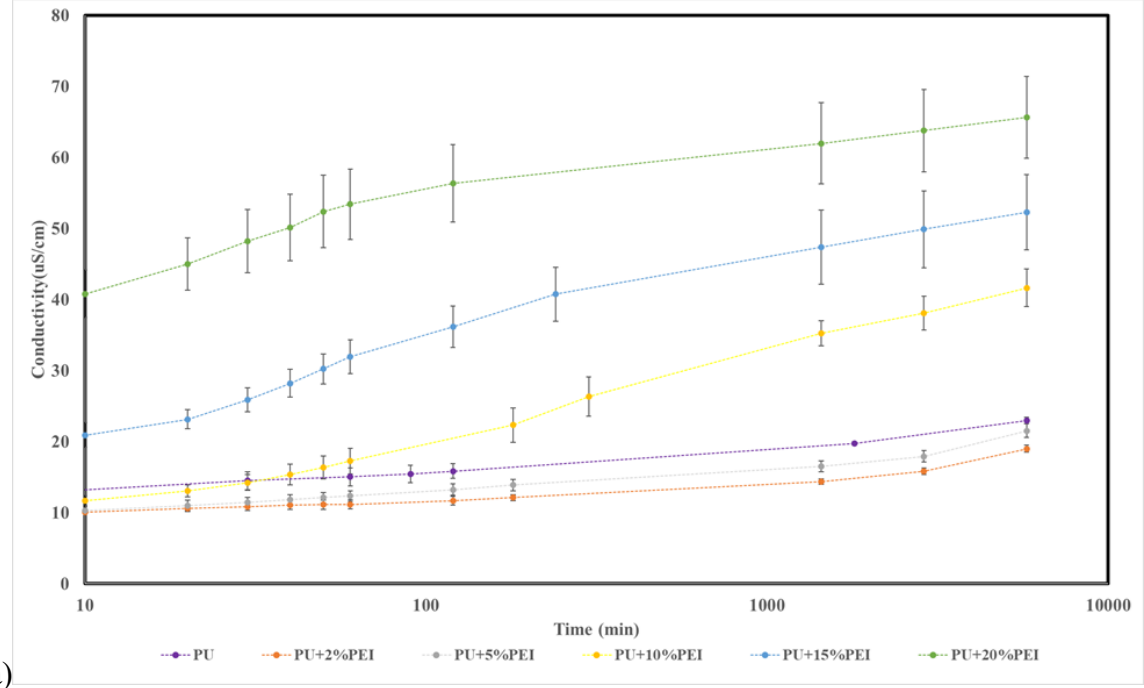

b)

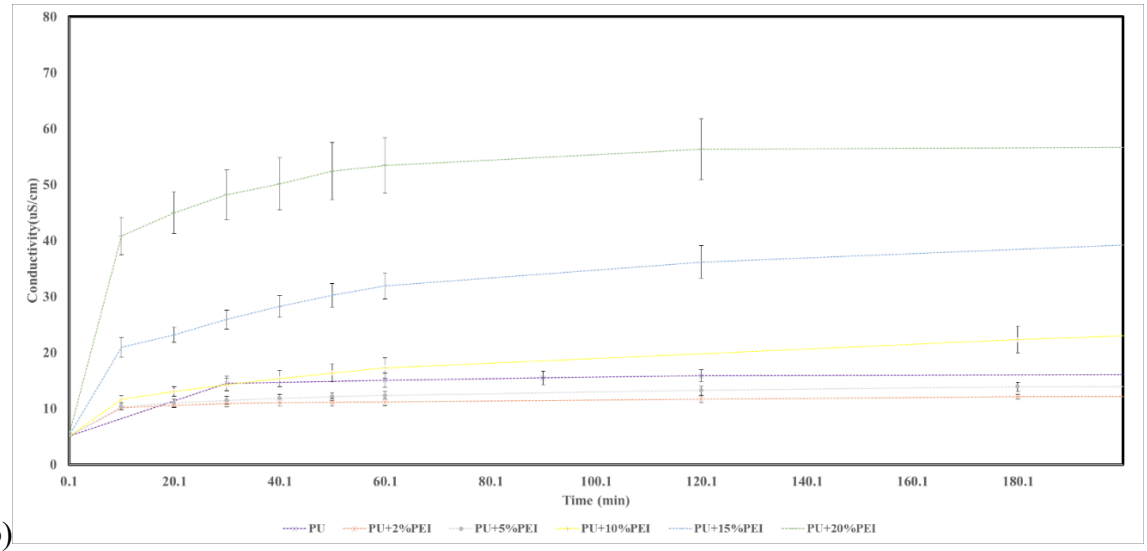

Figure 28. Conductivity of leaching solution after soaking PU/PEI composites at various time points over 1 week. a) Conductivity vs. Time (log); b) Conductivity vs. Time (linear).

Due to the complexity of conductivity conversion, a series of PEI solutions were made to calibrate the conductivity of each concentration for comparison with the conductivity of solutions with film

samples soaked in them for different time periods (Fig. 29). With the equation from the this calibration curve, we were able to convert the conductivity value into concentration of PEI in each leaching solution as shown in Fig. 30. This indicates the existence of mobile PEI molecules exist in the washing solution, which would provide ion-release activity of PU/PEI colloidal films. From Fig. 30, we can get the final PEI concentrations in each washing solution and convert it into the amount of PEI leached out following the calculation steps stated below.

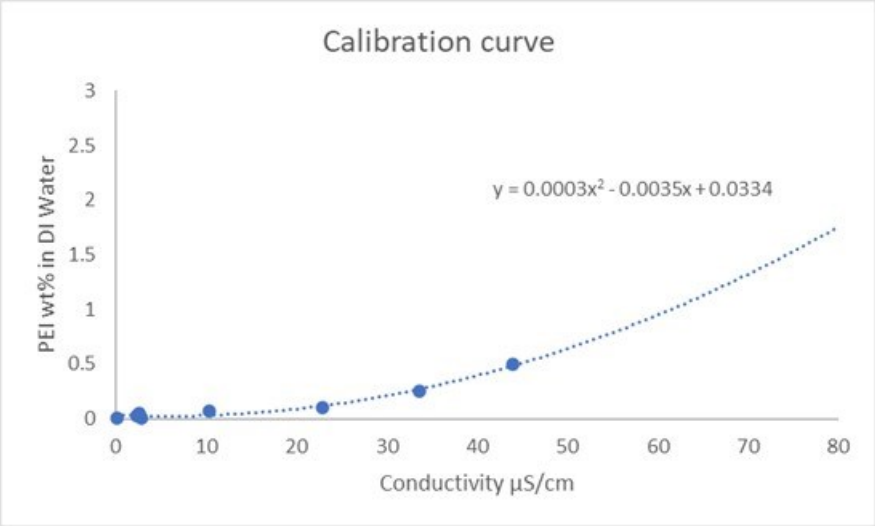

Figure 29. PEI Concentration (mg/mL) vs. Conductivity, Calibration curve of polyethyleneimine concentration.

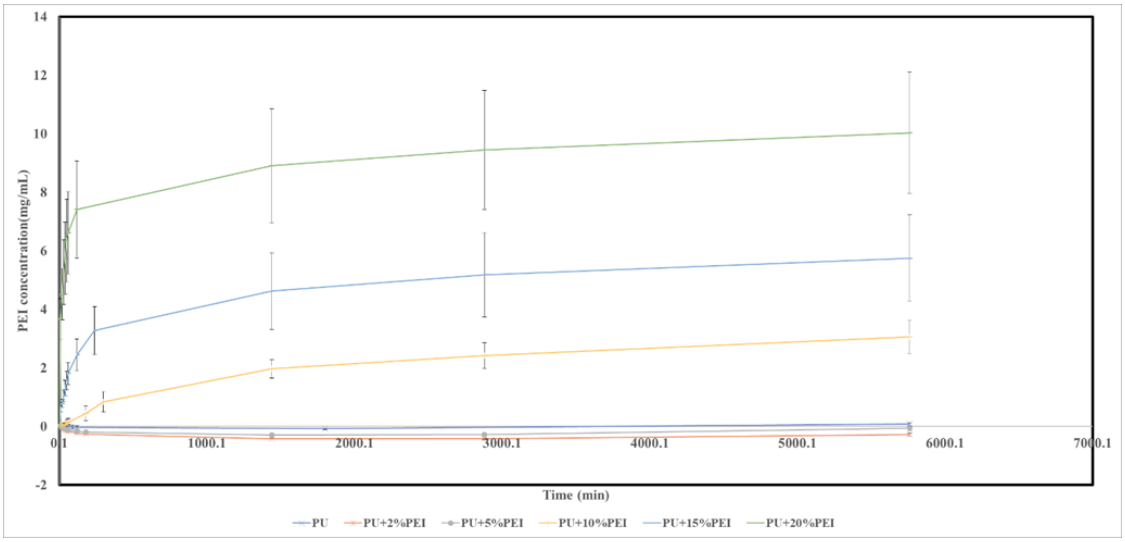

Figure 30. Converted concentration of PEI in leaching solutions vs. leaching time.

The amount of PEI in each piece of PU/PEI sample film (1 cm * 1 cm) can be found following the equation below: assuming the thickness of coating in petri dish is even.

$$Weight\ of\ PEI\ in\ each\ sample = \frac{1\ cm * 1\ \text{cm}}{(6/2)^2\pi} * weight\ of\ PEI\ in\ each\ petri\ dish$$

And the amount of PEI in each washing solution can be fund with an equation as:

$$Weight\ of\ PEI\ in\ solutions = PEI\ concentration * 10\ mL(volume\ of\ solution)$$

Comparing these two values of PEI weight, the difference can be an evidence that immobilized PEI existing in this PU/PEI system, supporting the existence of a contact-killing ability. However, the released PEI calculated does not match the calculated PEI in the sample. The ion-releasing

measurements for PEI containing samples were normalized by subtracting the calculated ion release of PU, to account for ions present in PU that were not PEI. It was found that the 2wt% and 5wt% samples showed a lower ion release rate than PU leading to the calculation of negative concentration values in the solution after normalizing the measurements compaired to PU. This was hypothesized to be due to the bound charged PEI in the PU attracting the unreacted DMPA or DMPA containing oligomers already present in the PU preventing its release into the solution. This behavior was inverted when the PU contained free PEI for 10, 15 and 20wt% samples with the PEI pulling unreacted DMPA or DMPA containing oligomers out of the PU film as it released. The calculated release was greater than the PEI present in the film. Since the ion releasing was calculated by the conductivity, the presence of unreacted DMPA or DMPA containing oligimers would significantly increase the conductivity of resulting solution. For this reason since the DMPA release cannot be determined, the calibration curve generated for this data was unsuitable for accurately measureing the release of PEI, but it can be used to measure the relative release of each composite relative to eachother. From the ion releasing measurements, we can see that 2wt% and 5wt% tend to reduce the release characteristics when compaired to neat PU. This behavior reaches a critical point at 10wt% when the conductivity is greater than neat PU, this is likely indicative of a structural change of the composite where above this point there is free PEI in the dried film and emulsion.

3.1.4.3 Water contact angle

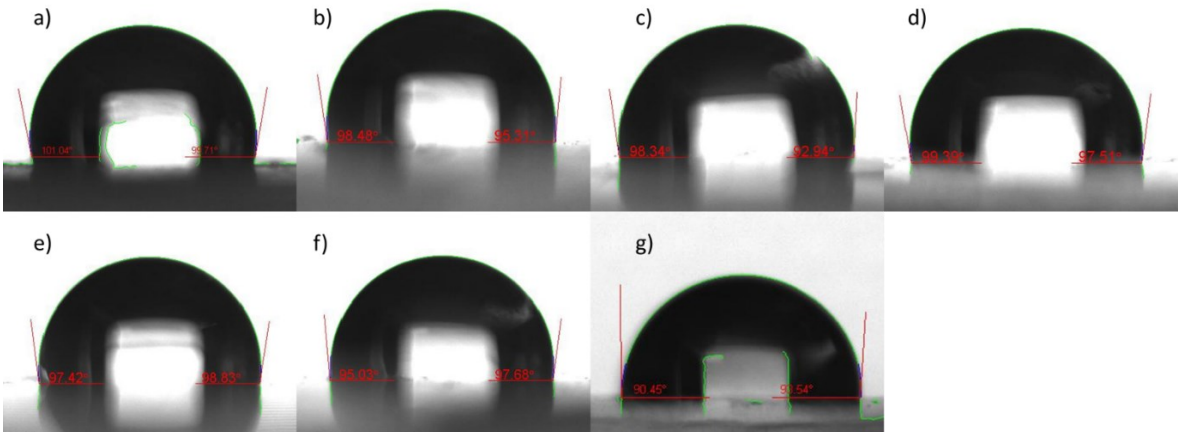

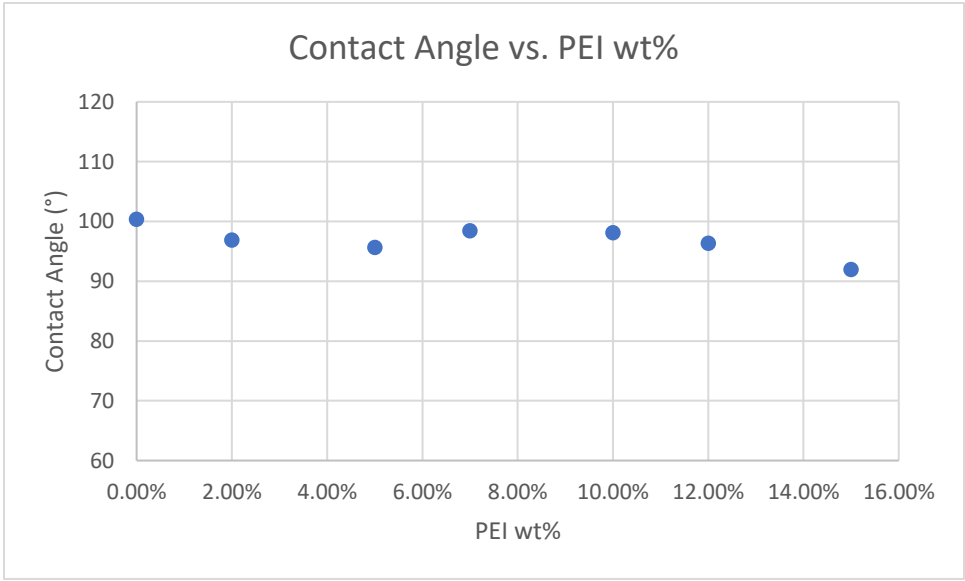

Figure 31. Top: Contact angle measurements of a) PU film; b) PU/2wt% PEI; c) PU/5wt% PEI; d) PU/7wt% PEI; e) PU/10wt% PEI; f) PU/12wt% PEI; g) PU/15wt% PEI.

The introduction of PEI into PU system slightly reduced the hydrophobicity compared to the polyurethane film seen in Fig. 31. However, with the highest concentration of PEI in these experiments (15wt%), the contact angle was still over 90°, indicating a hydrophobic surface. As the concentration of PEI increased, the film tended to become slightly more hydrophilic. As the PEI concentration is increased significantly there is not a significant reduction in contact angle indicating the PEI molecules are uniformly dispersed through the PU and do not segregate to the surface. These results indicate the PEI is contained mainly to the bulk of the material as expected from the hypothesized structure. It can also be hypothesized from these results that the composites show some degree of shielding of the PEI groups, where the hydrophobic portions of the PU molecule are segregated to the surface, with the charged PU sections and PEI remaining below the surface. This behavior could explain the increase in hydrophilicity at 2wt-5wt% PEI then increase in hydrophobicity at 7wt-10wt% PEI and finally a decrease as the PEI concentration increases over 12wt%. At low concentrations, the charges present are not high enough to drive significant segregation during drying leading to the presence of PEI on the surface. As the concentration increases the ionic interactions increase leading to less PEI present on the surface due to the increase in the segregation phenomenon. Finally, when the PEI concentration increases above a critical point the charged sections of the PU are saturated and can no longer bind the excess PEI leading to an increase in PEI on the surface.

3.1.4.4 Scanning electron microscope (SEM)

Fig. 32 shows SEM images of PU/15%wt PEI film surface and surfaces with treatment of DI water for 1 hour, 0.01M PBS buffer (pH 7.4 at 25°C) for 1 hour and UV Ozone (PSDP-UVT cleaner) at 25°C for 1 hour. From these images we can see soaking in DI water, soaking in PBS buffer and exposure under UV light for 1 hour did not affect the surface morphology of PU/PEI films. In the untreated samples, cracks can be seen throughout the surface. These cracks visible in Fig. 32 a) and b) are present in the DI water soaked samples [Fig. 32 c) and d)], the PBS buffer soaked samples [Fig. 32 e) and f)], and the UV treated samples [Fig. 32 g) and h)]. When performing SEM, the cracks were specifically focused on to see if there was propagation during the treatment. Of the different treatments, the UV exposure does not significantly change the surface morphology when compared to the untreated sample. Interestingly, the cracks present in the DI water and PBS treated samples have reduced in magnitude compared to both the untreated and UV exposed samples. This behavior is likely related to the self healing properties seen in PU/PEI composites[4]. When the water swelled the crack parts of it were able to contact and bond reducing the size of surface cracks. Based on this, UV treatment was chosen as the sterilization method for both antibacterial and antivirus testing. In addition, soaking the PU/PEI films in DI water was done for ion leaching purposes, and bacterial cells suspension in PBS buffer was utilized to contact with the PU/PEI sample films during the antibacterial testing.

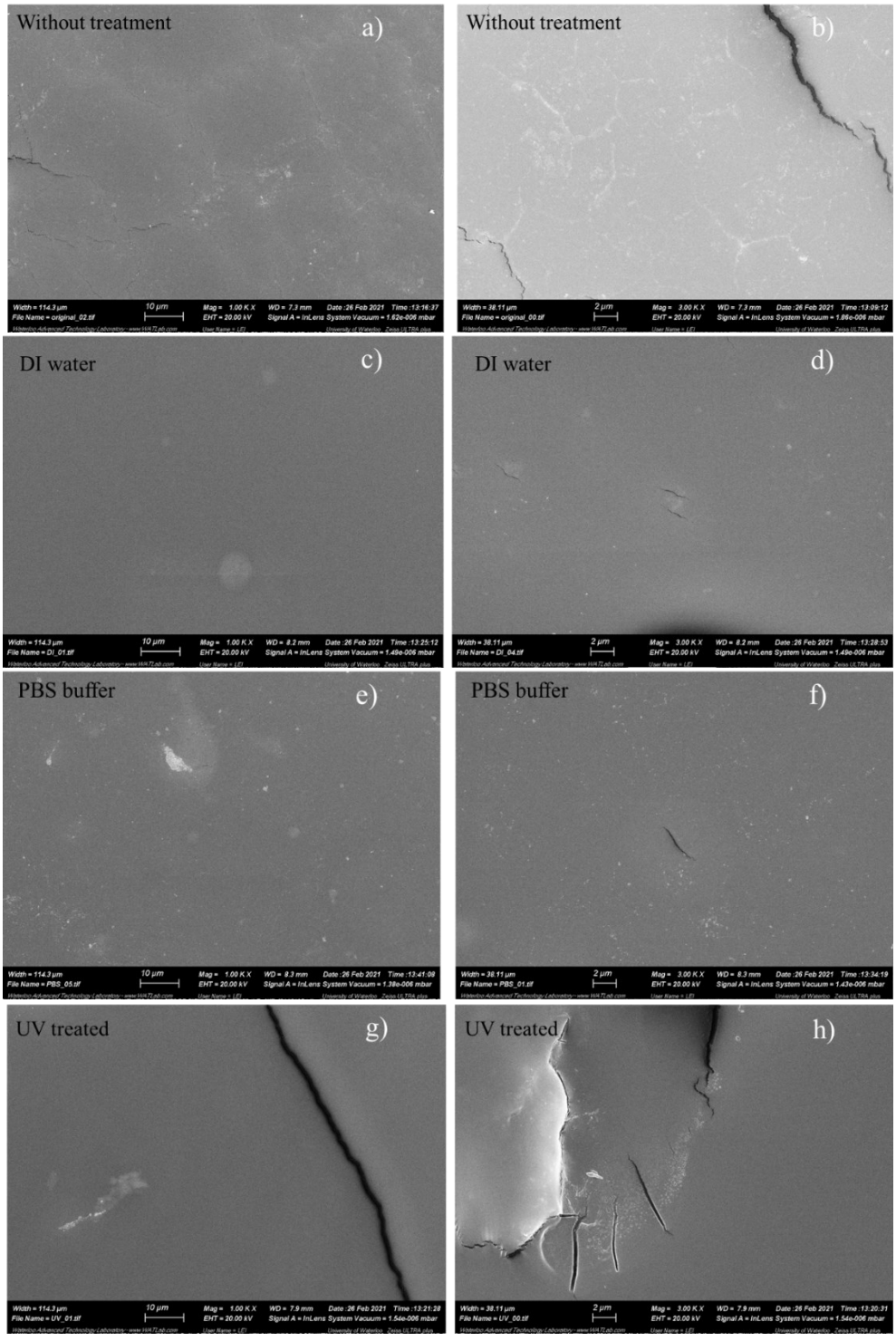

Figure 32. SEM of PU and PU/15wt% PEI films with a, b) no treatment; c, d) treatment of DI water; e, f) treatment of PBS buffer; and g, h) treatment of UV for 1 hour.

3.1.4.5 Dynamic light scattering (DLS) & Zeta-potential

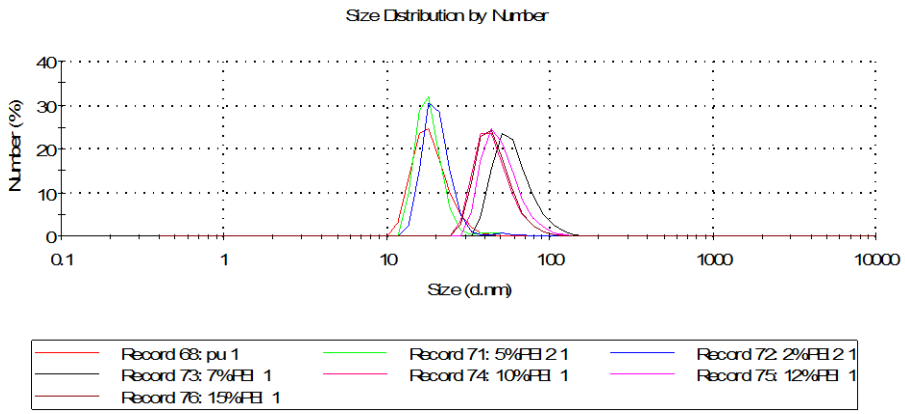

Figure 33. DLS measurements of PU/PEI emulsions.

The diagram of DLS (Fig. 33) shows with lower concentration of PEI, as 0%, 2wt% and 5wt%, the diameter of micro-emulsion particle is around 20 nm. With higher PEI concentrations the size of micro-emulsion particles increases, as 7wt%, 10wt%, 12wt% and 15wt% showing a 50 nm to 60 nm diameter. With the data shown by Zeta-potential, the results state the PU/PEI colloid system is stable. These results are also in line with the results seen in the contact angle measurements. At lower concentrations (2-4%) the PEI is more evenly dispersed through the system and do not show an increase in aggregation of the PU colloids. As the PEI concentration increases, the PU colloids increase to more than double in size. This sudden increase from 5-7% is hypothesised to be due to the switch of the PU colloids from micelles to liposomes. These liposomes likely contain high concentrations of PEI and would cause a change in the structure of the films produced by drying the resulting emulsions.

Table 2. Zeta potential of the prepared PU/PEI emulsions.

Samples	Zeta-potential (mV)
PU	-41.3
PU-2wt%PEI	-50.7
PU-5wt%PEI	-50.9
PU-7wt%PEI	-44.7
PU-10wt%PEI	-59.0
PU-12wt%PEI	-55.3
PU-15wt%PEI	-56.3

The zeta potential for the PU/PEI colloids showed relatively high charges (see Table 2), with a general trend of increasing as the PEI wt% is increased. As seen in the DLS results the 7wt% PEI shows a reduction in the zeta potential before an increase for higher wt%. This further indicates a change in the colloid morphology. Furthermore all the zeta potentials are near or below -50 mV, this indicates that the emulsion is stable and will not agglomerate over time[128].

3.1.4.6 Tensile test

To investigate the effect of different concentration of PEI into PU system on the mechanical strength of PU/PEI colloidal films, tensile tests were conducted on sample films of PU, PU/2wt% PEI, PU/5wt% PEI, PU/7wt% PEI, PU/12wt% PEI and PU/15wt% PEI (Fig. 34).

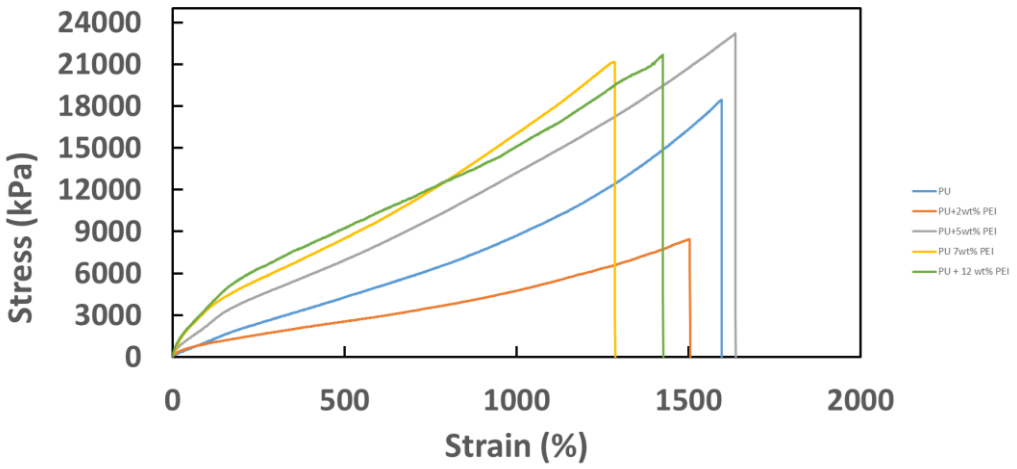

Figure 34. Stress-strain curves of various PU/PEI colloidal films.

When the PU/PEI composites were tested by UMT, the ultimate tensile strength compared to PU was generally increased through the addition of PEI. From fig.34 we can see the 5, 7 and 12 wt% PEI films all showed improved ultimate tensile strength compared to neat PU. Furthermore, the young's modulus of the higher wt% PU/PEI composites displayed a stiffening in the initial elastic region. Interestingly, the 2wt% PU displayed significantly lower mechanical properties compared to the PU. The reason for this was likely due to issues with the sample preparation. Due to the elasticity of the PU composites the tensile specimens had to be cut by hand to measure the elongation at break. Of the cutting dies that were available, the throat regions of the samples were too long and lead to the z axis travel of the UMT maxing out during elongation. It is likely that the

2wt% specimens had damage along the throat region of the sample or in the neck region where the width was reduced. This damage would likely cause the behavior that was shown in the 2wt% sample. This hypothesis was bolstered by the shape of the curve at ~200% elongation where other samples show a reduction in the slope while 2wt% does not. When comparing the other PU/PEI blends, it was found that 5wt% showed the greatest strength and strain at break compared to all the other samples. This behavior was likely due to the phenomena observed earlier in the DLS measurements and contact angle. Since the mechanism for the PEI strengthening of PU relates to the breaking and reforming of ionic bonds between the DMPA groups in the PU and PEI groups present in the PEI, it is likely that the nonhomogeneous dispersion of the PEI within the higher wt% PEI/PU composites leads to a reduction in overall strength. The homogeneous dispersion of the PEI in the 5wt% sample is likely what allowed it to have a significantly longer strain at break compared to other PU/PEI composites as well as a measurable longer strain at break compared to the neat PU. While there are strength differences between the various PU/PEI blends, at 5wt% and above the strength of the film is greater than neat PU and the main goal of this research is to optimize the antimicrobial activity of the resultant PU/PEI film. For this reason, from the tensile test, we can conclude that any film between 5wt% and 12% is suitable for coating dependant on their respective antimicrobial activity, as above that point cracking during drying becomes an issue and the strength is degraded.

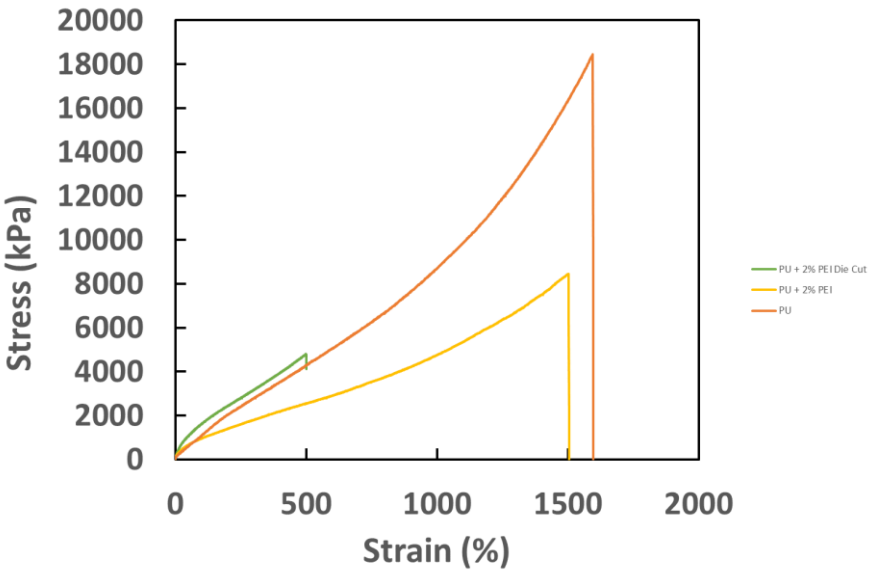

Figure 35. Stress-strain curve of different sample preparation methods of PU/2wt% PEI compared to PU.

With the assumption that the PU/2wt% PEI film showed incorrect measurements due to the hand-cut sample, a new PU/2wt% PEI sample cut with an ASTM die was prepared. Due to the limitations in available dies, the length of the sample was too long to reach its failure strain with the UMT reaching the end of Z-axis travel before this point. The result of tensile test is shown in Fig. 35. From this figure it can be seen that the die-cut PU/2wt% PEI sample had a higher stiffness than the hand-cut sample showing a slightly higher stiffness than PU. This is expected as the addition of charged molecules to allow for ionic crosslinking should increase the stiffness of the sample. It is expected that PU/2wt% PEI should show a stress-strain curve similar to PU with a slightly higher ultimate tensile strength if it was able to be fully extended.

3.1.4.7 Scratch test

To investigate the strength of the PU/PEI composite as a coating compared to the layer-by-layer process, a series of scratch tests were performed on each of the different formulations as seen in Fig. 36. When comparing each of the photos of the scratch [right side of Fig 36. a)-g)] all of the coatings showed spallation failure by buckling and wedging. The failure point of each of the coatings was determined by the point the coefficient of friction started to show vibrations that were mirrored by the Fz. This indicated that buckling or wedging was occurring as the tip would pass over a raised part of the coating and move into a trough, lowering both the Fx and the Fz read by the UMT. From the PU scratch test in Fig. 36 a), we can see the failure occurs around 1200 g with the characteristic oscillations associated with wedging with total failure of the coating occurring at around 4100 g. This behavior is similar to the PU/2wt% PEI seen in Fig. 36 b) with the beginning of buckling occurring around 1171 g with total failure occurring around 3500 g which was lower than the PU. This indicates that low wt% of PEI might cause a decrease in the strength of the coating, something that was noticed in the tensile tests, with additional measurements being performed to confirm the issue. Like the results found from the tensile strength retest, the initial strength of the PU/2wt% PEI coating was like that of the PU as the young's modulus of the two are quite similar. At high loads the coating failed earlier than the neat PU something that was seen in the initial tensile test measurements. Moving on to PU/5wt% PEI as seen in Fig. 36 c), initial buckling of the coating was seen at around 2000 g, these results mimic those seen in the tensile tests with 5wt% showing the greatest tensile strength and elongation at break of all the measurements. The 5wt% sample also showed total failure of the coating around 4000 g. As the PEI wt% was increased to 7% [Fig.36 d)] we see a decrease in the strength of the coating, like the tensile tests with initial failure occurring at 1545 g and total failure occurring at around 3500 g as

expected. This again was similar to tensile test results with the 7wt% showing weakening as the loading of PEI was over the capacity the PU could ionically bond to. The sample also displayed a delayed increase in force in the X and Z direction due to the meniscus that formed during drying in the Petri dish. Since the measurement was performed too close to the edge, the starting point of the probe was at a higher level than the majority of the sample. This led to the delayed increase of the values as the probe did not contact the sample for the first 3 mm of travel. For PU/10wt% PEI an initial failure of the coating was seen at 1400 g with total failure occurring at 3000 g as seen in Fig. 36 e). For PU/12wt% PEI an initial failure of the coating was seen at 1171 g with total failure occurring at 2800 g as seen in Fig. 36 f). Finally for the PU/15wt% PEI initial failure was seen around 1500 g and total failure seen at around 3000 g. From analysing the data as a set, it was found that the PEI could increase the strength of the PU composite coating significantly when added at 5wt%, but as more PEI is added the mechanical strength of the coating suffered. It was hypothesised that the excess PEI was interfering with the bonding between the polystyrene plate that allowed for delamination to occur sooner than coatings with just PU. This behaviour could be desirable for other surfaces though that are hydrophilic as the interactions between the PEI in the PU and the charged surface could increase the strength of the coating. While this is currently unknown it could be the subject of further research.

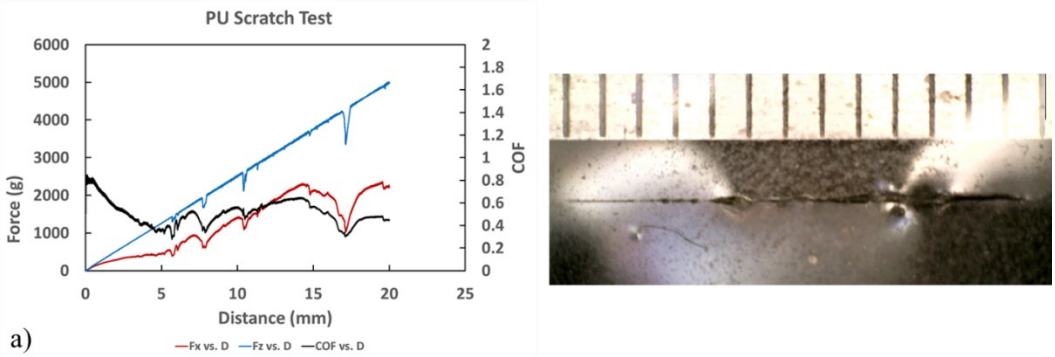

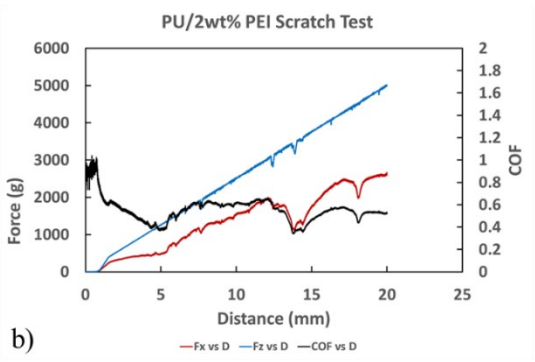
PU/2wt% PEI Scratch Test
Force (g)
COF
Distance (mm)
Fx vs D
Fz vs D
COF vs D

b)

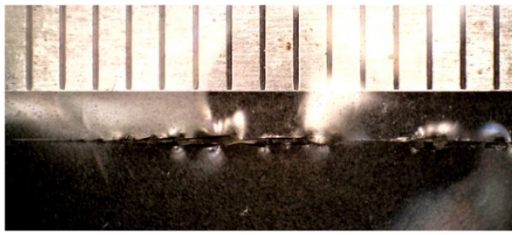

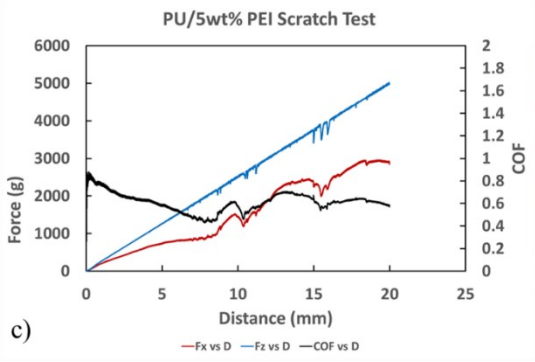
PU/5wt% PEI Scratch Test
Force (g)
COF
Distance (mm)
Fx vs D
Fz vs D
COF vs D

c)

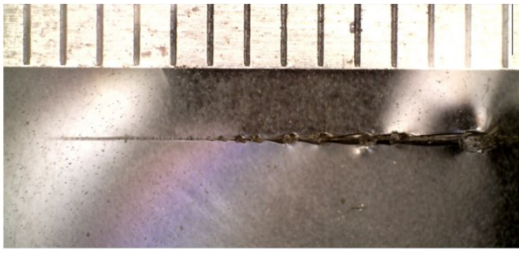

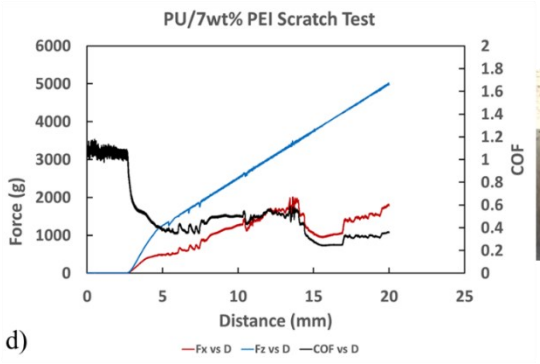
PU/7wt% PEI Scratch Test
Force (g)
COF
Distance (mm)
Fx vs D
Fz vs D
COF vs D

d)

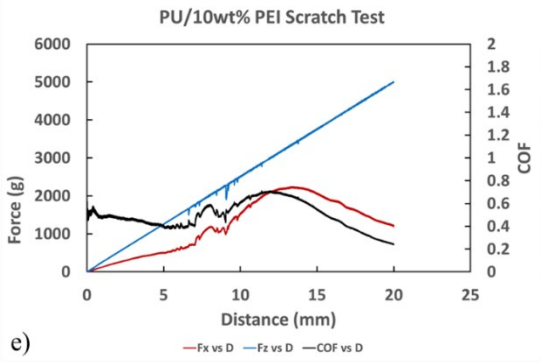
PU/10wt% PEI Scratch Test
Force (g)
COF
Distance (mm)
Fx vs D
Fz vs D
COF vs D

e)

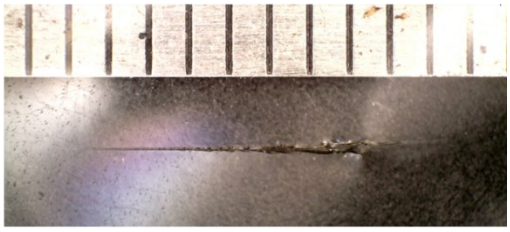

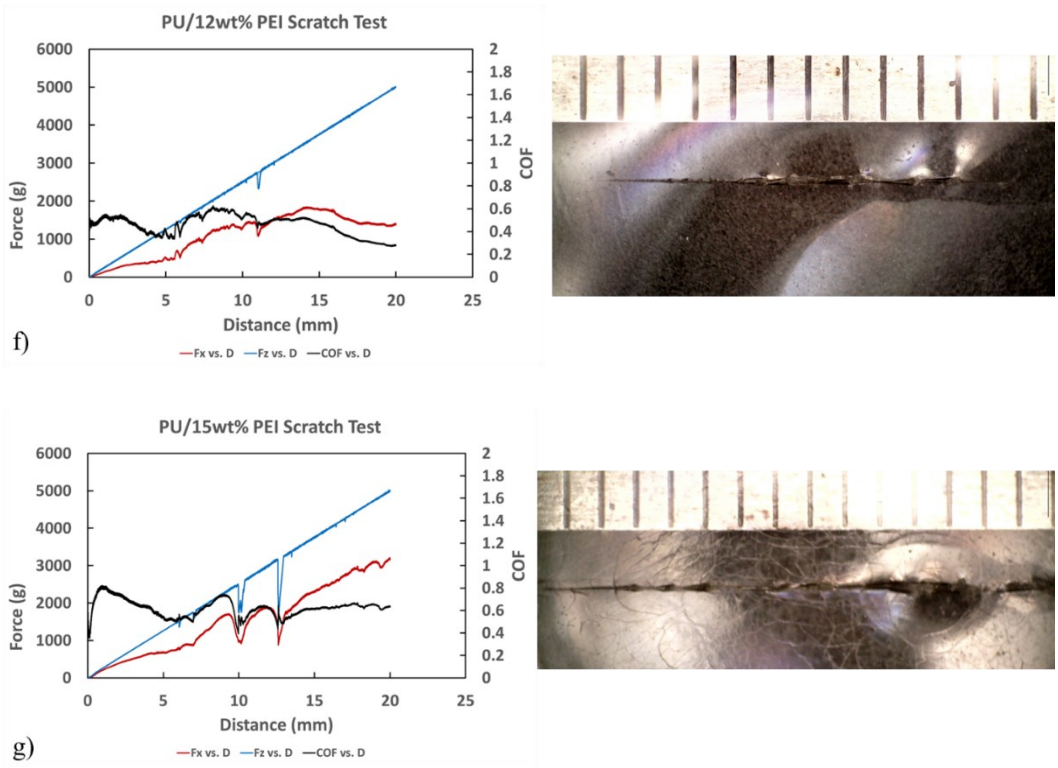

Figure 36. Force vs. Distance on a) PU; b) PU/2wt% PEI; c) PU/5wt% PEI; d) PU/7wt% PEI; e) PU/10wt% PEI; f) PU/12wt% PEI and g) PU/15wt% PEI coatings.

3.2 Ion-releasing killing activity of PU/PEI film

The antibacterial mechanism of mobile QA-PEI as polycations has been proved in previous work including disruption of the lipid bilayers of the cytoplasmic membrane. Additionally the outer-membrane of Gram-negative bacteria can also be broken through the electrolyte attraction between positively charged ammonium groups with the negatively charged bacterial surface and the replacement of divalent cations, calcium ions and magnesium ions from the cytoplasmic membrane[105], as shown in Fig. 37. A further damage of the bacterial cytoplasmic membrane can be caused by the interdigitation of the hydrophobic alkyl chain of QA-PEI molecules with the hydrophobic bacterial membrane leading to the loss of the proton motive force, leakage of

intracellular fluid and ultimate death of the bacterial cell[106–108]. While the mechanism of unquaternized PEI is not known, it is known that branched PEI has a propensity to protonate under neutral or acidic conditions to form a polycation. This behavior is expected to provide an antimicrobial activity similar to that of QA-PEI.

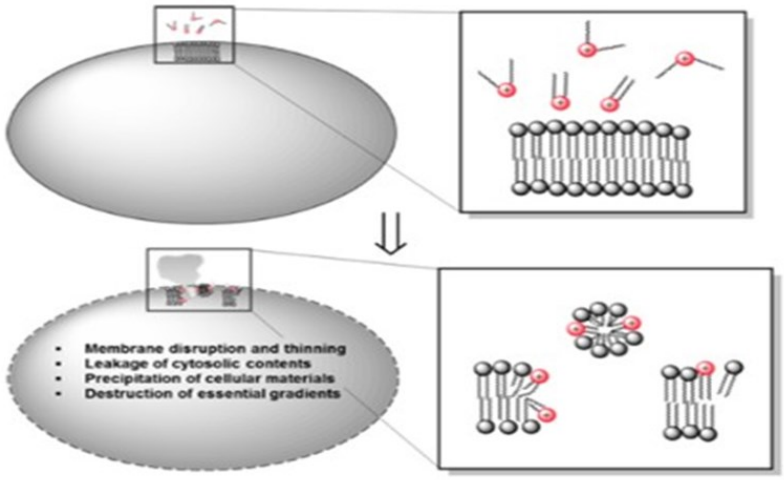

Figure 37. Antibacterial working principle of mobile QAC molecules[127]. Reproduced (adapted) with permission from ref 127. Copyright 2015 American Chemical Society.

As discussed in the section of WPUs synthesis in this project, the PU/PEI system contains three different dynamic non-covalent bonds. The PEI is introduced into PU matrix through ionic bonds. And these ionic bonds can be easily broken and rebuilt to distribute energy, offering the elongation property while the elastomeric film is stretched. When the ionic bonds break, the PU/PEI elastomer can partially release PEI molecules into the surroundings, leading to the occurrence of an antibacterial activity. However, an over-crosslinked PU/PEI network can be achieved from incorporation of excess PEI into the PU system based on the high ionic concentration. Due to the ionic interaction between the PEI and the PU, the PEI remains in the film for long periods of time.

While some can be released through the breaking of ionic bonds and diffusion of unbound PEI, the majority remains bound to the film due to the multiple tertiary amine groups present in the PEI requiring multiple ionic bonds to break to allow the release of bound PEI.

3.2.1 Materials and instruments

3.2.1.1 Materials

Escherichia coli (*E. coli*) was as the main bacteria for the antibacterial activity tests in this project. Lauryl sulfate broth purchased from Sigma Aldrich was used as the cultivation broth for *E. coli*. Agar plates were made of plate count agar from Difco. Phosphate buffered saline (0.01M) from Sigma Aldrich was used as buffer during the tests.

3.2.1.2 Instruments

All glassware used in this experiment was sterilized in an autoclave at 121°C. A mini centrifuge (from ARgosflexifuge) and Analog Vortex Mixer (from VWR) were used in the preparation of *E. coli* PBS suspension. The concentration of *E. coli* suspension was determined by diode array spectrophotometer (from Hewlett Packard) in this test. The bacterial broth and *E. coli* on agar plates were cultivated in the Isotemp incubator from Fisher Scientific. Sample solutions was sterilized in an auto clave.

3.2.2 Experiments of PU/PEI ion-releasing antibacterial activity

3.2.2.1 Preparation of bacteria

Cultivating *E.coli* in LSB (Lauryl sulfate Broth) at 37°C for 12 h-24 h, centrifuge 4 mL bacterial solution and suspend it in PBS buffer. 2-3 times of the suspension in PBS buffer was applied to confirm there is only negligible amount of LSB broth left in the PBS suspension. The OD (optical density) at 670 nm was utilized to determine the concentration of biomass (10^8 cells/mL) in the PBS buffer (OD670 = 0.03586). Then the *E.coli* PBS suspension was diluted 5 orders of magnification to 10^3 cells/mL which is the countable value on counting agar plates.

3.2.2.2 Antibacterial experiment of sample solutions

Every 12 mL DI water with one piece of PU/PEI sample films (0.5 inch * 0.5 inch) soaked in for 1 hour, 24 hours and over a week were kept in glass vials. After taking out the soaked sample films, the left solution in glass vials were sterilized in auto clave with a control vial of only 1 mL DI water in. Then 100 μL 10^3 cells/mL bacterial PBS buffer suspension was added into 100 μL of each sample solution in sterile 1.5 mL centrifuge tubes with acute mixing then for 2-3 minutes. Then all centrifuge tubes have the mixed solution in were left to set to give an adequate contact of the bacteria and sample solutions. After 1 hour of contacting, 100 μL mixture was taken from each tube after intense shaking by hands before applying the mixtures individually on agar plates since the final volume of final mixture of bacterial PBS suspension and each sample solution was 200 μL, but only 100 μL mixture was taken to incubate, even an acute mixing was applied, the 1hour

setting could have separated the homogenous suspension. These plates were cultivated in the biological incubator overnight at 37°C.

3.2.2.3 Absorption test of sample films

1 cm * 1 cm sample films of PU, PU/5wt% PEI, PU/10wt% PEI and PU/15wt% PEI were prepared. The thickness and weight of each sample film were recorded. After that, 12 mL DI water with each piece of the sample films soaked in for 1 hour, 24 hours and over a week were kept in glass vials at room temperature. Then the thickness and weight after absorption were recorded to compare with the values before soaking. Notably, while measuring the samples after absorption, the left water on surface of the samples needs to be gently wiped off without taking moisture out of the films, leading to a smaller change of absorption value.

3.2.3 Results and discussion

3.2.3.1 Ion-releasing antibacterial activity of PU/PEI films

From the results of counting agar plates, the control group of 10wt% PEI solution showed 0 colony which indicates that PEI molecules are significantly effective antibacterial agents. As stated in the experimental method of the antibacterial test, the final volume of the mixture of bacterial suspension and sample solution was 200 μL, the concentration of this 100 μL bacterial suspension was supposed to be diluted into a half of the initial concentration. Hence, the colony unit number of 50 μL bacterial PBS suspension was assumed as a more accurate result for the bacterial control group. In addition, the DI water control groups showed 8 colonies which is very close to the colony numbers from 50 μL bacterial control group (7 colonies). This also indicated the result of the

bacterial control group should be 7-8 colony units instead of 16 colony units shown from 100 µL bacterial PBS suspension.

Table 3. CFUs of washing solutions with PU and PU/5wt%, 10wt% and 15wt% PEI soaked in for 1h, 24h and 1 week.

Control groups	Colony forming units (cells)
50 µL bacterial PBS suspension	7
100 µL bacterial PBS suspension	16
1ml DI water	8
10wt% PEI solution	0

Samples	Colony units (cells)	Samples	Colony units (cells)	Samples	Colony units (cells)
PU 1h	5	PU 24h	15	PU 1week	6
5% 1h	4	5% 24h	8	5% 1week	7
10% 1h	4	10% 24h	7	10% 1week	11
15% 1h	2	15% 24h	11	15% 1week	9

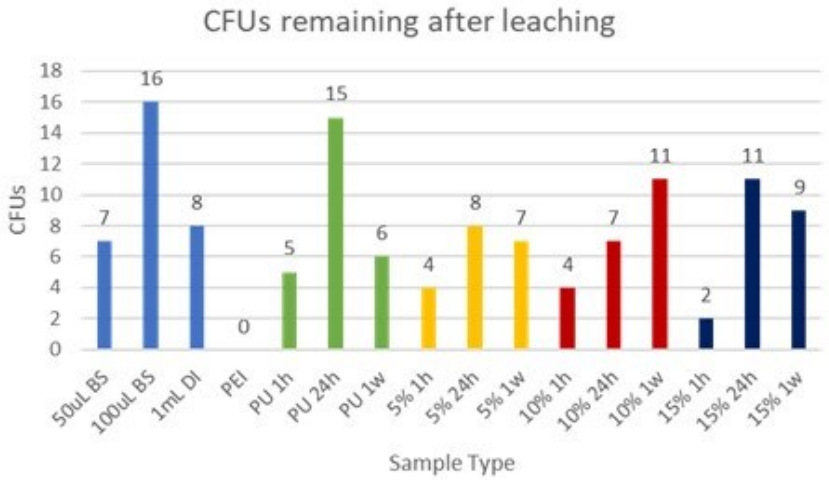

Figure 38. CFUs of washing solutions with PU and PU/5wt%, 10wt% and 15wt% PEI soaked in for 1h, 24h and 1 week.

The colony unit numbers from the sample solutions (see Table 3 and Fig. 38), the ones with PU/PEI films soaked in for 1hour showed the most effectiveness than the ones with films soaked for longer. Relevantly, the conductivity diagram discussed above shows the highest slope of conductivity of samples with 10wt%-20wt% PEI concentration within the first 20 minutes of leaching which indicates that most ion releasing occurred in this period. In addition, we noticed that with 1hour leaching, samples with concentrations from 5wt% to 10wt% of showed negligible difference in the resulting colony unit numbers, sample with 15wt% PEI shows stronger antibacterial efficiency which indicates that the killing efficiency is not linearly related to the concentration of PEI in the samples. After 24 hours of soaking, the samples showed an increase in the CFUs. This behaviour currently cannot be explained by our understanding of the system. It is likely that some compound is released from the polyurethane that either reduces the efficacy of antimicrobial compounds present in the solution or aids in the growth of the bacterial colonies. Interestingly, in all samples but 10% the colony counts reduce after 1 week of soaking. This could either be due to the degradation or reabsorption of the compound causing this behavior. Currently, there is no conclusive explanation for this behaviour and due to the magnitude of difference it could also be due to the variations of a biological system. Based on the assumption on reabsorption of these samples, an absorption test on sample films of PU, PU/5wt% PEI, PU/10wt% PEI and PU/15wt% PEI was applied to confirm the amount of absorption over 1 week of soaking. Additionally, it should be noted that multiple sets of this experiment were performed, but only the one was shown due to the O.D. measurements only being accurate to 1 order of magnitude of bacterial concentration. This led to significant variation when a new bacterial stock was used.

3.2.3.2 Absorption test

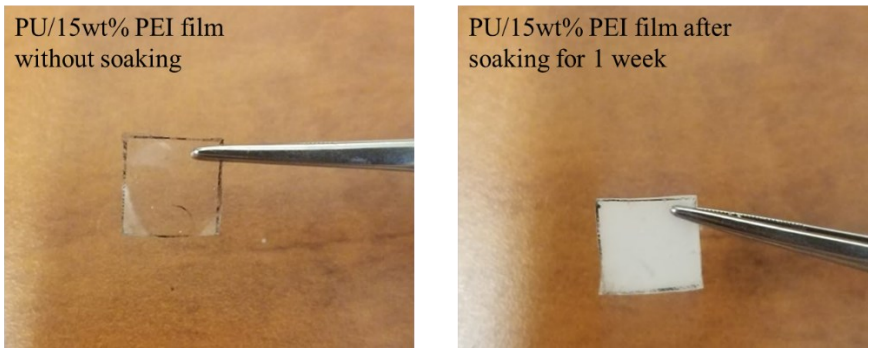

Figure 39. Visual change in PU/15wt% PEI film with soaking in DI water over 1 week.

Table 4. Thickness and weight changes of PU and PU/5wt%, 10wt%, 15wt% PEI soaking in DI water over 1 week. (N=3 replicates)

Sample films	Thickness change (%) after soaking for 7days	Weight change (%) after soaking for 7days	Weight loss (%) after drying out
PU	14.14±3.55	26.18±0.56	0.1127±0.53
PU/5wt%PEI	23.06±5.81	28.77±3.25	0.6229±0.13
PU/10wt%PEI	15.03±1.60	27.92±5.36	0.3924±0.06
PU/15wt%PEI	29.47±5.71	31.35±2.38	0.7092±0.50

$$Thickness\ change\ (\%) = \frac{thickness\ after\ soaking\ for\ 7\ days - original\ thickness}{original\ thickness}$$

$$Weight\ change\ (\%) = \frac{weight\ after\ soaking\ for\ 7\ days - original\ weight}{original\ weight}$$

$$Weight\ loss\ (\%) = \frac{original\ weight - weight\ after\ dring\ out}{original\ weight}$$

Fig. 39 shows the change in morphology of PU/15wt% PEI film after soaking in water over 1 week. This film changed from translucent to opaque with absorption of water, films with other concentration of PEI and PU film are not shown in figure but had the same phenomenon. This is the due to the refraction of light in the water PU matrix caused by the differences in the refractive index of water and PU.

From the results shown in Table. 4 above, the sample film with 15wt% PEI shows the most significant increase (47.09%) in thickness, PU sample shows the least change (15.53%) in thickness. From PU to PU/15wt% PEI, we can see the change in thickness is correlated to the increase in the concentration of PEI in the films. From the weight measurements we can see that the PU has the greatest increase in weight. This could be due to the PU without PEI not having significant ionic crosslinking allowing the chains to further extend and absorb more water. While the PEI containing PU composites showed greater thickness increase, but not a corresponding weight increase. This indicates the PEI containing samples are reducing in density and expanding, but not absorbing as much water as the neat PU.

3.3 Contact-killing antibacterial activity of PU/PEI colloid films

Despite claims and hypothesis of contact-killing surfaces discussed in Chapter 1, currently there is not an approval test can provide a direct investigation of contact-active antibacterial action. The most reliable and well-regarded method to prove this activity so far is by long-term leaching tests, constantly monitoring and comparing the antimicrobial performance of the concentrated washing solution with the polymer surface.

In addition, due to the high absorption of PU/PEI colloidal films, it was determined that agar plate counts were unreliable. This was due to the sample absorbing varying amounts of the bacterial solution leading to an unknown concentration of the bacterial solution removed from the sample and applied to the agar plate. Hence, a live-dead assay was applied in this project to more directly investigate the killing rate of bacterial cells on the sample surfaces.

3.3.1 Materials and instruments

3.3.1.1 Materials

Escherichia coli (*E. coli*) was used as the main bacteria for the antibacterial activity tests in this project. Lauryl sulfate broth purchased from Sigma Aldrich was used as the cultivation broth for *E. coli*. Agar plates were made of plate count agar from Difco. Phosphate buffered saline (0.01M) from Sigma Aldrich was used as buffer during the tests. Live/dead BacLight Bacterial Viability Kit (for microscopy & quantitative assays) from Thermo Fisher Scientific was used as fluorescent dye in this test.

3.3.1.2 Instruments

All glassware used in this experiment was sterilized in an auto clave. The bacterial broth was cultivated in a biological incubator. The mini centrifuge was used in the bacterial preparation step. The contacting steps of *E. coli* and sample films as well as the dying steps of the sample films after contact were completed in 24-well plate from Thermo Fisher Scientific. The concentration of *E. coli* suspension was determined by UV-Visible spectrophotometers in this test. Nikon Ti2 confocal microscope was used to observe the live-dead assay of *E. coli.*

3.3.2 Contact-active antibacterial activity of PU/PEI colloidal films

3.3.2.1 Fluorescent imaging

0.5 inch * 0.5 inch PU/PEI films with a PEI concentration of 0, 2, 5, 10, 12 and 15 wt% were soaked in DI water for 0, 1 h, 24 h, 48 h and over 1 week, and PDMS film with the same size as the control group were prepared as well. Each sample was placed in a cell of 24-well plate individually with a rubber ring pressed on the top of sample film as shown in Fig. 40 to ensure that the bacterial suspension only contact one surface (top surface) of the sample films and prevent the films from floating on the solution droplets, maximizing the contact area. Then 100 μL 10^8 cell/mL bacterial PBS suspension was applied to each cell into the rubber rings. A 1-hour contact of the bacterial suspension with the surfaces was provided after that. Next, the sample films were gently rinsed with PBS buffer to remove the excess bacterial cells which were not adhered on the surfaces to avoid the appearance of multilayers of cells under microscopic imaging. In addition, since the excess cells could pile up on the cells adhered on surfaces, they had no chance to contact the

surface, counting those number into the killing rate could show a significant error. After contacting, a LIVE/DEAD Bacterial Viability Kit was used for fluorescent imaging process. Following the instructions of the kit, 3 μL of compound A (SYTO9 and 3 μL of compound B (Propidium Iodide) were diluted in 1 mL PBS buffer, 100 μL dilution was then applied onto surface of each sample. The 24-well plate with samples being stained in were kept in the dark with the cover on to reduce the evaporation of solution within the plate for around 30 minutes. A rinse-off step was applied by PBS buffer in the end to remove the extra dye. Notably if the imaging is not implemented immediately, the stained samples need to be preserved at 4°C and wrapped with tinfoil to prevent light exposure.

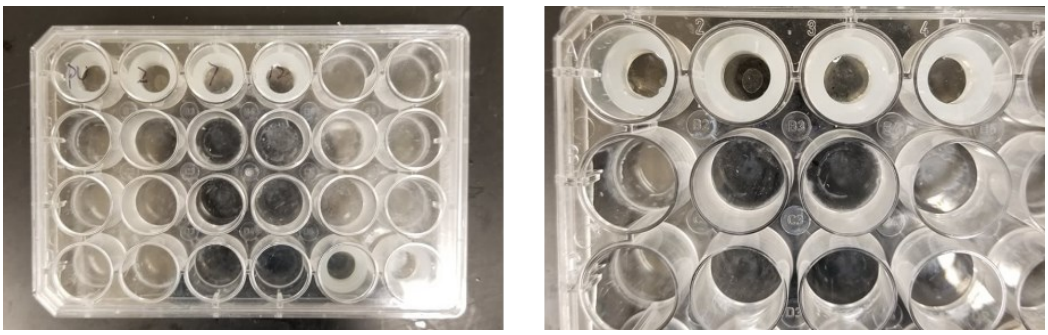

Figure 40. 24-well plate used in antibacterial live/dead assay.

The fluorescent images were taken by Nikon Ti2 confocal microscope with 40X magnification. This magnification was determined with laser off under optical mode of the microscope. To capture the live fluorescent images the light source was 488 nm and the measured wavelength was 520.5 nm. To capture the dead fluorescent images the light source used was 730 nm and the measured wavelength was 809.5 nm.

3.3.2.2 Image analysis

The images were analysed with Image J to find the total number of pixels that belong to live cells and the total that belong to dead cells. To generate this table, first each live or dead fluorescent image was filtered using the threshold function to get a black and white image where cells were black and the background was white. Once the live and dead images for a certain leaching time and PEI concentration were filtered, the 2 images were merged using the merge channel function with the live image representing the green channel and the dead image the red channel. Then to estimate the cells on the surface, the image was processed using the analyze particles function, since cells can agglomerate and this function would only count multiple cells as 1, the summed area of detected particles was used. This was performed twice, once with a red threshold for detection and once with a green threshold to detect live and dead cells independently. Once the number of pixels for the live and dead portions of the image were measured independently, they were plotted against each other for an estimate of the ratio of live to dead cells on the surface.

3.3.3 Results and discussions

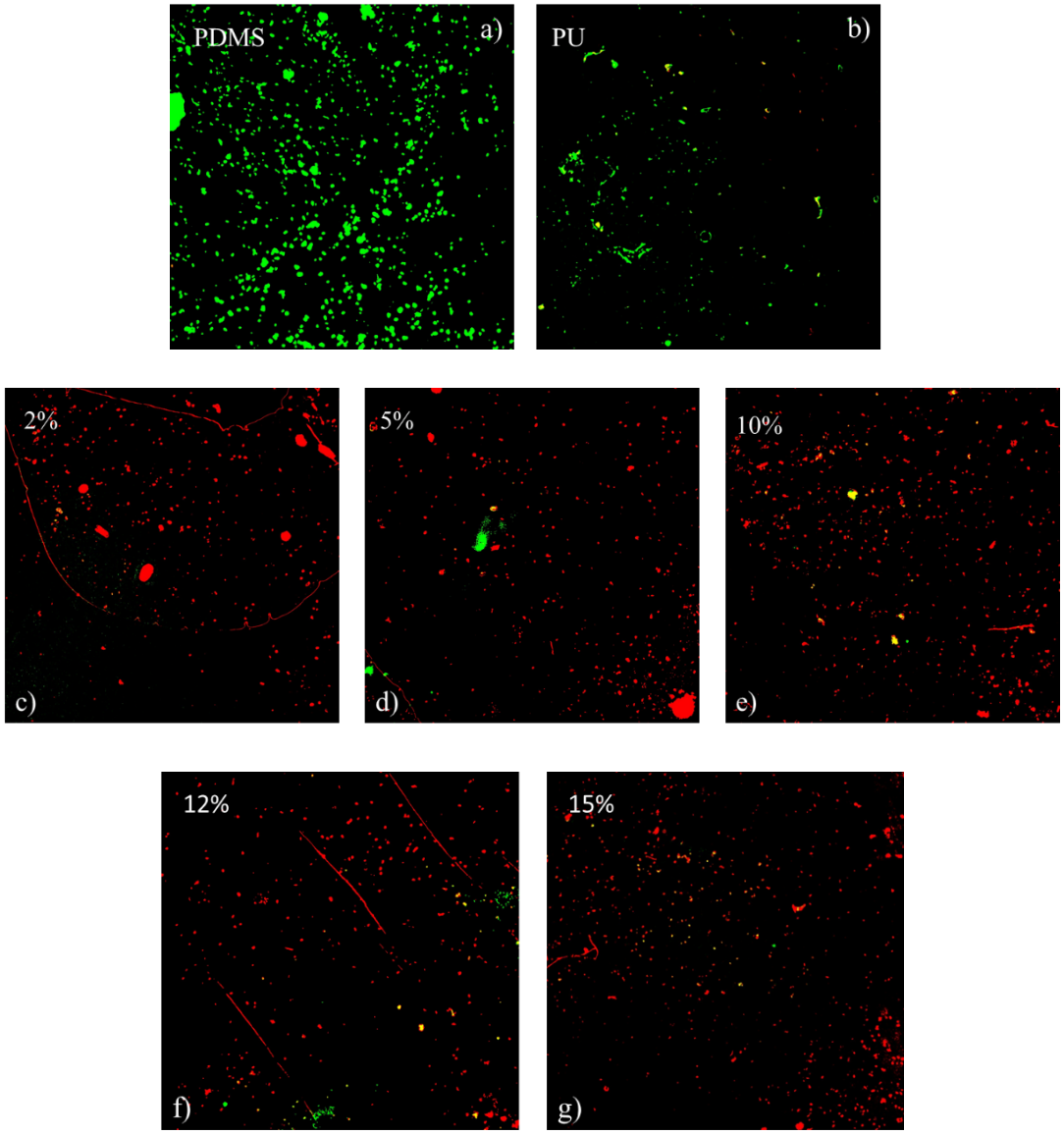

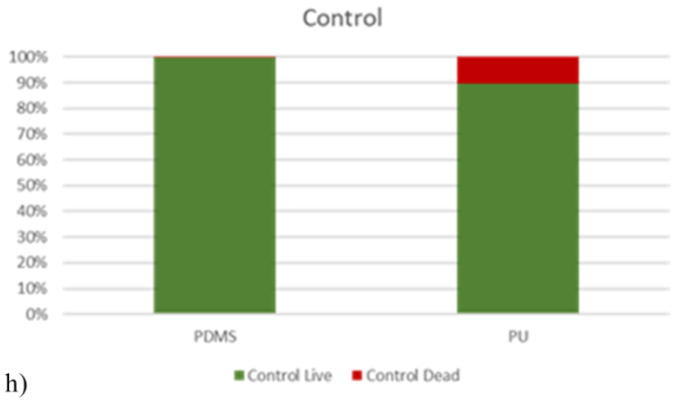

h)

Figure 41. E. coli dead (red) and alive (green) on a) PDMS surface; b) PU surface; c) PU/2wt%PEI surface; d) PU/5wt%PEI surface; e) PU/10wt%PEI surface; f) PU/12wt%PEI surface; g) PU/15wt%PEI surface; h) Killing rate of PDMS control surface and PU surface.

From the images shown above, the original PU film shows mostly green spots which is a similar result in antibacterial activity as the PDMS control surface shows. The table of killing efficiency further proved that both original PU film and PDMS control surface have negligible antibacterial activity with less than 10% killing rate. Conversely, the previous discussion of that the incorporation of even small amount of PEI can show significant antimicrobial activities has been proved in Fig. 41 c) and d), where with 2wt% and 5wt% PEI, the PU/PEI films barely have green spots on the surfaces. From the diagrams of killing rate, we can see that PU/2wt% PEI exhibited over 95% killing efficiency and over 80% killing efficiency was shown from PU/5wt% PEI of *E. coli.* From Fig. 41 e)-g), we see no appreciable increase in the rate of red spots over green spots. The diagrams of killing rate (as shown in Fig. 44-46) provided a more direct display of the killing efficiency. Around 90% killing rate of film with 10wt% PEI, 80% killing rate of PU/12wt% PEI and over 95% killing efficiency shown from PU/15wt% PEI. Respectively, comparing to films with low concentration (2wt% and 5wt%) of PEI, films with high PEI concentration did not shown

an apparent increase in bacterial killing efficiency. Therefore, for freshly prepared PU/PEI films, the killing efficiency is relatively consistent across the concentration range used in this work.

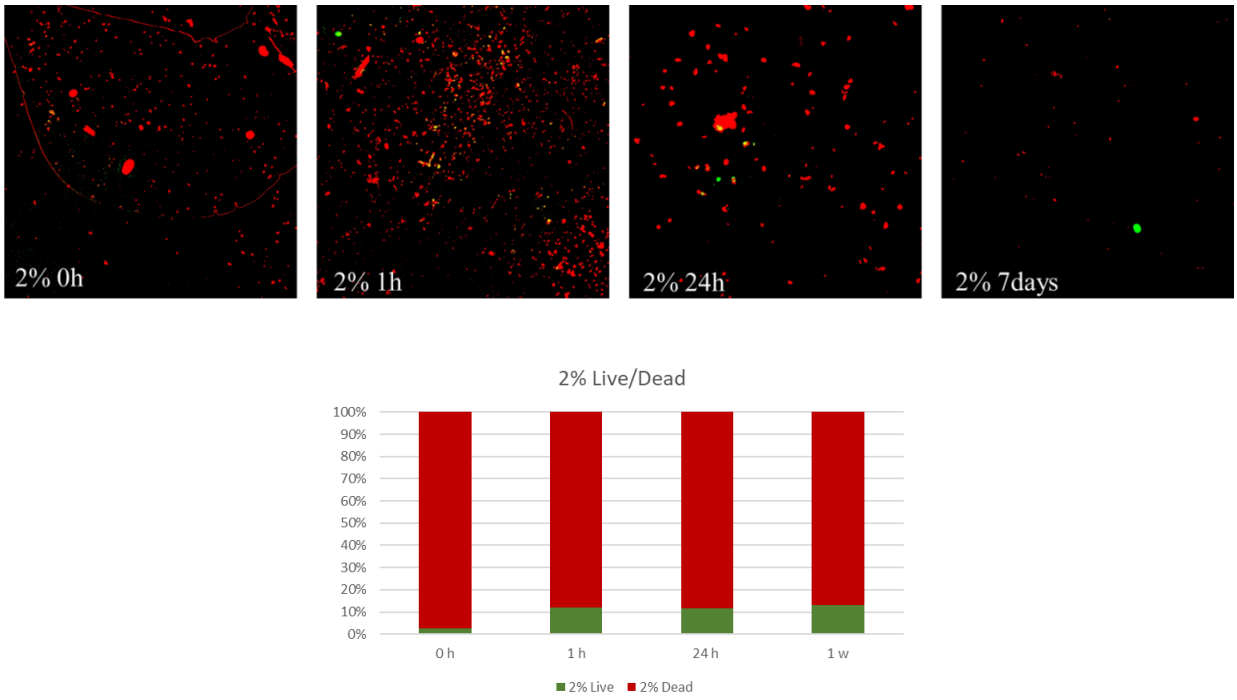

Figure 42. E. coli dead (red) and alive (green). Killing rate of PU/2wt% PEI surface with (left to right) 0, 1, 24 h and over 1 week leaching treatment.

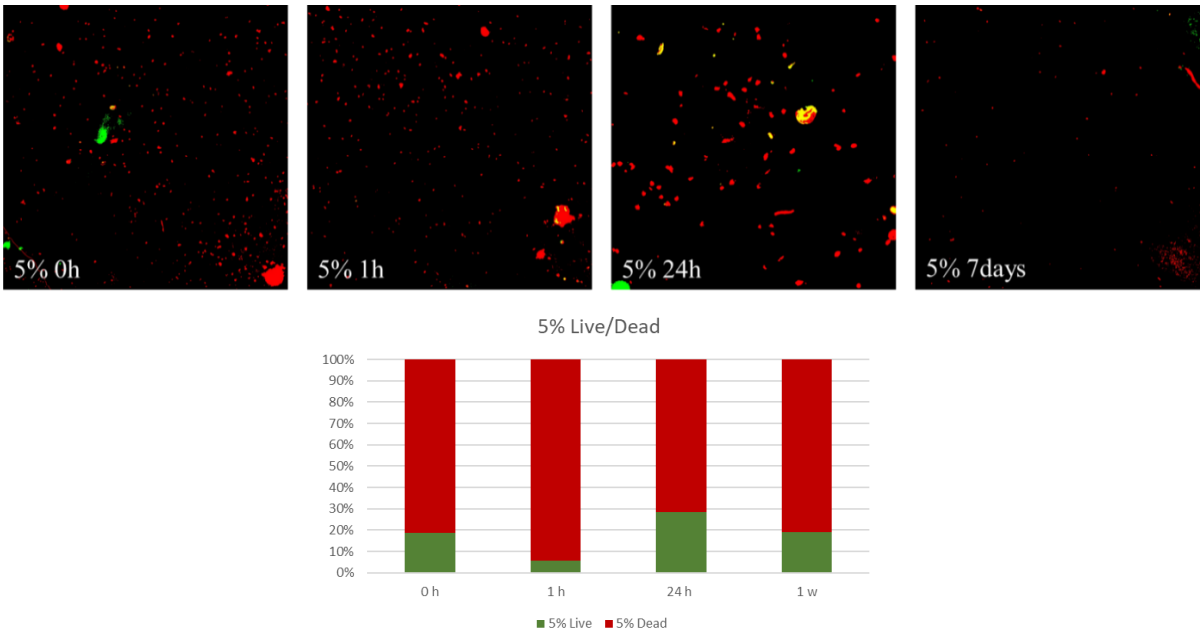

Figure 43. E. coli dead (red) and alive (green). Killing rate of PU/5wt% PEI surface with (left to right) 0, 1, 24 h and over 1 week leaching treatment.

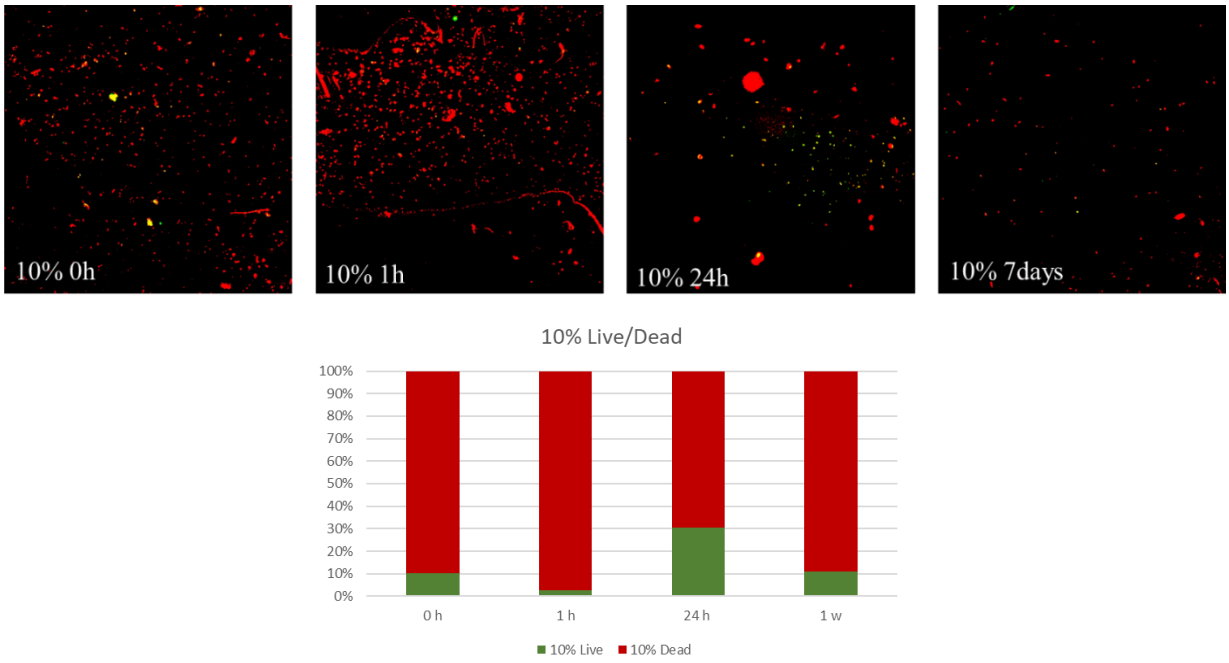

Figure 44. E. coli dead (red) and alive (green). Killing rate of PU/10wt% PEI surface with (left to right) 0, 1, 24 h and over 1 week leaching treatment.

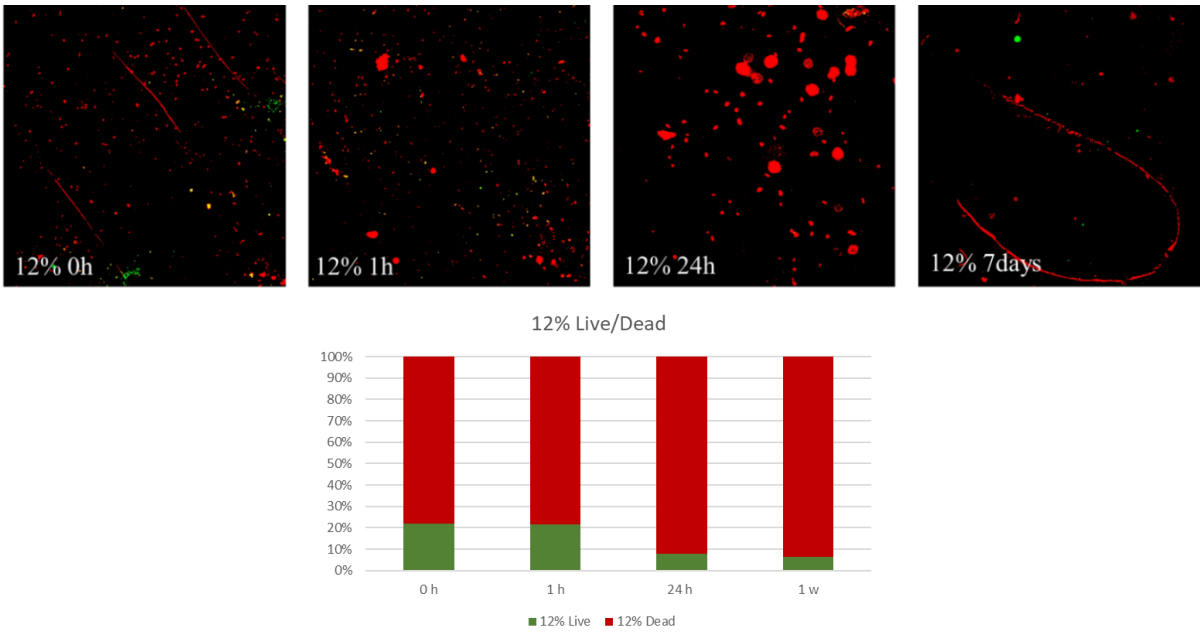

Figure 45. E. coli dead (red) and alive (green). Killing rate of PU/12wt% PEI surface with (left to right) 0, 1, 24 h and over 1 week leaching treatment.

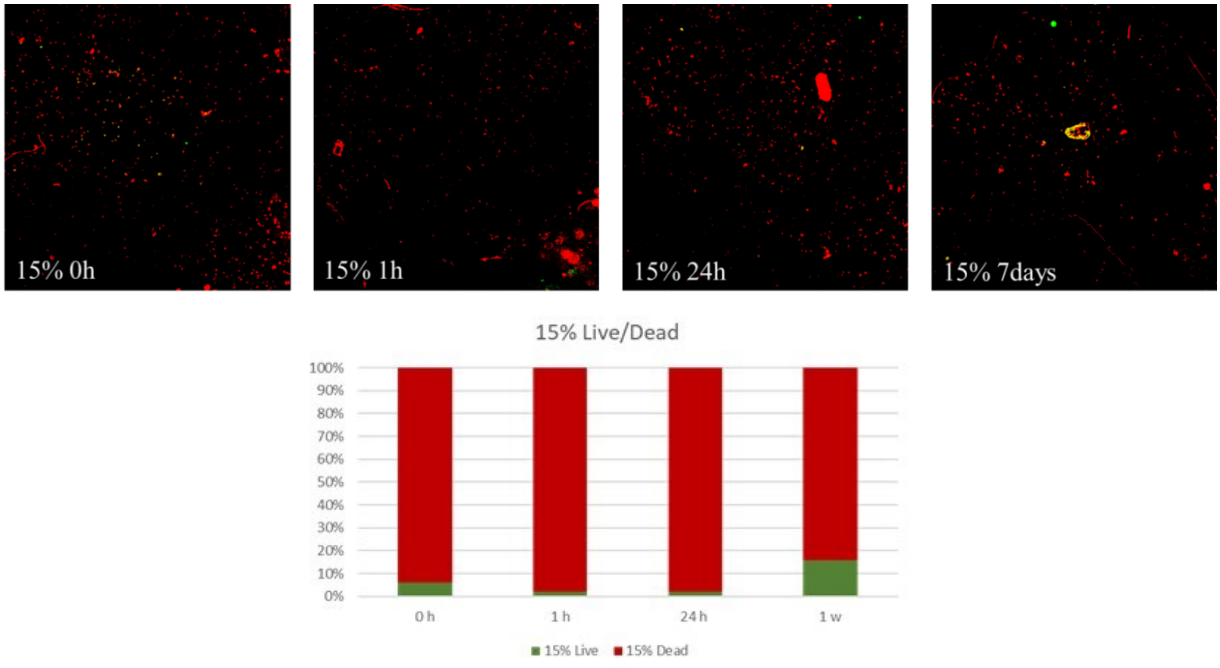

Figure 46. E. coli dead (red) and alive (green). Killing rate of PU/)15wt% PEI surface with (left to right) 0, 1, 24 h and over 1 week leaching treatment.

After comparing the bacterial killing rate with the increase on PEI in PU/PEI sample films. The influence from leaching time was also investigated. As seen in Fig. 42-46, we can see the general trends in the PU/PEI films as they are exposed to leaching for increasing periods of time. With concentration of 2wt%, 5wt% and 10wt% the killing efficiency tends to reduce around 10% with the washing time going from 0 hour to 24 hours. Over 24-hour leaching, the results of live/dead rate for 1-week leaching varied, but we noticed that the total amount of spots which refers to the number of cells on the surfaces reduced significantly comparing to the amount on sample surfaces with less leaching time. Therefore, the images were analysed with image j to find the total number of pixels that on each sample surface including all live cells and dead cells. As seen in Table. 5, over one week of soaking, the sum of cells on the surfaces of PU with 2wt%-10wt% PEI dramatically decreased comparing to the total pixel numbers on surfaces with shorter time of leaching, the greatest reduction of each concentration was up to around 1 order of magnitude. Based on this, we suspected that as the leaching time increased from 0 hour to 7 days, the adhesion of the surface was reduced with fewer spots seen in the fluorescent images and less pixels captured by the image analysis program. Interestingly, the exceptions were found of PU with 12wt% and 15wt% PEI, investigation from the number of pixels in Table. 5, the significant decrease did not occur in either PU/12wt% PEI or PU/15wt% PEI, which indicates the adhesion of PU films with 12wt% and 15wt% of PEI do not reduce after an extended leaching time. This was hypothesised to be due to the higher PEI concentration which allowed the surface to maintain its surface charge after extended contact with water. It is unlikely that leaching times in excess of 1 week would cause these surfaces to lose adhesion, as the ion-releasing results (Fig. 28) show a tapering off of release after 48 hours. Additionally, during the measurement of the fluorescent images, replicates were performed, but due to limitations with image processing they could not be included. The PU

film tended to be very absorbent, this was an issue analysing the images as some had stains of the fluorescent dye due to the “coffee ring effect” which were falsely identified as cells skewing results. Additionally, it appeared as though cells were absorbed into the sample as for certain samples it was impossible to focus on all the cells visible. It appeared as they resided on different focal planes leading to blurry cells not being identified during image analysis. For this reason, images that had these issues were excluded as they could not provide an accurate measure of the surface’s properties. However, the changes of cell numbers found in the performed images were large enough to be conclusive without a “T test”.

Table 5. The sum of pixels on PU/PEI surface image.

	0h	1h	24h	1 week
PU/2wt%PEI	22015	43928	13224	1631
PU/5wt%PEI	11770	14191	8812	2636
PU/10wt%PEI	26681	50322	13922	4119
PU/12wt%PEI	6721	15484	16747	14403
PU/15wt%PEI	26140	20860	22491	13728

Chapter 4. Antiviral property of the PU/PEI colloidal film.

4.1 Introduction

Quaternized PEI (QA-PEI) as a QACs polycation has been demonstrated to have antiviral activities against enveloped viruses, such as hepatitis B virus (HBV), hepatitis C virus (HCV), human immunodeficiency virus (HIV), and influenza viruses, since those viruses have a similar membrane structure to that of bacterial cells, constituting bilayers of phospholipid due to their infection and replication approaches[118]. As seen in Figure. 47, the antiviral working principle of QACs is supposed to follow the same route as its antibacterial action, disrupting the phospholipid bilayer of the viral membrane.

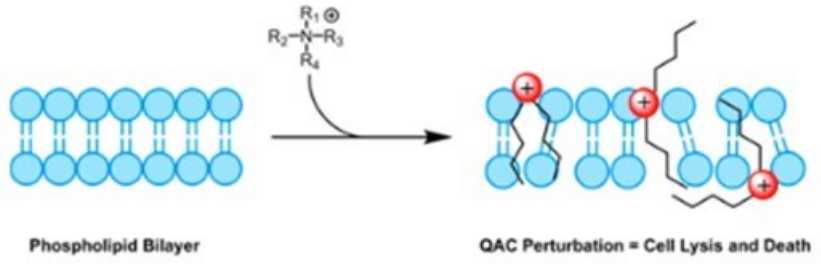

Figure 47. Concept of QACs' antibacterial and antiviral working principle[118]. Reproduced (adapted) with permission from ref 118. Copyright 2020 American Chemical Society.

In this project, baculovirus was used as the antiviral activity testing material of PU/PEI colloidal film because of its low cytotoxicity and biosafety as baculovirus are insect-specific viruses but not pathogenic to humans[129] with extra evidence provided by its incapability of replication within mammalian cells[130]. In addition, baculovirus was chosen in this work since it included a viral

envelope (as seen in Fig. 48) which could be targeted by QACs. However, the branched PEI used in this project was not quaternized. While it does not include quats, depending on conditions the tertiary amino groups in PEI can protonate. For this reason, we wanted to test the samples to see if the PEI could act as a pseudo QAC against enveloped viruses when immobilized within PU.

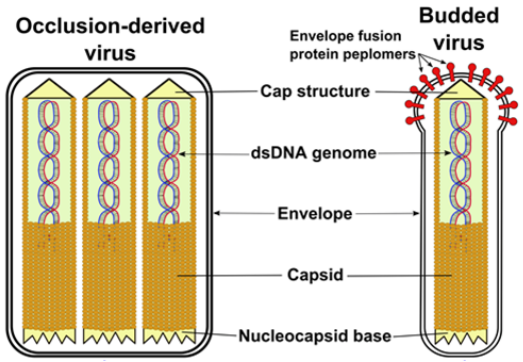

Figure 48. Structures of two virion phenotypes of baculovirus[131]. Reproduced with permission from ref 131. Copyright 2018 Microbiology Society.

4.2 Materials and instruments

4.2.1 Materials

Baculovirus (Autographa californica multiple nucleopolyhedrovirus) (AcMNPV) vector (from Applied Virus and Complex Biologics Bioprocessing Research Lab) was used as testing virus in this work. mKOκ (a red fluorescent protein) was used to measure expression of the baculovirus. Sf-9 (ATCC CRL-1711) insect cells were applied as the viral hosts in end-point dilution assays, and the cell growth medium was Sf-900 III SFM purchased from Thermo Fisher Scientific.

4.2.2 Instruments

Sample surfaces were sterilized by UV-C irradiation. A 6-well plate was used while applying the virus suspension onto surfaces, and a 96-well plate (96 F plate) from VWR was used for the end-point dilution assay. A fluorescent microscope from Zeiss Axiovert 200 with HBO 50 and HAL 100 was applied to observe the quantity of virus as determined by the red fluorescent protein.

4.3 Antiviral experiments of PU/PEI colloidal films

PU and PU/15wt% PEI sample films were sterilized by UV-C irradiation for 1 minute with a dose of approximately 10 mJ/cm^2.

In the preliminary test, a plastic control, a control surface of PU film and testing surface of PU/12wt% PEI were prepared. Then 25 μL of the cultured virus suspension (was applied to each surface in a 6-well plate. The viral droplets were left on the surfaces for approximately 2 hours with the plates being covered to prevent the droplets being dried out. After that, the virus droplets were resuspended in the inset cell growth medium Sf-900 III SFM. Notably, only one time point was performed for the testing surface of PU/12wt% PEI as an exploratory experiment to see if any effect was visible before the comprehensive test was performed.

In the comprehensive test, a plastic control, a control surface of PU film and testing surface of PU/15wt% PEI were prepared. Similarly, 25 μL of the cultured virus suspension same initial concentration as used in the preliminary test) was applied to each surface. To optimize the testing method, the droplets were allowed to dry at ambient conditions. In addition, virus droplets tended

to dry out after approximately 1.5 hours. The samples were covered up after drying and let sit at room temperature for 8 hours. Then 250 μL of DI water was then repeatedly pipetted on to the area where the virus solution had dried and then drawn back into the micropipette. Due to the 1 in 10 dilution that occurred the assay numbers found during quantification were multiplied by a factor of 10.

In both preliminary and comprehensive tests, baculovirus were quantified by an end-point dilution assay on confluent monolayers of *Spodoptera frugiperda* insect cells [Sf9 (ATCC CRL-1711)] in a 96-well plate. Wells were scored as positive or negative for virus by the presence or absence of red fluorescence when observed under a fluorescent microscope with excitation wavelength around 520 nm and emission wavelength around 570 nm.

4.4 Results and discussion

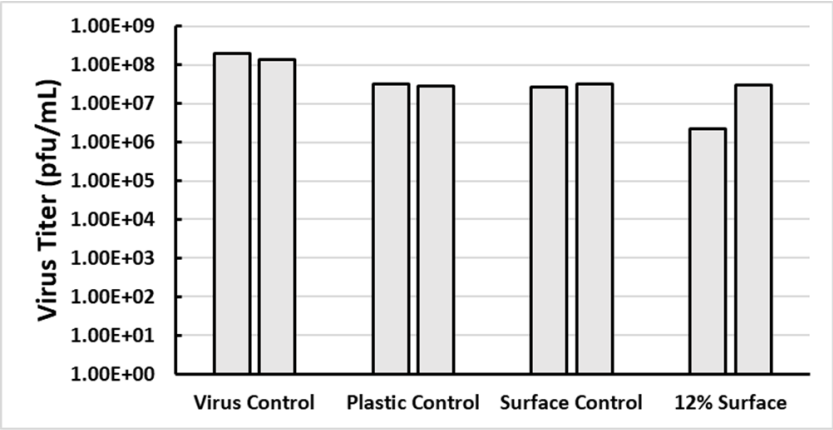

Figure 49. Preliminary end-point dilution assay results of PU/12wt% PEI.

The antiviral results of PU/PEI films in the preliminary test, as shown in Fig. 49. The reduction in virus titer was shown in the group of surface control (neat PU films) comparing to the virus control, which is expected, and it normally occurs. In addition, it is positive that there is no significant difference showing in the virus titer results between the group of surface control (neat PU) and the plastic control surfaces, which means it is expected to be easy to resuspend the virus from the sample surfaces after the step of contact. However, the results seen in Fig. 49 of PU/12wt% PEI films varied between two replicates. The value of virus titer in one of the duplicates showed approximately the same as the results of control surfaces while the other duplicate appeared to have about a 1-log reduction in viral titer. Hence, the replicate showed reduction in viral titer result was suspected to be an outlier. Additionally, it was also hypothesized that it was due to the minor contact of the virus and sample surface (PU/12wt% PEI film). Since the size and weight of virus were tiny, when the viral droplet was applied onto the sample surface, the virus in the droplet did not contact the surface sufficiently as they could not settle out of the solution and allow for the PEI to damage their membrane on contact. Based on these hypotheses, the testing method was optimized with the viral droplet was allowed to dry out on the surface during the contact time.

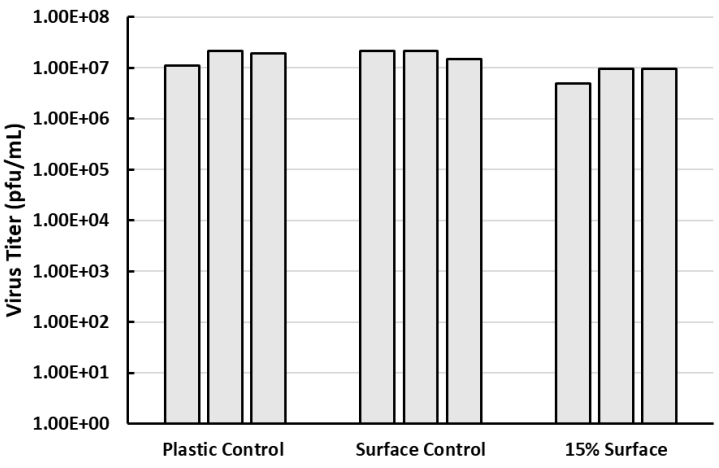

Sample ID	Virus Titer (pfu/mL)
Plastic Control A	1.11E+07
Plastic Control B	2.18E+07
Plastic Control C	1.89E+07
Surface Control A	2.18E+07
Surface Control B	2.18E+07
Surface Control C	1.49E+07
15% Surface A	4.97E+06
15% Surface B	9.59E+06
15% Surface C	9.59E+06

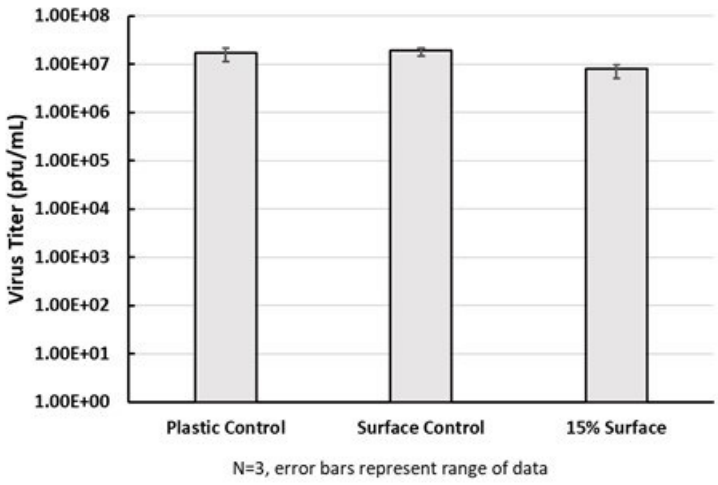

Figure 50. Comprehensive end-point dilution assay results of PU/15wt% PEI.

As seen in Fig. 50, the viral titer of plastic controls lost about 1-log virus titer comparing to the virus control in Fig. 49, which is expected with the viral droplets being dried out on the surfaces. (Since the initial concentration was the same in both the exploratory experiment and the comprehensive test, the results of virus control are supposed to show same value in viral titer.) In addition, as our expectation, similar virus recovery showed in the control group of plastic surfaces and the group of surface control (neat PU films). The resulting virus titer of PU/15wt% PEI sample surfaces is slightly lower than it of the plastic control and neat PU surface control with a reduction

of less than 0.5-log. However, an inactivation over 1-log in virus titer is typically conclusive in virucidal effects, the PU/15wt% PEI sample surfaces did not show sufficient evidence to conclude its antiviral property. It is unclear why the PU/PEI composites did not show significant killing efficiency. One hypothesis is the structure of the baculovirus. There are two phenotypes of baculovirus as shown in Fig. 48, occlusion-derived virus (ODV form) and budded virus (BV form). The envelope structure of phospholipid bilayer exists in both phenotypes. However, the composition of envelope structure varies in these two forms such as phosphatidylserine is contained in BV's envelope while phosphatidylcholine is the composition of ODV's envelope structure[132]. The effects of these differences on virucidal activity requires further studies. More likely as we discussed above, within a neutral solution PEI with positive charges is more likely to act as a vector of gene delivery with its lysosomal buffering capacity[121–123]rather than antiviral agent.

Chapter 5. Conclusions and future work

5.1 Conclusions

The main goal of this project is to evaluate the antimicrobial activities including multifunctional antibacterial activity with both ion-releasing and contact-active working principles, and antiviral activity of the PU/PEI colloidal film. After the successful synthesis of waterborne PU and incorporation of PEI into PU emulsion was confirmed by the FTIR results, the results of DLS and Zeta-potential stated the stability of this PU/PEI emulsion. In addition, tensile test and contact angle measurements proved that the incorporation PEI into PU colloidal system did not significantly affect its mechanical property. Based on the understanding of PU/PEI crosslinked network (as shown in Fig. 25), it was suspected that the highest wt% of PEI introduced in PU in this project (15wt%) was not excess the threshold of ion concentration to over-crosslink the PU/PEI network, leading to a reduction in mechanical properties. Furthermore, PU/PEI colloidal films showed significant abrasion resistance during the scratch test. Overall, mechanical tests concluded excellent mechanical properties of this PU/PEI colloidal film and the best mechanical properties shown in both scratch test and tensile test at 5wt%.

Results shown in the ion-releasing antibacterial experiment within 24 hours followed the same trend as the conductivity test of PEI cations' leaching. However, the increase of CFUs after 24h could not be proved by changes of the conductivity curve. This was hypothesized due to some unclear compounds leaching out from PU films interfered the antibacterial activity of PEI in

solution. The reduction of colony unit forms after 1 week also cannot be explained. Additionally, the change of colony unit forms with the increase of PEI concentration was not as expected showing linear relation, this was also found in the contact-active antibacterial experiment. Significant antibacterial activity of PU/PEI films was noticed in contact-active antibacterial test with over 80% killing rate showing in all sample films. Meanwhile, it was found that with low wt% PEI (2-10wt%), the adhesion of bacterial cells reduced over 1-week leaching time, but this behavior did not occur in PU with high wt% PEI (12wt%-15wt%). Though minor decrease of the virus titer was found in the antiviral test of PU/PEI films, with a less than 0.5-log reduction, the virucidal property of such material cannot be concluded.

5.2 Future work

To further build on the work presented above, future work should focus on further characterization of the PU/PEI composites investigated. One important area to focus on is the leaching behaviour of the PU/PEI samples. It is likely unknown compounds in the leaching solution interfered with the ion-releasing antibacterial results. In addition, an optimal experimental method for conductivity test could better support the existence of the ion-releasing antibacterial activity of PU/PEI colloidal films. The optimization can be achieved by improving the PEI calibration curve, such as instead of using DI water, making PEI calibration in DI water with PU films soaked in with the consideration of the leaching of other unknown molecules.

More fundamentally, it is currently unclear of the details of how the PU/PEI composites are structured and a further characterization of the ionic interaction of PU and PEI would be helpful to determine the method of bonding in between these two components. Additionally, it would be

useful to investigate the composition of the surface through atomic force microscopy to determine if higher PEI wt% samples have homogeneously or heterogeneously dispersed PEI, this could be done with a functionalized probe to detect the charges in PEI.

To improve the antibacterial tests, more replicates should be included to remove variation of the biological system, providing more analytical results. Additionally, an additional PEI solution control group can also be added into antiviral experiments to test the virucidal effect of PEI polycation on baculovirus. Also, more types of enveloped virus should be tested with PU/PEI films, especially ones that have been used in previous QACs virucidal activity studies, such as influenza viruses. Furthermore, adding a quaternization step of PEI to form QA-PEI might improve its antibacterial and antiviral activities but it is not clear how it could affect the formation of PU/PEI colloidal film. Future investigations are needed.

References

(1) HAI Data | CDC https://www.cdc.gov/hai/data/index.html (accessed 2021 -05 -12).

(2) Wei, T.; Tang, Z.; Yu, Q.; Chen, H. Smart Antibacterial Surfaces with Switchable Bacteria-Killing and Bacteria-Releasing Capabilities. *ACS Appl. Mater. Interfaces* **2017**, *9* (43), 37511–37523. https://doi.org/10.1021/acsami.7b13565.

(3) Si, P. Water Based Polyurethane Multi-Functional Composites, University of Waterloo, 2020.

(4) Si, P.; Jiang, F.; Cheng, Q. S.; Rivers, G.; Xie, H.; Kyaw, A. K. K.; Zhao, B. Triple Non-Covalent Dynamic Interactions Enabled a Tough and Rapid Room Temperature Self-Healing Elastomer for next-Generation Soft Antennas. *J. Mater. Chem. A* **2020**, *8* (47), 25073–25084. https://doi.org/10.1039/D0TA06613C.

(5) Cornell, R. J.; Donaruma, L. G. 2-METHACRYLOXYTROPONES. INTERMEDIATES FOR THE SYNTHESIS OF BIOLOGICALLY ACTIVE POLYMERS. *J. Med. Chem.* **1965**, *8*, 388–390. https://doi.org/10.1021/jm00327a025.

(6) Siedenbiedel, F.; Tiller, J. C. Antimicrobial Polymers in Solution and on Surfaces: Overview and Functional Principles. *Polymers* **2012**, *4* (1), 46–71. https://doi.org/10.3390/polym4010046.

(7) Vogl, O.; Tirrell, D. Functional Polymers with Biologically Active Groups. *J. Macromol. Sci. Part - Chem.* **1979**, *13* (3), 415–439. https://doi.org/10.1080/00222337908068110.

(8) Panarin, E. F.; Solovskii, M. V.; Ekzemplyarov, O. N. Synthesis and Anti Microbial Properties of Polymers Containing Quaternary Ammonium Groups. *Pharm. Chem. J. Engl. Transl. Khimiko-Farmatsevticheskii Zhurnal* **1972**, *5* (7), 406–4081971.

(9) Julieta. Bioseguridad: Recent Advances in Antimicrobial Polymers: A Mini-Review. *Bioseguridad*, 2016.

(10) López, D.; Vlamakis, H.; Kolter, R. Biofilms. *Cold Spring Harb. Perspect. Biol.* **2010**, *2* (7), a000398. https://doi.org/10.1101/cshperspect.a000398.

(11) Hall-Stoodley, L.; Costerton, J. W.; Stoodley, P. Bacterial Biofilms: From the Natural Environment to Infectious Diseases. *Nat. Rev. Microbiol.* **2004**, *2* (2), 95–108. https://doi.org/10.1038/nrmicro821.

(12) Aggarwal, S.; Stewart, P. S.; Hozalski, R. M. Biofilm Cohesive Strength as a Basis for Biofilm Recalcitrance: Are Bacterial Biofilms Overdesigned? *Microbiol. Insights* **2016**, *8* (Suppl 2), 29–32. https://doi.org/10.4137/MBI.S31444.

(13) Peddinti, B. S. T.; Scholle, F.; Vargas, M. G.; Smith, S. D.; Ghiladi, R. A.; Spontak, R. J. Inherently Self-Sterilizing Charged Multiblock Polymers That Kill Drug-Resistant Microbes in Minutes. *Mater. Horiz.* **2019**, *6* (10), 2056–2062. https://doi.org/10.1039/C9MH00726A.

(14) Vasudevan, R. Biofilms: Microbial Cities of Scientific Significance. *J. Microbiol. Exp.* **2014**, *1* (3). https://doi.org/10.15406/jmen.2014.01.00014.

(15) Zhang, H.; Chiao, M. Anti-Fouling Coatings of Poly(Dimethylsiloxane) Devices for Biological and Biomedical Applications. *J. Med. Biol. Eng.* **2015**, *35* (2), 143–155. https://doi.org/10.1007/s40846-015-0029-4.

(16) Francolini, I.; Donelli, G.; Crisante, F.; Taresco, V.; Piozzi, A. Antimicrobial Polymers for Anti-Biofilm Medical Devices: State-of-Art and Perspectives. *Adv. Exp. Med. Biol.* **2015**, *831*, 93–117. https://doi.org/10.1007/978-3-319-09782-4_7.

(17) Liu, L.; Li, W.; Liu, Q. Recent Development of Antifouling Polymers: Structure, Evaluation, and Biomedical Applications in Nano/Micro-Structures. *Wiley Interdiscip. Rev. Nanomed. Nanobiotechnol.* **2014**, *6* (6), 599–614. https://doi.org/10.1002/wnan.1278.

(18) Ye, Q.; Zhou, F. Antifouling Surfaces Based on Polymer Brushes. In *Antifouling Surfaces and Materials: From Land to Marine Environment*; Zhou, F., Ed.; Springer: Berlin, Heidelberg, 2015; pp 55–81. https://doi.org/10.1007/978-3-662-45204-2_3.

(19) Yu, K.; Mei, Y.; Hadjesfandiari, N.; Kizhakkedathu, J. N. Engineering Biomaterials Surfaces to Modulate the Host Response. *Colloids Surf. B Biointerfaces* **2014**, *124*, 69–79. https://doi.org/10.1016/j.colsurfb.2014.08.009.

(20) GRIESSER, H. J.; Doran, M. R.; MICHL, T. D.; KRASIMIR, A. V. Bacteriostatic Surfaces. WO2015184492A1, December 10, 2015.

(21) Xue, Y.; Xiao, H.; Zhang, Y. Antimicrobial Polymeric Materials with Quaternary Ammonium and Phosphonium Salts. *Int. J. Mol. Sci.* **2015**, *16* (2), 3626–3655. https://doi.org/10.3390/ijms16023626.

(22) Pankey, G. A.; Sabath, L. D. Clinical Relevance of Bacteriostatic versus Bactericidal Mechanisms of Action in the Treatment of Gram-Positive Bacterial Infections. *Clin. Infect. Dis.* **2004**, *38* (6), 864–870. https://doi.org/10.1086/381972.

(23) Fernandes, P. B.; Bailer, R.; Swanson, R.; Hanson, C. W.; McDonald, E.; Ramer, N.; Hardy, D.; Shipkowitz, N.; Bower, R. R.; Gade, E. In Vitro and in Vivo Evaluation of A-56268 (TE-031), a New Macrolide. *Antimicrob. Agents Chemother.* **1986**, *30* (6), 865–873. https://doi.org/10.1128/aac.30.6.865.

(24) Observations on Mode of Action of Erythromycin. - Thomas H. Haight, Maxwell Finland, 1952 https://journals.sagepub.com/doi/abs/10.3181/00379727-81-19817 (accessed 2021 -05 -13).

(25) Piscitelli, S. C.; Danziger, L. H.; Rodvold, K. A. Clarithromycin and Azithromycin: New Macrolide Antibiotics. *Clin. Pharm.* **1992**, *11* (2), 137–152.

(26) Retsema, J.; Girard, A.; Schelkly, W.; Manousos, M.; Anderson, M.; Bright, G.; Borovoy, R.; Brennan, L.; Mason, R. Spectrum and Mode of Action of Azithromycin (CP-62,993), a New 15-Membered-Ring Macrolide with Improved Potency against Gram-Negative Organisms. *Antimicrob. Agents Chemother.* **1987**, *31* (12), 1939–1947. https://doi.org/10.1128/aac.31.12.1939.

(27) Feder, H. M.; Osier, C.; Maderazo, E. G. Chloramphenicol: A Review of Its Use in Clinical Practice. *Rev. Infect. Dis.* **1981**, *3* (3), 479–491. https://doi.org/10.1093/clinids/3.3.479.

(28) Rahal, J. J.; Simberkoff, M. S. Bactericidal and Bacteriostatic Action of Chloramphenicol against Memingeal Pathogens. *Antimicrob. Agents Chemother.* **1979**, *16* (1), 13–18. https://doi.org/10.1128/aac.16.1.13.

(29) Turk, D. C. A Comparison of Chloramphenicol and Ampicillin as Bactericidal Agents for Haemophilus Influenzae Type B. *J. Med. Microbiol.* **1977**, *10* (1), 127–131. https://doi.org/10.1099/00222615-10-1-127.

(30) Weeks, J. L.; Mason, E. O.; Baker, C. J. Antagonism of Ampicillin and Chloramphenicol for Meningeal Isolates of Group B Streptococci. *Antimicrob. Agents Chemother.* **1981**, *20* (3), 281–285. https://doi.org/10.1128/aac.20.3.281.

(31) Bostic, G. D.; Perri, M. B.; Thal, L. A.; Zervos, M. J. Comparative in Vitro and Bactericidal Activity of Oxazolidinone Antibiotics against Multidrug-Resistant Enterococci. *Diagn. Microbiol. Infect. Dis.* **1998**, *30* (2), 109–112. https://doi.org/10.1016/s0732-8893(97)00210-1.

(32) Zurenko, G. E.; Yagi, B. H.; Schaadt, R. D.; Allison, J. W.; Kilburn, J. O.; Glickman, S. E.; Hutchinson, D. K.; Barbachyn, M. R.; Brickner, S. J. In Vitro Activities of U-100592 and U-100766, Novel Oxazolidinone Antibacterial Agents. *Antimicrob. Agents Chemother.* **1996**, *40* (4), 839–845. https://doi.org/10.1128/AAC.40.4.839.

(33) Delgado, G.; Neuhauser, M. M.; Bearden, D. T.; Danziger, L. H. Quinupristin-Dalfopristin: An Overview. *Pharmacotherapy* **2000**, *20* (12), 1469–1485. https://doi.org/10.1592/phco.20.19.1469.34858.

(34) Lamb, H. M.; Figgitt, D. P.; Faulds, D. Quinupristin/Dalfopristin: A Review of Its Use in the Management of Serious Gram-Positive Infections. *Drugs* **1999**, *58* (6), 1061–1097. https://doi.org/10.2165/00003495-199958060-00008.

(35) Jain, A.; Duvvuri, L. S.; Farah, S.; Beyth, N.; Domb, A. J.; Khan, W. Antimicrobial Polymers. *Adv. Healthc. Mater.* **2014**, *3* (12), 1969–1985. https://doi.org/10.1002/adhm.201400418.

(36) Demir, B.; Broughton, R. M.; Qiao, M.; Huang, T.-S.; Worley, S. D. N-Halamine Biocidal Materials with Superior Antimicrobial Efficacies for Wound Dressings. *Molecules* **2017**, *22* (10), 1582. https://doi.org/10.3390/molecules22101582.

(37) Martins, A. F.; Facchi, S. P.; Follmann, H. D. M.; Pereira, A. G. B.; Rubira, A. F.; Muniz, E. C. Antimicrobial Activity of Chitosan Derivatives Containing N-Quaternized Moieties in Its Backbone: A Review. *Int. J. Mol. Sci.* **2014**, *15* (11), 20800–20832. https://doi.org/10.3390/ijms151120800.

(38) Chamy, R. *Biodegradation: Life of Science*; BoD – Books on Demand, 2013.

(39) Aquino, R. P.; Auriemma, G.; Mencherini, T.; Russo, P.; Porta, A.; Adami, R.; Liparoti, S.; Della Porta, G.; Reverchon, E.; Del Gaudio, P. Design and Production of Gentamicin/Dextrans Microparticles by Supercritical Assisted Atomisation for the Treatment of Wound Bacterial Infections. *Int. J. Pharm.* **2013**, *440* (2), 188–194. https://doi.org/10.1016/j.ijpharm.2012.07.074.

(40) Hornyák, I.; Madácsi, E.; Kalugyer, P.; Vácz, G.; Horváthy, D. B.; Szendrői, M.; Han, W.; Lacza, Z. Increased Release Time of Antibiotics from Bone Allografts through a Novel Biodegradable Coating. *BioMed Res. Int.* **2014**, *2014*, 459867. https://doi.org/10.1155/2014/459867.

(41) Macha, I. J.; Cazalbou, S.; Ben-Nissan, B.; Harvey, K. L.; Milthorpe, B. Marine Structure Derived Calcium Phosphate-Polymer Biocomposites for Local Antibiotic Delivery. *Mar. Drugs* **2015**, *13* (1), 666–680. https://doi.org/10.3390/md13010666.

(42) Su, L.-C.; Xie, Z.; Zhang, Y.; Nguyen, K. T.; Yang, J. Study on the Antimicrobial Properties of Citrate-Based Biodegradable Polymers. *Front. Bioeng. Biotechnol.* **2014**, *2*, 23. https://doi.org/10.3389/fbioe.2014.00023.

(43) Tashiro, T. Antibacterial and Bacterium Adsorbing Macromolecules. *Macromol. Mater. Eng.* **2001**, *286* (2), 63–87. https://doi.org/10.1002/1439-2054(20010201)286:2<63::AID-MAME63>3.0.CO;2-H.

(44) Kawabata, N. Capture of Micro-Organisms and Viruses by Pyridinium-Type Polymers and Application to Biotechnology and Water Purification. *Prog. Polym. Sci.* **1992**, *17* (1), 1–34. https://doi.org/10.1016/0079-6700(92)90015-Q.

(45) Nathan, A.; Zalipsky, S.; Ertel, S. I.; Agathos, S. N.; Yarmush, M. L.; Kohn, J. Copolymers of Lysine and Polyethylene Glycol: A New Family of Functionalized Drug Carriers. *Bioconjug. Chem.* **1993**, *4* (1), 54–62. https://doi.org/10.1021/bc00019a008.

(46) Dizman, B.; Elasri, M. O.; Mathias, L. J. Synthesis, Characterization, and Antibacterial Activities of Novel Methacrylate Polymers Containing Norfloxacin. *Biomacromolecules* **2005**, *6* (1), 514–520. https://doi.org/10.1021/bm049383+.

(47) Lawson, M. C.; Shoemaker, R.; Hoth, K. B.; Bowman, C. N.; Anseth, K. S. Polymerizable Vancomycin Derivatives for Bactericidal Biomaterial Surface Modification:

Structure−Function Evaluation. *Biomacromolecules* **2009**, *10* (8), 2221–2234. https://doi.org/10.1021/bm900410a.

(48) Turos, E.; Shim, J.-Y.; Wang, Y.; Greenhalgh, K.; Reddy, G. S. K.; Dickey, S.; Lim, D. V. Antibiotic-Conjugated Polyacrylate Nanoparticles: New Opportunities for Development of Anti-MRSA Agents. *Bioorg. Med. Chem. Lett.* **2007**, *17* (1), 53–56. https://doi.org/10.1016/j.bmcl.2006.09.098.

(49) Timofeeva, L.; Kleshcheva, N. Antimicrobial Polymers: Mechanism of Action, Factors of Activity, and Applications. *Appl. Microbiol. Biotechnol.* **2011**, *89* (3), 475–492. https://doi.org/10.1007/s00253-010-2920-9.

(50) Deka, S. R.; Sharma, A. K.; Kumar, P. Cationic Polymers and Their Self-Assembly for Antibacterial Applications. *Curr. Top. Med. Chem.* **2015**, *15* (13), 1179–1195. https://doi.org/10.2174/1568026615666150330110602.

(51) Kanazawa, A.; Ikeda, T.; Endo, T. Antibacterial Activity of Polymeric Sulfonium Salts. *J. Polym. Sci. Part Polym. Chem.* **1993**, *31* (11), 2873–2876. https://doi.org/10.1002/pola.1993.080311126.

(52) Polymeric phosphonium salts as a novel class of cationic biocides. IV. Synthesis and antibacterial activity of polymers with phosphonium salts in the main chain - Kanazawa - 1993 - Journal of Polymer Science Part A: Polymer Chemistry - Wiley Online Library https://onlinelibrary.wiley.com/doi/abs/10.1002/pola.1993.080311219 (accessed 2021 -05 - 17).

(53) Kanazawa, A.; Ikeda, T.; Endo, T. Novel Polycationic Biocides: Synthesis and Antibacterial Activity of Polymeric Phosphonium Salts. *J. Polym. Sci. Part Polym. Chem.* **1993**, *31* (2), 335–343. https://doi.org/10.1002/pola.1993.080310205.

(54) Pasquier, N.; Keul, H.; Heine, E.; Moeller, M.; Angelov, B.; Linser, S.; Willumeit, R. Amphiphilic Branched Polymers as Antimicrobial Agents. *Macromol. Biosci.* **2008**, *8* (10), 903–915. https://doi.org/10.1002/mabi.200800121.

(55) Beyth, N.; Farah, S.; Domb, A. J.; Weiss, E. I. Antibacterial Dental Resin Composites. *React. Funct. Polym.* **2014**, *75*, 81–88. https://doi.org/10.1016/j.reactfunctpolym.2013.11.011.

(56) Tew, G. N.; Scott, R. W.; Klein, M. L.; DeGrado, W. F. De Novo Design of Antimicrobial Polymers, Foldamers, and Small Molecules: From Discovery to Practical Applications. *Acc. Chem. Res.* **2010**, *43* (1), 30–39. https://doi.org/10.1021/ar900036b.

(57) Tew, G. N.; Liu, D.; Chen, B.; Doerksen, R. J.; Kaplan, J.; Carroll, P. J.; Klein, M. L.; DeGrado, W. F. De Novo Design of Biomimetic Antimicrobial Polymers. *Proc. Natl. Acad. Sci.* **2002**, *99* (8), 5110–5114. https://doi.org/10.1073/pnas.082046199.

(58) Ilker, M. F.; Nüsslein, K.; Tew, G. N.; Coughlin, E. B. Tuning the Hemolytic and Antibacterial Activities of Amphiphilic Polynorbornene Derivatives. *J. Am. Chem. Soc.* **2004**, *126* (48), 15870–15875. https://doi.org/10.1021/ja045664d.

(59) Gabriel, G. J.; Madkour, A. E.; Dabkowski, J. M.; Nelson, C. F.; Nüsslein, K.; Tew, G. N. Synthetic Mimic of Antimicrobial Peptide with Nonmembrane-Disrupting Antibacterial Properties. *Biomacromolecules* **2008**, *9* (11), 2980–2983. https://doi.org/10.1021/bm800855t.

(60) Lienkamp, K.; Madkour, A. E.; Musante, A.; Nelson, C. F.; Nüsslein, K.; Tew, G. N. Antimicrobial Polymers Prepared by ROMP with Unprecedented Selectivity: A Molecular Construction Kit Approach. *J. Am. Chem. Soc.* **2008**, *130* (30), 9836–9843. https://doi.org/10.1021/ja801662y.

(61) Zasloff, M. Antimicrobial Peptides of Multicellular Organisms. *Nature* **2002**, *415* (6870), 389–395. https://doi.org/10.1038/415389a.

(62) Shai, Y. Mechanism of the Binding, Insertion and Destabilization of Phospholipid Bilayer Membranes by α-Helical Antimicrobial and Cell Non-Selective Membrane-Lytic Peptides. *Biochim. Biophys. Acta BBA - Biomembr.* **1999**, *1462* (1), 55–70. https://doi.org/10.1016/S0005-2736(99)00200-X.

(63) Nüsslein, K.; Arnt, L.; Rennie, J.; Owens, C.; Tew, G. N. Y. 2006. Broad-Spectrum Antibacterial Activity by a Novel Abiogenic Peptide Mimic. *Microbiology 152* (7), 1913–1918. https://doi.org/10.1099/mic.0.28812-0.

(64) Waschinski, C. J.; Tiller, J. C. Poly(Oxazoline)s with Telechelic Antimicrobial Functions. *Biomacromolecules* **2005**, *6* (1), 235–243. https://doi.org/10.1021/bm049553i.

(65) Waschinski, C. J.; Herdes, V.; Schueler, F.; Tiller, J. C. Influence of Satellite Groups on Telechelic Antimicrobial Functions of Polyoxazolines. *Macromol. Biosci.* **2005**, *5* (2), 149–156. https://doi.org/10.1002/mabi.200400169.

(66) Waschinski, C. J.; Barnert, S.; Theobald, A.; Schubert, R.; Kleinschmidt, F.; Hoffmann, A.; Saalwächter, K.; Tiller, J. C. Insights in the Antibacterial Action of Poly(Methyloxazoline)s with a Biocidal End Group and Varying Satellite Groups. *Biomacromolecules* **2008**, *9* (7), 1764–1771. https://doi.org/10.1021/bm7013944.

(67) Chlorhexidine Facts: Mechanism of Action https://www.chlorhexidinefacts.com/mechanism-of-action.html (accessed 2021 -05 -18).

(68) Rodriguez, L. C.; Palmer, K.; Montagner, F.; Rodrigues, D. C. A Novel Chlorhexidine-Releasing Composite Bone Cement: Characterization of Antimicrobial Effectiveness and Cement Strength. *J. Bioact. Compat. Polym.* **2015**, *30* (1), 34–47. https://doi.org/10.1177/0883911514566130.

(69) New Biocidal N-Halamine-PEG Polymers - M. W. Eknoian, S. D. Worley, J. M. Harris, 1998

https://journals.sagepub.com/doi/abs/10.1177/088391159801300205?casa_token=n7BJrV6qtJgAAAAA:FZ-Ks5OyMAKVHiTl-d5dTvlEu0rAeosRWkY8p5h-HmyV9ONmQekI8xpexFzlv7PrydhSWNkjwros (accessed 2021 -05 -18).

(70) A new cyclic N-halamine biocidal polymer | Industrial & Engineering Chemistry Research https://pubs.acs.org/doi/abs/10.1021/ie00025a022 (accessed 2021 -05 -18).

(71) Liang, J.; Barnes, K.; Akdag, A.; Worley, S. D.; Lee, J.; Broughton, R. M.; Huang, T.-S. Improved Antimicrobial Siloxane. *Ind. Eng. Chem. Res.* **2007**, *46* (7), 1861–1866. https://doi.org/10.1021/ie061583+.

(72) Spadaro, J. A.; Berger, T. J.; Barranco, S. D.; Chapin, S. E.; Becker, R. O. Antibacterial Effects of Silver Electrodes with Weak Direct Current. *Antimicrob. Agents Chemother.* **1974**, *6* (5), 637–642. https://doi.org/10.1128/AAC.6.5.637.

(73) Feng, Q. L.; Wu, J.; Chen, G. Q.; Cui, F. Z.; Kim, T. N.; Kim, J. O. A Mechanistic Study of the Antibacterial Effect of Silver Ions on Escherichia Coli and Staphylococcus Aureus. *J. Biomed. Mater. Res.* **2000**, *52* (4), 662–668. https://doi.org/10.1002/1097-4636(20001215)52:4<662::AID-JBM10>3.0.CO;2-3.

(74) Bragg, P. D.; Rainnie, D. J. The Effect of Silver Ions on the Respiratory Chain of Escherichia Coli. *Can. J. Microbiol.* **2011**. https://doi.org/10.1139/m74-135.

(75) Interaction of Silver(I) Ions with the Respiratory Chain of Escherichia coli: An Electrochemical and Scanning Electrochemical Microscopy Study of the Antimicrobial Mechanism of Micromolar Ag+ | Biochemistry https://pubs.acs.org/doi/10.1021/bi0508542 (accessed 2021 -05 -19).

(76) Lyutakov, O.; Hejna, O.; Solovyev, A.; Kalachyova, Y.; Svorcik, V. Polymethylmethacrylate Doped with Porphyrin and Silver Nanoparticles as Light-Activated Antimicrobial Material. 20.

(77) Yin, I. X.; Zhang, J.; Zhao, I. S.; Mei, M. L.; Li, Q.; Chu, C. H. The Antibacterial Mechanism of Silver Nanoparticles and Its Application in Dentistry. *Int. J. Nanomedicine* **2020**, *15*, 2555–2562. https://doi.org/10.2147/IJN.S246764.

(78) Tiller, J. C.; Liao, C.-J.; Lewis, K.; Klibanov, A. M. Designing Surfaces That Kill Bacteria on Contact. *Proc. Natl. Acad. Sci.* **2001**, *98* (11), 5981–5985. https://doi.org/10.1073/pnas.111143098.

(79) Chrószcz, M.; Barszczewska-Rybarek, I. Nanoparticles of Quaternary Ammonium Polyethylenimine Derivatives for Application in Dental Materials. *Polymers* **2020**, *12* (11). https://doi.org/10.3390/polym12112551.

(80) Ding, X.; Duan, S.; Ding, X.; Liu, R.; Xu, F.-J. Versatile Antibacterial Materials: An Emerging Arsenal for Combatting Bacterial Pathogens. *Adv. Funct. Mater.* **2018**, *28* (40), 1802140. https://doi.org/10.1002/adfm.201802140.

(81) Bieser, A. M.; Tiller, J. C. Mechanistic Considerations on Contact-Active Antimicrobial Surfaces with Controlled Functional Group Densities. *Macromol. Biosci.* **2011**, *11* (4), 526–534. https://doi.org/10.1002/mabi.201000398.

(82) Isquith, A. J.; Abbott, E. A.; Walters, P. A. Surface-Bonded Antimicrobial Activity of an Organosilicon Quaternary Ammonium Chloride. *Appl. Microbiol.* **1972**, *24* (6), 859–863.

(83) Chen, R.; Li, Y.; Tang, L.; Yang, H.; Lu, Z.; Wang, J.; Liu, L.; Takahashi, K. Synthesis of Zinc-Based Acrylate Copolymers and Their Marine Antifouling Application. *RSC Adv.* **2017**, *7* (63), 40020–40027. https://doi.org/10.1039/C7RA04840H.

(84) Kuo, P.-L.; Chuang, T.-F.; Wang, H.-L. Surface-Fragmenting, Self-Polishing, Tin-Free Antifouling Coatings. *J. Coat. Technol.* **1999**, *71* (893), 77–83. https://doi.org/10.1007/BF02697909.

(85) Laloyaux, X.; Fautré, E.; Blin, T.; Purohit, V.; Leprince, J.; Jouenne, T.; Jonas, A. M.; Glinel, K. Temperature-Responsive Polymer Brushes Switching from Bactericidal to Cell-Repellent. *Adv. Mater.* **2010**, *22* (44), 5024–5028. https://doi.org/10.1002/adma.201002538.

(86) Liang, J.; Chen, Y.; Barnes, K.; Wu, R.; Worley, S. D.; Huang, T.-S. N-Halamine/Quat Siloxane Copolymers for Use in Biocidal Coatings. *Biomaterials* **2006**, *27* (11), 2495–2501. https://doi.org/10.1016/j.biomaterials.2005.11.020.

(87) Li, Z.; Lee, D.; Sheng, X.; Cohen, R. E.; Rubner, M. F. Two-Level Antibacterial Coating with Both Release-Killing and Contact-Killing Capabilities. *Langmuir ACS J. Surf. Colloids* **2006**, *22* (24), 9820–9823. https://doi.org/10.1021/la0622166.

(88) Yudovin-Farber, I.; Golenser, J.; Beyth, N.; Weiss, E. I.; Domb, A. J. Quaternary Ammonium Polyethyleneimine: Antibacterial Activity. *J. Nanomater.* **2010**, *2010*, e826343. https://doi.org/10.1155/2010/826343.

(89) Brissault, B.; Kichler, A.; Guis, C.; Leborgne, C.; Danos, O.; Cheradame, H. Synthesis of Linear Polyethylenimine Derivatives for DNA Transfection. *Bioconjug. Chem.* **2003**, *14* (3), 581–587. https://doi.org/10.1021/bc0200529.

(90) Shen, C.; Li, J.; Zhang, Y.; Li, Y.; Shen, G.; Zhu, J.; Tao, J. Polyethylenimine-Based Micro/Nanoparticles as Vaccine Adjuvants. *Int. J. Nanomedicine* **2017**, *Volume 12*, 5443–5460. https://doi.org/10.2147/IJN.S137980.

(91) Yemul, O.; Imae, T. Synthesis and Characterization of Poly(Ethyleneimine) Dendrimers. *Colloid Polym. Sci.* **2008**, *286* (6), 747–752. https://doi.org/10.1007/s00396-007-1830-6.

(92) Lungu, C. N.; Diudea, M. V.; Putz, M. V.; Grudziński, I. P. Linear and Branched PEIs (Polyethylenimines) and Their Property Space. *Int. J. Mol. Sci.* **2016**, *17* (4), 555. https://doi.org/10.3390/ijms17040555.

(93) Overview of Amines - Course Hero https://www.coursehero.com/sg/organic-chemistry/overview-of-amines/ (accessed 2021 -05 -26).

(94) Primary, Secondary, Tertiary, and Quaternary in Organic Chemistry. *Master Organic Chemistry*, 2010.

(95) Gibney, K.; Sovadinova, I.; Lopez, A. I.; Urban, M.; Ridgway, Z.; Caputo, G. A.; Kuroda, K. Poly(Ethylene Imine)s as Antimicrobial Agents with Selective Activity. *Macromol. Biosci.* **2012**, *12* (9), 1279–1289. https://doi.org/10.1002/mabi.201200052.

(96) El-Banna, A.; Sherief, D.; Fawzy, A. S. 7 - Resin-Based Dental Composites for Tooth Filling. In *Advanced Dental Biomaterials*; Khurshid, Z., Najeeb, S., Zafar, M. S., Sefat, F., Eds.; Woodhead Publishing, 2019; pp 127–173. https://doi.org/10.1016/B978-0-08-102476-8.00007-4.

(97) Zafar, M. S.; Alnazzawi, A. A.; Alrahabi, M.; Fareed, M. A.; Najeeb, S.; Khurshid, Z. 18 - Nanotechnology and Nanomaterials in Dentistry. In *Advanced Dental Biomaterials*; Khurshid, Z., Najeeb, S., Zafar, M. S., Sefat, F., Eds.; Woodhead Publishing, 2019; pp 477–505. https://doi.org/10.1016/B978-0-08-102476-8.00018-9.

(98) Hora, P. I.; Pati, S. G.; McNamara, P. J.; Arnold, W. A. Increased Use of Quaternary Ammonium Compounds during the SARS-CoV-2 Pandemic and Beyond: Consideration of Environmental Implications. *Environ. Sci. Technol. Lett.* **2020**, *7* (9), 622–631. https://doi.org/10.1021/acs.estlett.0c00437.

(99) Gerba, C. P. Quaternary Ammonium Biocides: Efficacy in Application. *Appl. Environ. Microbiol.* **2015**, *81* (2), 464–469. https://doi.org/10.1128/AEM.02633-14.

(100) Jiao, Y.; Niu, L.-N.; Ma, S.; Li, J.; Tay, F. R.; Chen, J.-H. Quaternary Ammonium-Based Biomedical Materials: State-of-the-Art, Toxicological Aspects and Antimicrobial Resistance. *Prog. Polym. Sci.* **2017**, *71*, 53–90. https://doi.org/10.1016/j.progpolymsci.2017.03.001.

(101) Chen, Z.; Lv, Z.; Sun, Y.; Chi, Z.; Qing, G. Recent Advancements in Polyethyleneimine-Based Materials and Their Biomedical, Biotechnology, and Biomaterial Applications. *J. Mater. Chem. B* **2020**, *8* (15), 2951–2973. https://doi.org/10.1039/c9tb02271f.

(102) Yew, P. Y. M.; Chee, P. L.; Cally, O.; Zhang, K.; Liow, S. S.; Loh, X. J. Quarternized Short Polyethylenimine Shows Good Activity against Drug-Resistant Bacteria. *Macromol. Mater. Eng.* **2017**, *302* (9), 1700186. https://doi.org/10.1002/mame.201700186.

(103) Venkatesh, M.; Barathi, V. A.; Goh, E. T. L.; Anggara, R.; Fazil, M. H. U. T.; Ng, A. J. Y.; Harini, S.; Aung, T. T.; Fox, S. J.; Liu, S.; Yang, L.; Barkham, T. M. S.; Loh, X. J.; Verma, N. K.; Beuerman, R. W.; Lakshminarayanan, R. Antimicrobial Activity and Cell Selectivity of Synthetic and Biosynthetic Cationic Polymers. *Antimicrob. Agents Chemother.* **2017**, *61* (10). https://doi.org/10.1128/AAC.00469-17.

(104) Chemistry (IUPAC), T. I. U. of P. and A. IUPAC - quaternary ammonium compounds (Q05003) https://goldbook.iupac.org/terms/view/Q05003 (accessed 2021 -08 -16). https://doi.org/10.1351/goldbook.Q05003.

(105) Jucker, B. A.; Harms, H.; Zehnder, A. J. Adhesion of the Positively Charged Bacterium Stenotrophomonas (Xanthomonas) Maltophilia 70401 to Glass and Teflon. *J. Bacteriol.* **1996**, *178* (18), 5472–5479.

(106) Asri, L. A. T. W.; Crismaru, M.; Roest, S.; Chen, Y.; Ivashenko, O.; Rudolf, P.; Tiller, J. C.; Mei, H. C. van der; Loontjens, T. J. A.; Busscher, H. J. A Shape-Adaptive, Antibacterial-Coating of Immobilized Quaternary-Ammonium Compounds Tethered on Hyperbranched Polyurea and Its Mechanism of Action. *Adv. Funct. Mater.* **2014**, *24* (3), 346–355. https://doi.org/10.1002/adfm.201301686.

(107) Gilbert, P.; Moore, L. E. Cationic Antiseptics: Diversity of Action under a Common Epithet. *J. Appl. Microbiol.* **2005**, *99* (4), 703–715. https://doi.org/10.1111/j.1365-2672.2005.02664.x.

(108) Friedrich, C. L.; Moyles, D.; Beveridge, T. J.; Hancock, R. E. W. Antibacterial Action of Structurally Diverse Cationic Peptides on Gram-Positive Bacteria. *Antimicrob. Agents Chemother.* **2000**, *44* (8), 2086–2092.

(109) Kenawy, E.-R. Biologically Active Polymers. IV. Synthesis and Antimicrobial Activity of Polymers Containing 8-Hydroxyquinoline Moiety. *J. Appl. Polym. Sci.* **2001**, *82* (6), 1364–1374. https://doi.org/10.1002/app.1973.

(110) Cakmak, I.; Ulukanli, Z.; Tuzcu, M.; Karabuga, S.; Genctav, K. Synthesis and Characterization of Novel Antimicrobial Cationic Polyelectrolytes. *Eur. Polym. J.* **2004**, *40* (10), 2373–2379. https://doi.org/10.1016/j.eurpolymj.2004.06.004.

(111) Jeong, J.-H.; Byoun, Y.-S.; Lee, Y.-S. Poly(Styrene-Alt-Maleic Anhydride)-4-Aminophenol Conjugate: Synthesis and Antibacterial Activity. *React. Funct. Polym.* **2002**, *50* (3), 257–263. https://doi.org/10.1016/S1381-5148(01)00120-1.

(112) Palermo, E. F.; Kuroda, K. Chemical Structure of Cationic Groups in Amphiphilic Polymethacrylates Modulates the Antimicrobial and Hemolytic Activities. *Biomacromolecules* **2009**, *10* (6), 1416–1428. https://doi.org/10.1021/bm900044x.

(113) Gilbert, P.; Al-taae, A. Antimicrobial Activity of Some Alkyltrimethylammonium Bromides. *Lett. Appl. Microbiol.* **1985**, *1* (6), 101–104. https://doi.org/10.1111/j.1472-765X.1985.tb01498.x.

(114) Birch, B. J.; Hall, D. G. Heats of Dilution of Sub-Micellar Aqueous Surfactant Solutions. *J. Chem. Soc. Faraday Trans. 1 Phys. Chem. Condens. Phases* **1972**, *68* (0), 2350–2355. https://doi.org/10.1039/F19726802350.

(115) He, J.; Söderling, E.; Vallittu, P. K.; Lassila, L. V. J. Investigation of Double Bond Conversion, Mechanical Properties, and Antibacterial Activity of Dental Resins with Different Alkyl Chain Length Quaternary Ammonium Methacrylate Monomers (QAM). *J. Biomater. Sci. Polym. Ed.* **2013**, *24* (5), 565–573. https://doi.org/10.1080/09205063.2012.699709.

(116) US EPA, O. About List N: Disinfectants for Coronavirus (COVID-19) https://www.epa.gov/coronavirus/about-list-n-disinfectants-coronavirus-covid-19-0 (accessed 2021 -05 -27).

(117) Haldar, J.; An, D.; Cienfuegos, L. Á. de; Chen, J.; Klibanov, A. M. Polymeric Coatings That Inactivate Both Influenza Virus and Pathogenic Bacteria. *Proc. Natl. Acad. Sci.* **2006**, *103* (47), 17667–17671. https://doi.org/10.1073/pnas.0608803103.

(118) Schrank, C. L.; Minbiole, K. P. C.; Wuest, W. M. Are Quaternary Ammonium Compounds, the Workhorse Disinfectants, Effective against Severe Acute Respiratory Syndrome-Coronavirus-2? *ACS Infect. Dis.* **2020**, *6* (7), 1553–1557. https://doi.org/10.1021/acsinfecdis.0c00265.

(119) Ansaldi, F.; Banfi, F.; Morelli, P.; Valle, L.; Durando, P.; Sticchi, L.; Contos, S.; Gasparini, R.; Crovari, P. SARS-CoV, Influenza A and Syncitial Respiratory Virus Resistance against Common Disinfectants and Ultraviolet Irradiation. *J. Prev. Med. Hyg.* **2004**, *45* (1–2), 5–8.

(120) Tuladhar, E.; de Koning, M. C.; Fundeanu, I.; Beumer, R.; Duizer, E. Different Virucidal Activities of Hyperbranched Quaternary Ammonium Coatings on Poliovirus and Influenza Virus. *Appl. Environ. Microbiol.* **2012**, *78* (7), 2456–2458. https://doi.org/10.1128/AEM.07738-11.

(121) Behr, J.-P. The Proton Sponge: A Trick to Enter Cells the Viruses Did Not Exploit. *Chim. Int. J. Chem.* **1997**, *51* (1–2), 34–36.

(122) Demeneix, null; Behr, null; Boussif, null; Zanta, null; Abdallah, null; Remy, null. Gene Transfer with Lipospermines and Polyethylenimines. *Adv. Drug Deliv. Rev.* **1998**, *30* (1–3), 85–95. https://doi.org/10.1016/s0169-409x(97)00109-9.

(123) Fischer, D.; Bieber, T.; Li, Y.; Elsässer, H.-P.; Kissel, T. A Novel Non-Viral Vector for DNA Delivery Based on Low Molecular Weight, Branched Polyethylenimine: Effect of Molecular Weight on Transfection Efficiency and Cytotoxicity. *Pharm. Res.* **1999**, *16* (8), 1273–1279. https://doi.org/10.1023/A:1014861900478.

(124) Noreen, A.; Zia, K. M.; Zuber, M.; Tabasum, S.; Saif, M. J. Recent Trends in Environmentally Friendly Water-Borne Polyurethane Coatings: A Review. *Korean J. Chem. Eng.* **2016**, *33* (2), 388–400. https://doi.org/10.1007/s11814-015-0241-5.

(125) Honarkar, H. Waterborne Polyurethanes: A Review. *J. Dispers. Sci. Technol.* **2018**, *39* (4), 507–516. https://doi.org/10.1080/01932691.2017.1327818.

(126) Akindoyo, J. O.; Beg, M. D. H.; Ghazali, S.; Islam, M. R.; Jeyaratnam, N.; Yuvaraj, A. R. Polyurethane Types, Synthesis and Applications – a Review. *RSC Adv.* **2016**, *6* (115), 114453–114482. https://doi.org/10.1039/C6RA14525F.

(127) Jennings, M. C.; Minbiole, K. P. C.; Wuest, W. M. Quaternary Ammonium Compounds: An Antimicrobial Mainstay and Platform for Innovation to Address Bacterial Resistance. *ACS Infect. Dis.* **2015**, *1* (7), 288–303. https://doi.org/10.1021/acsinfecdis.5b00047.

(128) Lu, G. W.; Gao, P. CHAPTER 3 - Emulsions and Microemulsions for Topical and Transdermal Drug Delivery. In *Handbook of Non-Invasive Drug Delivery Systems*; Kulkarni, V. S., Ed.; Personal Care & Cosmetic Technology; William Andrew Publishing: Boston, 2010; pp 59–94. https://doi.org/10.1016/B978-0-8155-2025-2.10003-4.

(129) Lu, H.-Y.; Chen, Y.-H.; Liu, H.-J. Baculovirus as a Vaccine Vector. *Bioengineered* **2012**, *3* (5), 271–274. https://doi.org/10.4161/bioe.20679.

(130) Summers, M. *Baculoviruses for Insect Pest Control: Safety Considerations : Selected Papers from EPA-USDA Working Symposium, Bethesda, Maryland*; American Society for Microbiology, 1975.

(131) Harrison, R. L.; Herniou, E. A.; Jehle, J. A.; Theilmann, D. A.; Burand, J. P.; Becnel, J. J.; Krell, P. J.; van Oers, M. M.; Mowery, J. D.; Bauchan, G. R.; ICTV Report ConsortiumYR 2018. ICTV Virus Taxonomy Profile: Baculoviridae. *J. Gen. Virol. 99* (9), 1185–1186. https://doi.org/10.1099/jgv.0.001107.

(132) Slack, J.; Arif, B. M. The Baculoviruses Occlusion-Derived Virus: Virion Structure and Function. *Adv. Virus Res.* **2006**, *69*, 99–165. https://doi.org/10.1016/S0065-3527(06)69003-9.